



universität
wien

MASTERARBEIT / MASTER'S THESIS

Titel der Masterarbeit / Title of the Master's Thesis

When Inertia Matters Simulating Underdamped Active Particles in a Harmonic Potential

verfasst von / submitted by

Mag. rer. nat. Alexander Hummelbrunner, BSc

angestrebter akademischer Grad / in partial fulfilment of the requirements for the degree of

Master of Science (MSc)

Wien, 2018 / Vienna, 2018

Studienkennzahl lt. Studienblatt /
degree programme code as it appears on
the student record sheet:

A 066 876

Studienrichtung lt. Studienblatt /
degree programme as it appears on
the student record sheet:

Masterstudium Physik

Betreut von / Supervisor:

Univ.-Prof. Dr. Christoph Dellago

Danksagung

Zuerst möchte ich mich bei einigen Personen bedanken, die diese Arbeit erst ermöglicht haben.

Zuallererst bedanke ich mich bei meinem Betreuer Prof. Christoph Dellago, der mir nicht nur ermöglichte, ein eigenes Thema zu verfolgen, sondern mir auch die nötige Zeit dafür gab. Er fand für meine Anliegen stets Zeit und die Diskussionen mit ihm haben der Arbeit neuen Schwung verliehen. Ebenso möchte ich mich bei den weiteren Mitgliedern des “Stochastic Thermodynamics”-Teams Max Innerbichler und Victor Wenin bedanken, die bei unseren regelmäßigen Treffen meine Fortschritte kritisch unter die Lupe nahmen.

Mein Dank gilt auch meinen Studienkolleginnen und Studienkollegen ohne deren Unterstützung der Abschluss des Studiums schwieriger geworden wäre und nicht so viel Freude bereitet hätte.

Zu guter Letzt danke ich meiner Familie, insbesondere meiner Frau Barbara, die mein Studium von Beginn an förderte. Nur ihre fortwährende Unterstützung erlaubte es mir neben der Betreuung unseres Sohnes auch diese Arbeit fertig zu stellen.

Abstract

A single underdamped and self-propelled Brownian particle in a three dimensional harmonic trap was studied theoretically and simulated using Langevin dynamics. The direction of the particle's propelling force is undergoing underdamped rotational diffusion. In the limit of small rotational diffusion constants compared to the trap frequency the second moments of the velocity and the position are found analytically. Outside of this limit the second moments can be described using the power spectrum of the propelling direction. Using numerical integration the second moments show resonant behaviour with respect to the rotational diffusion constant.

In the limit of fast rotational diffusion it can be shown that the equipartition theorem is fulfilled and an effective temperature can be ascribed to the particle.

The theoretical work is supported by Langevin dynamics simulations.

Zusammenfassung

Die Statistik eines einzelnen aktiven brownischen Teilchens in einem harmonischen Potential wurde bei niedriger Reibung theoretisch untersucht und mittels Langevin-Dynamik simuliert. Die Richtung der Aktivität des Teilchens unterlag dabei der brownischen Bewegung. Im Grenzfall sehr langsamer Rotationsdiffusion der Aktivitätsrichtung im Vergleich zur Frequenz des Potentials konnten die zweiten Momente der Position und der Geschwindigkeit des Teilchens analytisch hergeleitet werden. Außerhalb dieses Grenzfalles können diese zweiten Momente bestimmt werden, indem das Leistungsspektrum der Aktivitätsrichtung ausgewertet wird. Mittels numerischer Integration der zweiten Momente zeigen sich Resonanzeffekte in Abhängigkeit der Rotationsdiffusionskonstante.

Nur im Grenzfall rascher Rotationsdiffusion lässt sich zeigen, dass dem Gleichverteilungsgesetz genüge getan wird und dem Teilchen eine effektive Temperatur zugeordnet werden kann.

Die theoretische Arbeit wird durch die Ergebnisse der Langevin-Dynamik-Simulation bestätigt.

Contents

1. Brownian Motion	5
1.1. The freely diffusing particle - from Einstein to Langevin	5
1.1.1. The Einstein formula	5
1.1.2. The Langevin equation	8
1.1.3. The Fokker-Planck equation	11
1.1.4. The Wiener-Khinchin theorem	14
1.2. Brownian motion in a harmonic potential	15
1.2.1. Inactive particle in an oscillatory shear flow	19
1.3. Threedimensional case	21
1.3.1. Free Brownian motion	21
1.3.2. Brownian motion in a harmonic potential	22
2. Active Particles	25
2.1. Introduction	25
2.2. Overdamped active particles	25
2.3. Underdamped active particles	27
2.3.1. Underdamped and freely rotating	27
2.4. Active particles in a harmonic potential	30
2.4.1. Overdamped case	30
2.4.2. Underdamped and freely rotating	31
2.4.2.1. Slow rotation	32
2.4.2.2. Rotation period near oscillation period	34
2.4.2.3. Fast rotation	37
3. Simulations	41
3.1. The algorithms	41
3.1.1. Moving source-dynamics	41
3.1.2. Rotating sphere-dynamics	44
3.1.3. Translational motion	46
3.2. Underdamped active particles	47
3.3. Underdamped active particles in a harmonic potential	51
3.3.1. Units and particle properties	51
3.3.2. Slow rotation	51
3.3.3. Rotation period near oscillation period	56
3.3.4. Fast rotation	62
4. Conclusion	67

Contents

A. Testing the Simulation	69
A.1. Brownian particle	69
A.1.1. Free particle	69
A.1.2. In harmonic potential	69
A.2. Overdamped active particle	69
B. Supplementary Calculations	73
B.1. Overdamped active particles	73
B.1.1. Position's expectation value	73
B.1.2. Mean squared displacement	74

Introduction

The statistical description of systems far from equilibrium is a growing research topic in physics. Especially so-called “active particles” and the related “active matter” have been extensively investigated experimentally and theoretically in the last decade. Active particles refer to a whole class of biological and physical entities, which can take up energy from the environment and transform it into kinetic energy, e.g. motile cells, molecular motors and Janus particles, the term can also be used for describing the movement of higher organisms such as birds and fish and even humans [21].

The experiments and theoretical descriptions range from the first modeling of the motile cells’ erratic movement [3] to today’s studies of the behaviour in complex and crowded environments [2]. These particles show new properties, that might be used to transport nanoscopic cargoes, for example in health care.

Most of this research is focused on active motion in low Reynold’s number regimes - neglecting inertia. This approach is justified, when studying motile cells and molecular motors in water and similar fluids. But e.g. active particles in dusty plasmas [22] would be subject to inertia. The first self-propelled particles in such a regime have been theoretically proposed [1]. In an underdamped regime new phenomena could occur. For example Kählert and Löwen describe the case of a harmonically trapped inactive particle subject to an externally imposed oscillatory shear flow. They find resonant behaviour in this case [11].

The present work generalizes this approach to an active Brownian particle, like a Janus particle, in three dimensions and studies it’s simulated behaviour in a harmonic potential. The work from Kählert and Löwen suggests that there might be a resonance - this shall be further investigated using Langevin dynamics simulations on a general model for underdamped active particles.

This thesis is organized as follows:

I will review the theoretical foundation for Brownian (inactive) particles in Chapter 1 “Brownian Motion”. On the one hand should the simulation for small activity strengths converge to this case, and on the other will results and mathematical tools introduced in this chapter be important for the theoretical description of active particles.

In Chapter 2 “Active Particles” the widely used overdamped case and the model of the freely rotating, underdamped case, that has been studied for the present thesis, are discussed in theoretical terms. With an emphasis on the case of the underdamped, freely rotating particle in a harmonic potential.

The results of the simulation and the comparison with the theoretical hypothesis from Chapter 2 are found in Chapter 3 “Simulations”, as are the descriptions of the algorithms used.

Contents

In Chapter 4 “Conclusions” the important results will be reviewed and an outlook for further research will be given.

A major part of this work was the development and the testing of the simulation. Some results of the extensive simulation testing are given in the appendix.

1. Brownian Motion

1.1. The freely diffusing particle - from Einstein to Langevin

The Brownian motion and Brownian particle is named after the British botanist Robert Brown (1773 - 1858) who described in 1827 the erratic motion of pollen grains in water. Studying Brownian motion one stands on the shoulders of giants like Albert Einstein, Marian Smoluchowski, George Uhlenbeck, Leonard Ornstein and Paul Langevin. That seems like a lot of brain power working on a problem that started with the botanist's observation. But by studying the particle's erratic movement the concept of stochastic differential equations had to be introduced. Today stochastic differential equations are present in physics, biology and even finance mathematics, describing stock prices.

1.1.1. The Einstein formula

Albert Einstein (1879 - 1955) proposed 1905 a mathematical theory for the erratic movement of the pollen grains based on the atomistic concept [9] - at a time when the atomistic concept was still a hypothesis and controversially debated in the physics community [13]. Einstein assumed, that the grain pollens move, because they are hit by water molecules. These collisions are of random strength and direction, and will cancel each other out over long periods of time. But for short times it's possible to have more molecules colliding with, for example, the right side of the particle - driving it to the left. He first showed, that for small spheres suspended in a liquid the diffusion constant D depends only on the coefficient of viscosity η and on the radius of the suspended particles r :

$$D = \frac{RT}{N_A} \cdot \frac{1}{6\pi\eta r} \quad (1.1)$$

where R is the universal gas constant (well known from experiments at that time), T the temperature of the liquid and N_A the Avogadro constant. One way to put the atomistic theory on firm ground was measuring the Avogadro constant in different ways, hoping for results which were in good accordance to each other. Einstein's theory provided another way to measure the Avogadro constant.

Let τ be a time interval big enough to neglect inertia, like Einstein proposed, and therefore assume the displacements of the suspended particles as mutually independent. The displacements Δ should follow a symmetric probability density ϕ , where $\phi(\Delta)$ is bigger than zero only for small values of Δ . Following Einstein one can write a particle distribution function $\rho(x, t)$ for n particles distributed on the x-axis at time t . Hence:

$$\int_{-\infty}^{\infty} \rho(x, t) dx = n \quad (1.2)$$

1. Brownian Motion

Using the small time interval τ one can write

$$\rho(x, t + \tau) = \rho(x, t) + \tau \cdot \frac{\partial \rho(x, t)}{\partial t} \quad (1.3)$$

Another way to obtain $\rho(x, t + \tau)$ is by using the distribution of displacements $\phi(\Delta)$. The number of the particles in the interval $[x, x + dx]$ at a time $t + \tau$ can be expressed using $\phi(\Delta)$ and the distribution function $\rho(x, t)$ at time t as:

$$\rho(x, t + \tau) dx = dx \cdot \int_{-\infty}^{\infty} \rho(x + \Delta, t) \phi(\Delta) d\Delta$$

Let's expand $\rho(x + \Delta, t)$ in powers of Δ

$$\rho(x + \Delta, t) = \rho(x, t) + \Delta \frac{\partial \rho}{\partial x} + \frac{\Delta^2}{2} \frac{\partial^2 \rho}{\partial x^2} + \dots$$

then

$$\rho(x, t + \tau) dx = dx \cdot \left(\rho(x, t) \int_{-\infty}^{\infty} \phi(\Delta) d\Delta + \frac{\partial \rho}{\partial x} \int_{-\infty}^{\infty} \Delta \phi(\Delta) d\Delta + \frac{\partial^2 \rho}{\partial x^2} \int_{-\infty}^{\infty} \frac{\Delta^2}{2} \phi(\Delta) d\Delta + \dots \right)$$

Using that the integral $\int_{-\infty}^{\infty} \Delta^k \phi(\Delta) d\Delta$ vanishes if k is odd or $k = 0$:

$$\rho(x, t + \tau) dx = dx \cdot \left(\rho(x, t) + \frac{\partial^2 \rho}{\partial x^2} \int_{-\infty}^{\infty} \frac{\Delta^2}{2} \phi(\Delta) d\Delta + \dots \right) \quad (1.4)$$

Because we assumed $\phi(\Delta)$ to be only bigger than zero for small displacements, powers of Δ^4 upwards will be neglected. Comparing (1.3) to (1.4) Einstein arrived at

$$\tau \frac{\partial \rho(x, t)}{\partial t} = \int_{-\infty}^{\infty} \frac{\Delta^2}{2} \phi(\Delta) d\Delta \cdot \frac{\partial^2 \rho(x, t)}{\partial x^2}$$

and, after defining $D = \frac{1}{\tau} \int_{-\infty}^{\infty} \frac{\Delta^2}{2} \phi(\Delta) d\Delta$, one arrives at the well-known diffusion equation

$$\frac{\partial \rho(x, t)}{\partial t} = D \frac{\partial^2 \rho(x, t)}{\partial x^2}$$

Assuming as initial condition $\rho(x, 0) = n \cdot \delta(x)$, with $\delta(x)$ being the delta-distribution, the solution is known as:

$$\rho(x, t) = \frac{n}{\sqrt{4\pi D}} \cdot \frac{e^{-x^2/4Dt}}{\sqrt{t}}$$

Now let's calculate the mean squared distance from the origin for one particle (setting $n = 1$):

$$\begin{aligned} \langle x^2 \rangle &= \int_{-\infty}^{\infty} x^2 \rho(x, t) dx \\ &= \frac{1}{\sqrt{4\pi D t}} \int_{-\infty}^{\infty} x^2 e^{-x^2/4Dt} dx \end{aligned}$$

1.1. The freely diffusing particle - from Einstein to Langevin

In x -direction the distribution function is equal to a normal distribution with mean zero and variance $2Dt$ and therefore we obtain the so-called Einstein formula:

$$\langle x^2 \rangle = 2Dt \quad (1.5)$$

As can be seen in Fig. 1.1 the trajectories and MSD for different instances of the process can differ widely from each other. But statistical properties can still be derived and will be obeyed.

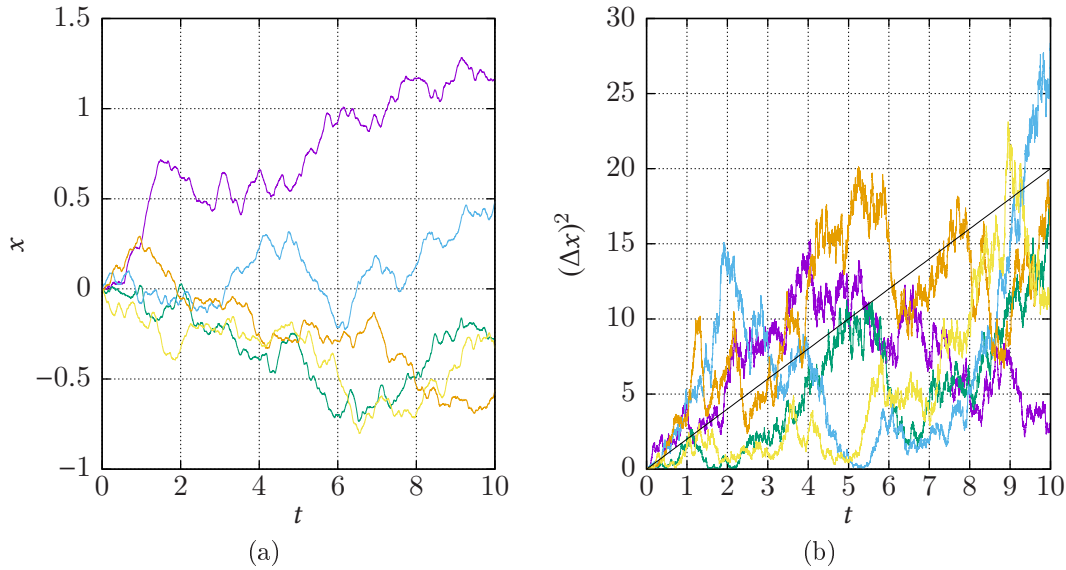


Figure 1.1.: (a) Five simulated typical trajectories for one-dimensional Brownian particles (b) the theoretical mean square displacement $2Dt$ as a black line and five simulated square displacements.

Combining the two results for D , eqs. (1.1) and (1.5), one gets

$$\frac{\langle x^2 \rangle}{2t} = \frac{RT}{N_A} \cdot \frac{1}{6\pi\eta r}$$

and therefore the Avogadro constant could be measured indirectly by determining the mean squared displacement of the particle with respect to time:

$$N_A = \frac{2t}{\langle x^2 \rangle} \cdot \frac{RT}{6\pi\eta r}$$

A Nobel Prize has been awarded to the french physicist Jean-Baptiste Perrin (1870 - 1942) in 1926 for the measurement of the Avogadro constant in different ways, including the one formulated above.

1. Brownian Motion

1.1.2. The Langevin equation

For a Langevin Dynamics simulation, as was used for the present work, it's important to know the underlying equations of motion. While Einstein obtained his results using the distribution function $\rho(x, t)$ for the Brownian particles, Langevin proposed the governing equations of motion. Changing the Newtonian ansatz from a known force $F(x, t)$ to a sum of forces, one represented by a random variable $F_r(t)$, and the other the force of friction $-\gamma_0 v$, one gets the Langevin equation in a similar notation as de Haas-Lorentz [8] used first in 1913:

$$m \dot{v} = -\gamma_0 v + F_r(t) \quad (1.6)$$

The random force is not wholly unknown. It should model the random interactions between the Brownian particle and the molecules of the medium. Over a long period of time the average of F_r should be zero, otherwise we would get a net flow of Brownian particles over time. And the force should have no “memory”. Writing this in mathematical terms, using the Dirac-delta δ :

$$\langle F_r(t) \rangle = 0 \quad (1.7)$$

$$\langle F_r(t) F_r(t') \rangle = 2 m^2 S \delta(t - t') \quad (1.8)$$

where S symbolizes the “strength” of the random force.

Following Ornstein's approach in “On the Brownian Motion” [15] we will calculate the important statistical values for this equation.

Using $\xi = \frac{\gamma_0}{m}$ and $A = \frac{F_r}{m}$, one can integrate the Langevin equation (1.6):

$$v = v_0 e^{-\xi t} + e^{-\xi t} \int_0^t e^{\xi s} A(s) ds \quad (1.9)$$

where v_0 is the initial velocity of the particle. Calculating the expectation value of Eq. (1.9) and using the first property (1.7) of $F_r(t)$, one finds

$$\langle v \rangle = v_0 e^{-\xi t} \quad (1.10)$$

where the expectation value should be understood as an ensemble average. Einstein used a time interval τ large enough to neglect any memory effects of the displacements, but the Langevin equation leads to a memory effect for the velocity. Einsteins time interval needs to be much bigger than $\frac{m}{\gamma}$ to justify his assumption.

Let's look at the second moment of the velocity, first squaring Eq. (1.9), then averaging and again using the first property (1.7) of $F_r(t)$, the result is

$$\langle v^2 \rangle = v_0^2 e^{-2\xi t} + e^{-2\xi t} \cdot \left\langle \left(\int_0^t e^{\xi s} A(s) ds \right)^2 \right\rangle \quad (1.11)$$

The integral in the second term deserves a closer look, the product of the integrals can be written as a two-dimensional integral:

$$\left\langle \int_0^t \int_0^t e^{\xi s} e^{\xi s'} A(s) A(s') ds ds' \right\rangle$$

1.1. The freely diffusing particle - from Einstein to Langevin

The value of $e^{\xi(s+s')}$ is, with respect to the ensemble average, constant and we can write

$$\int_0^t \int_0^t e^{\xi(s+s')} \langle A(s) A(s') \rangle ds ds'$$

Now using the second property (1.8) of the random force leads to

$$\int_0^t \int_0^t e^{\xi(s+s')} 2S \delta(s-s') ds ds'$$

Integrating over s using the delta-distribution's definition $\int f(x) \delta(x-x_0) dx = f(x_0)$

$$2S \int_0^t e^{2\xi s'} ds' = \frac{S}{\xi} \cdot (e^{2\xi t} - 1)$$

inserting this in Eq. (1.11):

$$\langle v^2 \rangle = v_0^2 e^{-2\xi t} + \frac{S}{\xi} \cdot (1 - e^{-2\xi t}) \quad (1.12)$$

In the limit $t \rightarrow \infty$ the particle should eventually arrive at a mean squared velocity dictated by the equipartition theorem as $\langle v^2 \rangle = \frac{k_B T}{m}$, where k_B is the Boltzmann constant and T the temperature of the solvent. Comparing this to the Eq. (1.12) from above, one can calculate the strength S as

$$S = \xi \frac{k_B T}{m} \quad (1.13)$$

Let's look at the mean squared displacement (MSD) next by multiplying the Langevin equation with x , ($\frac{dx}{dt} = v$):

$$\frac{d^2 x}{dt^2} x = -\xi \frac{dx}{dt} x + Ax$$

Using $\frac{d^2 x}{dt^2} \cdot x = \frac{1}{2} \frac{d^2 x^2}{dt^2} - v^2$ and $\frac{dx}{dt} x = \frac{1}{2} \frac{dx^2}{dt}$ does change the equation to

$$\frac{1}{2} \cdot \left(\frac{d^2 x^2}{dt^2} + \xi \frac{dx^2}{dt} \right) = v^2 + Ax$$

Taking the ensemble average, one arrives at

$$\frac{d^2}{dt^2} \langle x^2 \rangle + \xi \frac{d}{dt} \langle x^2 \rangle = 2 \langle v^2 \rangle + \langle Ax \rangle$$

We know $\langle v^2 \rangle$ from Eq. (1.12), therefore we only have to take a closer look at $\langle Ax \rangle$. Integrating Eq. (1.9) again, one obtains

$$x = x_0 + \frac{v_0}{\xi} (1 - e^{-\xi t}) + \frac{1}{\xi} \int_0^t A(s) \cdot (1 - e^{\xi(s-t)}) ds$$

1. Brownian Motion

multiplying this equation with $A(t)$ and taking the ensemble average

$$\langle Ax \rangle = \langle A \rangle x_0 + \langle A \rangle \frac{v_0}{\xi} \left(1 - e^{-\xi t}\right) + \frac{1}{\xi} \int_0^t \langle A(t)A(s) \rangle \left(1 - e^{-\xi(s-t)}\right) ds$$

If one uses both properties (1.7) and (1.8) of the random force F_r , then

$$\langle Ax \rangle = \frac{1}{\xi} \int_0^t 2S \delta(t-s) \left(1 - e^{-\xi(s-t)}\right) ds = 0$$

This only holds for equal times $\langle A(t)x(t) \rangle$ as Manoliu and Kittel [14] showed. This is also in accordance with our physical intuition of the problem. While the random acceleration should not be depending on the position of the particle at that time, these accelerations have an impact on the particle's position at a later time. Now we'll use this result and Eq. (1.12) averaging over all initial velocities ($\langle v_0^2 \rangle = \frac{S}{\xi}$):

$$\frac{d^2}{dt^2} \langle x^2 \rangle + \xi \frac{d}{dt} \langle x^2 \rangle = 2 \frac{S}{\xi}$$

This can be solved by using the following ansatz:

$$\langle x^2 \rangle = c_0 + c_1 e^{-\xi t} + 2 \frac{S}{\xi^2} t$$

The integration constants can be calculated, assuming that at $t = 0$ the MSD and its first derivative are zero. Hence the solution reads:

$$\langle x^2 \rangle = \frac{2S}{\xi^3} \left(\xi t - 1 + e^{-\xi t} \right) \quad (1.14)$$

While S only determines the slope of the MSD, the value of ξ is also responsible for the shape of the curve, as can be seen in Fig. 1.2. For short times, meaning $\xi t \ll 1$, the curve mimics a particle in a ballistic regime. In the limit of $\xi t \gg 1$ one arrives at a linear function for the MSD

$$\langle x^2 \rangle = \frac{2S}{\xi^2} t$$

which is exactly the Einstein formula (1.5), if one uses Eq. (1.13) and identifies $D = \frac{k_B T}{m\xi}$. This diffusion constant D is identical to the diffusion constant Einstein was using, defined in Eq. (1.1), if one keeps in mind that $k_B = \frac{R}{N_A}$ and Einstein uses the Stokes friction for a spherical particle with radius r , hence $\xi = \frac{6\pi r \eta}{m}$.

The autocorrelation function $\langle v(t)v(t+\tau) \rangle$ is easily obtained from Eq. (1.9). Rewriting this equation to $v_0 = v(t)$ and $v(t+\tau)$, and multiplying by $v(t)$, one gets

$$v(t)v(t+\tau) = v(t)^2 e^{-\xi\tau} + v_0 e^{-\xi\tau} \int_0^\tau e^{\xi s} A(s) ds$$

where $\tau > 0$. Now taking the average and using the equilibration limit $\langle v(t)^2 \rangle = \frac{S}{\xi}$

$$\langle v(t)v(t+\tau) \rangle = \frac{S}{\xi} \cdot e^{-\xi\tau}$$

1.1. The freely diffusing particle - from Einstein to Langevin

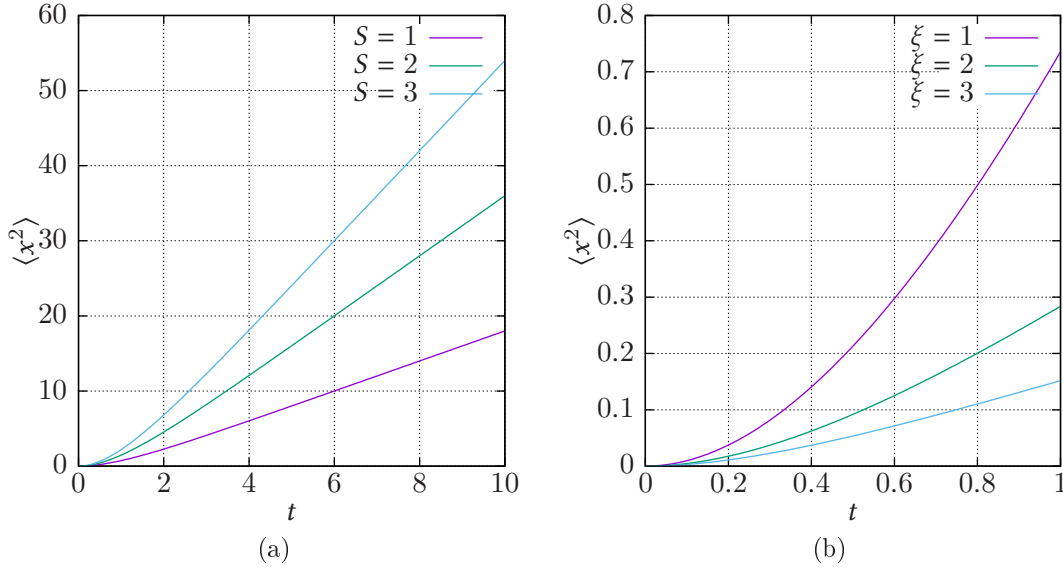


Figure 1.2.: The MSD for Brownian particles following Eq. (1.14) (a) for three different values of S with $\xi = 1$ (b) for three different values of ξ with $S = 1$

1.1.3. The Fokker-Planck equation

Instead of solving the equation of motion, in our case the Langevin equation, one can also take a look at the time dependent probability distribution function for the problem. The equation that describes the time dependence of the probability distribution function for Markovian processes is called Fokker-Planck equation. Each Langevin equation has an equivalent Fokker-Planck equation. First we will derive the general form of the Fokker-Planck equation and then apply it to the problem of the free Brownian particle, which we have discussed in the previous section.

We want to derive the differential equation describing the time dependence of a two-dimensional probability distribution function $p(a, t)$, where a is a continuous variable - called state - and t denotes the time, as usual. The expression $p(a, t) da$ describes the probability to find the system in a state $[a, a+da]$ at time t . It should describe a Markovian process with the transition rate $\omega(a, a'; t)$ denoting the probability to transition from state a' to state a at the time t . The corresponding Master-Equation¹ reads

$$\frac{\partial p(a; t)}{\partial t} = \int da' [\omega(a, a'; t) p(a', t) - \omega(a', a; t) p(a, t)]$$

This equation describes the influx to $p(a, t)$ by summing all other states' probability distribution at a' up, weighted by their transition probability to land in a . It also describes the outflux by subtracting the transition probability to leave the state a in

¹more on Markovian processes and the Master equation is found e.g. in G. Röpke, "Statistische Mechanik und das Nichtgleichgewicht" [18]

1. Brownian Motion

favor of state a' . Let's rewrite the equation a little bit

$$\frac{\partial p(a, t)}{\partial t} = \int \omega(a, a'; t) p(a', t) da' - p(a, t) \int \omega(a', a; t) da'$$

It's reasonable to assume, that the changes of a are small, i.e. that $\omega(a, a'; t)$ is a sharply peaked function around a' . Substitutions will lead us to

$$\frac{\partial p(a, t)}{\partial t} = \int \omega(a, a - b; t) p(a - b, t) db - p(a, t) \int \omega(a + b, a; t) db$$

We can Taylor expand $\omega(a, a - b; t) p(a - b, t)$ at $a = a + b$:

$$\begin{aligned} \omega(a, a - b; t) p(a - b, t) &= \sum_{n=0}^{\infty} \frac{(a - (a + b))^n}{n!} \frac{\partial^n}{\partial a^n} \left[\omega(a + b, a; t) p(a, t) \right] \\ &= \omega(a + b, a; t) p(a, t) + \sum_{n=1}^{\infty} \frac{(-b)^n}{n!} \frac{\partial^n}{\partial a^n} \left[\omega(a + b, a; t) p(a, t) \right] \end{aligned}$$

Hence

$$\begin{aligned} \frac{\partial p(a, t)}{\partial t} &= \int \omega(a + b, a; t) p(a, t) db + \int \sum_{n=1}^{\infty} \frac{(-b)^n}{n!} \frac{\partial^n}{\partial a^n} \left[\omega(a + b, a; t) p(a, t) \right] db \\ &\quad - p(a, t) \int \omega(a + b, a; t) db \end{aligned}$$

The first and third term on the right hand side cancel each other out, and if we rewrite the second term and substitute $b = a' - a$, we arrive at the Kramers-Moyal Expansion:

$$\begin{aligned} \frac{\partial p(a, t)}{\partial t} &= \sum_{n=1}^{\infty} \frac{(-1)^n}{n!} \left(\frac{\partial}{\partial a} \right)^n \left[\alpha_n(a, t) p(a, t) \right] \\ \alpha_n &= \int (a' - a)^n \omega(a', a; t) da' \\ &= \lim_{\Delta t \rightarrow 0} \frac{1}{\Delta t} \int (a' - a)^n P(a', t + \Delta t | a, t) da' \end{aligned}$$

where $P(a', t + \Delta t | a, t)$ denotes the conditional probability, that the system is in state a' at time $t + \Delta t$ if at time t the system was in state a . The α_n are called moments of the transition probabilities.

If $\alpha_n = 0$ for all $n \geq 3$, then the Kramers-Moyal expansion ends after the second term and the resulting equation is called Fokker-Planck equation:

$$\frac{\partial p(a, t)}{\partial t} = -\frac{\partial}{\partial a} [\alpha_1(a, t) p(a, t)] + \frac{1}{2} \frac{\partial^2}{\partial a^2} [\alpha_2(a, t) p(a, t)]$$

After formulating the Fokker-Planck equation we will apply it to the Langevin equation of the free Brownian particle (1.6) and calculate the time-dependent probability distribution of the velocity $p(v, t)$. We integrated the Langevin equation in the last section

1.1. The freely diffusing particle - from Einstein to Langevin

and obtained a solution for $v(t)$ under the assumption that the initial velocity is v_0 , see Eq. (1.9). Let's calculate the moments of the transition probabilities α_1 and α_2 :

$$\alpha_1 = \lim_{\Delta t \rightarrow 0} \frac{1}{\Delta t} \int_{-\infty}^{\infty} (v - v_0) \cdot P(v, t_0 + \Delta t | v_0, t_0) dv$$

The integral is equal to the expectation value of $(v(t_0 + \Delta t) - v_0)$ under the assumption that $v(t_0) = v_0$, hence:

$$\alpha_1 = \lim_{\Delta t \rightarrow 0} \frac{1}{\Delta t} \langle v(t_0 + \Delta t) - v(t_0) \rangle$$

Using the Eq. (1.10) and $t_0 = 0$, one obtains

$$\begin{aligned} \alpha_1 &= \lim_{\Delta t \rightarrow 0} \frac{1}{\Delta t} \cdot \left(v(0) e^{-\xi \cdot \Delta t} - v(0) \right) \\ &= -\xi v(0) \end{aligned}$$

because the right hand side of the first line equals the first derivative of $v(t)$ at $t = 0$.

For the second moment we will use the Eq. (1.12) for $\langle v(t)^2 \rangle$:

$$\begin{aligned} \alpha_2 &= \lim_{\Delta t \rightarrow 0} \frac{1}{\Delta t} \langle (v(\Delta t) - v_0)^2 \rangle \\ &= \lim_{\Delta t \rightarrow 0} \frac{1}{\Delta t} \left[v_0^2 \cdot e^{-2\xi \Delta t} + \frac{S}{\xi} \cdot \left(1 - e^{-2\xi \Delta t} \right) - 2v_0^2 e^{-\xi \Delta t} + v_0^2 \right] \\ &= -\frac{S}{\xi} \underbrace{\lim_{\Delta t \rightarrow 0} \frac{1}{\Delta t} \left(e^{-2\xi \Delta t} - 1 \right)}_{-2\xi} + v_0^2 \underbrace{\lim_{\Delta t \rightarrow 0} \frac{1}{\Delta t} \left(e^{-2\xi \Delta t} + 1 \right)}_{-2\xi} - 2v_0^2 \underbrace{\lim_{\Delta t \rightarrow 0} \frac{e^{-\xi \Delta t}}{\Delta t}}_{-\xi} \\ &= 2S \end{aligned}$$

Using de l'Hospital to calculate the last two limits. The Fokker-Planck equation for the velocity of the Brownian motion therefore reads

$$\frac{\partial p(v, t)}{\partial t} = \xi \frac{\partial}{\partial v} [v p(v, t)] + S \frac{\partial^2}{\partial v^2} p(v, t)$$

From this equation one can get the stationary solution $p_0(v)$ for $p(v, t)$ by setting $\frac{\partial p(v, t)}{\partial t} = 0$.

$$\frac{d^2}{dv^2} p_0(v) + \frac{\xi}{S} \frac{d}{dv} [v \cdot p_0(v)] = 0$$

integrating this equation leaves us with the well-known Maxwell-Boltzmann velocity distribution

$$p_0(v) = \left(\frac{\xi}{2\pi S} \right)^{1/2} \cdot e^{-\xi v^2 / 2S} \quad (1.15)$$

While the thermal fluctuations, represented by S , broadens the curve, if the temperature rises, the friction ξ sharpens the peak and counteracts the thermal fluctuations, see Fig. 1.3.

1. Brownian Motion

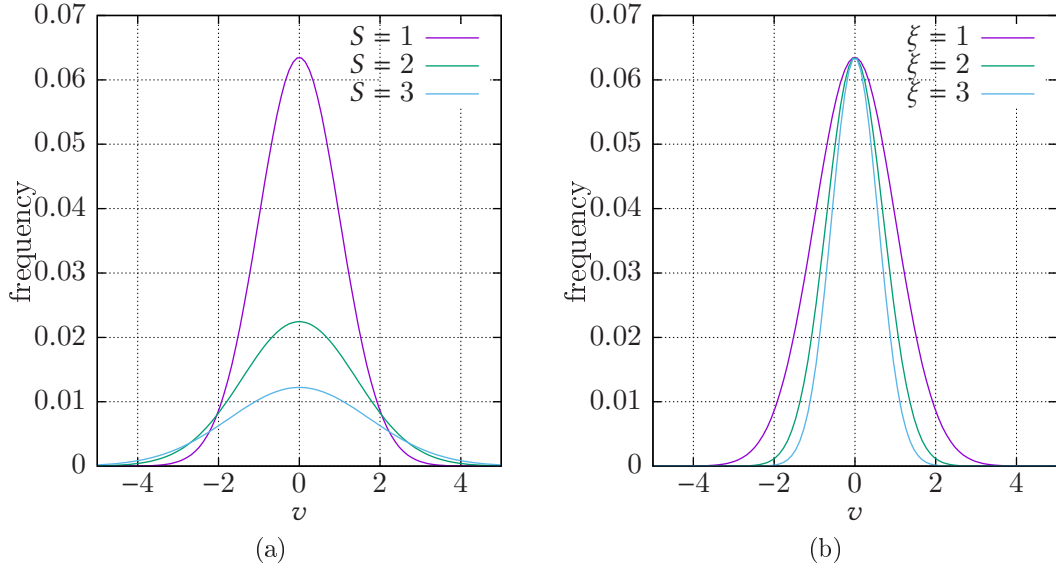


Figure 1.3.: The velocity distribution for Brownian particles following Eq. (1.15) (a) for three different values of S with $\xi = 1$ (b) for three different values of ξ with $S = 1$

1.1.4. The Wiener-Khinchin theorem

Let's denote the Fourier transform $\tilde{a}(\omega)$ of a function $a(t)$ defined as

$$\tilde{a}(\omega) = \int_{-\infty}^{\infty} a(t) e^{-i\omega t} dt$$

and the inverse Fourier transform

$$a(t) = \frac{1}{2\pi} \int_{-\infty}^{\infty} \tilde{a}(\omega) e^{i\omega t} d\omega$$

The power spectrum of the function is then defined as

$$S_a(\omega) = \langle |\tilde{a}(\omega)|^2 \rangle$$

and $S_a(\omega) d\omega$ is physically the mean intensity in the frequency interval $[\omega, \omega + d\omega]$. The theorem of Wiener and Khinchin states the connection between the autocorrelation function (ACF) $\langle a(t) a(t + \tau) \rangle$ and the spectral density $S_a(\omega)$:

$$S_a(\omega) = \int_{-\infty}^{\infty} \langle a(t) a(t + \tau) \rangle e^{-i\omega\tau} d\tau$$

$$\langle a(t) a(t + \tau) \rangle = \frac{1}{2\pi} \int_{-\infty}^{\infty} S_a(\omega) e^{i\omega\tau} d\omega$$

Now we will apply this theorem to the Langevin equation to calculate the velocity's power spectrum $\langle |\tilde{v}(\omega)|^2 \rangle$. In Fourier space the time differential can be easily rewritten

1.2. Brownian motion in a harmonic potential

as:

$$\frac{d}{dt}v(t) = \frac{d}{dt} \int \tilde{v}(\omega) e^{i\omega t} d\omega = \int i\omega \tilde{v} \cdot e^{i\omega t} d\omega$$

hence

$$\left(\frac{d\tilde{v}}{dt} \right) = i\omega \tilde{v}$$

Therefore we can rewrite the Langevin equation in Fourier space as:

$$\begin{aligned} \frac{d}{dt}v(t) &= -\xi v(t) + A(t) \\ (i\omega + \xi) \tilde{v}(\omega) &= \tilde{A}(\omega) \\ S_v(\omega) = \langle |\tilde{v}(\omega)|^2 \rangle &= \frac{\langle |\tilde{A}(\omega)|^2 \rangle}{\xi^2 + \omega^2} \end{aligned}$$

with $A(t)$ being a stochastic process, still having the properties we defined earlier in subsec. 1.1.2, namely $\langle A(t) \rangle = 0$ and $\langle A(t) A(t') \rangle = 2S \delta_{t-t'}$. Then the power spectrum of the random acceleration can be calculated using the Wiener-Khinchin theorem

$$\begin{aligned} \langle |\tilde{A}(\omega)|^2 \rangle &= \int_{-\infty}^{\infty} \langle A(t) A(t + \tau) \rangle e^{-i\omega\tau} d\tau \\ &= \int_{-\infty}^{\infty} 2S \delta(\tau) e^{-i\omega\tau} d\tau \\ &= 2S \end{aligned} \tag{1.16}$$

and therefore

$$S_v(\omega) = \frac{2S}{\xi^2 + \omega^2} \tag{1.17}$$

Using this result, we can also calculate the power spectrum of the position $S_x(\omega)$, using $\frac{d}{dt}x = v$, hence

$$i\omega \tilde{x} = \tilde{v}$$

and by squaring and averaging

$$S_x(\omega) = \langle |\tilde{x}(\omega)|^2 \rangle = \frac{1}{\omega^2} \langle |\tilde{v}|^2 \rangle = \frac{1}{\omega^2} \cdot \frac{2S}{\xi^2 + \omega^2}$$

1.2. Brownian motion in a harmonic potential

The problem of a Brownian particle in a harmonic trap will be discussed using the Langevin equation with an additional force. The potential reads $U = \frac{k_s}{2} x^2$ with k_s

1. Brownian Motion

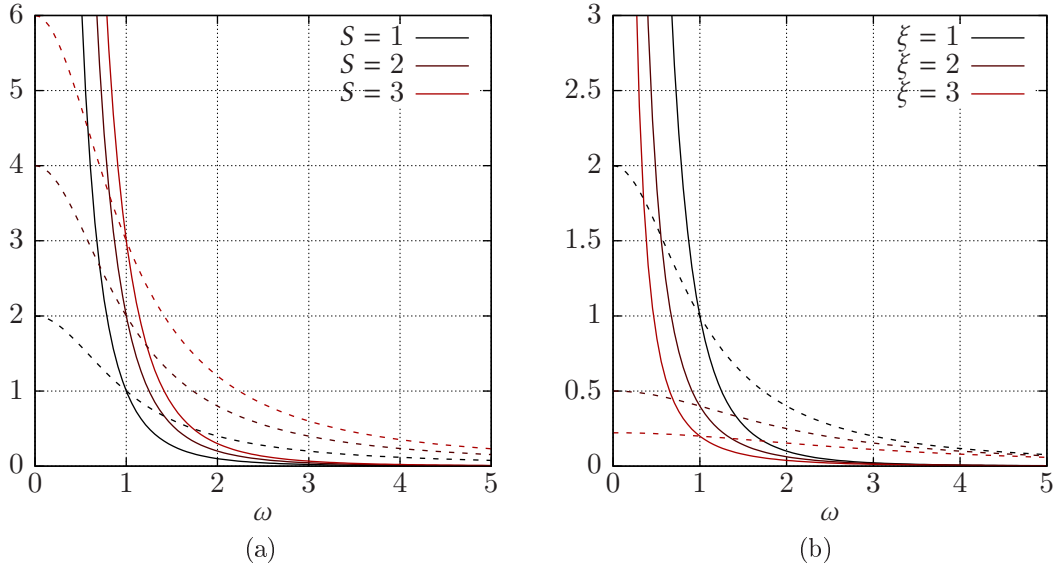


Figure 1.4.: The power spectra $S_x(\omega)$ (full) and $S_v(\omega)$ (dashed) for Brownian particles following Eq. (1.4) (a) for three different values of S with $\xi = 1$ (b) for three different values of ξ with $S = 1$

denoting the spring constant of the force $F = -\nabla U = -k_s x$. Putting it all together one arrives at the two coupled differential equations:

$$\begin{aligned} \frac{dx}{dt} &= v \\ m \frac{dv}{dt} &= -\gamma v + F_r(t) - k_s x \end{aligned}$$

For the random force $F_r(t)$ the same restrictions are still in place:

$$\begin{aligned} \langle F_r(t) \rangle &= 0 \\ \langle F_r(t) F_r(t') \rangle &= 2m^2 S \cdot \delta(t - t') \end{aligned}$$

For brevity's sake we will write the equation, using $\omega_0^2 = \frac{k_s}{m}$, $A(t) = \frac{F_r(t)}{m}$ and $\xi = \frac{\gamma}{m}$:

$$\frac{dv}{dt} = -\xi v + A(t) - \omega_0^2 x$$

The corresponding Fokker-Planck equation for the probability density $p(x, v, t)$ reads

$$\frac{\partial p}{\partial t} + v \frac{\partial p}{\partial x} - \omega_0^2 x \frac{\partial p}{\partial v} = S \frac{\partial^2 p}{\partial x^2} + \frac{\partial}{\partial v} (\xi v p)$$

This equation can be solved in the stationary limit $\frac{\partial p_0}{\partial t} = 0$:

$$p_0(x, v, t) = C \cdot e^{-\xi k_s x^2 / 2S} \cdot e^{-\xi v^2 / 2S}$$

1.2. Brownian motion in a harmonic potential

The obtained solution equals two Maxwellian distributions, one for the velocity and one for the position. The constant C can be easily calculated by requiring

$$\int_{-\infty}^{\infty} \int_{-\infty}^{\infty} p_0(x, v) dx dv = 1$$

One can calculate the autocorrelation functions for the position first and then follow up with differentiation of the obtained result to get the crosscorrelation for position and velocity and finally the autocorrelation for the velocity. To do this we will follow Coffey's "The Langevin equation" [7] by rewriting the Langevin equation for the positions

$$\frac{d^2}{dt^2}x(t) + \xi \frac{d}{dt}x(t) + \omega_0^2 x(t) = A(t)$$

Now changing to Fourier space

$$-\omega^2 \tilde{x} + i\omega \tilde{x} + \omega_0^2 \tilde{x} = \tilde{A}(\omega)$$

and calculating the power spectrum, using $S_A(\omega) = 2S$, see Eq. (1.16):

$$S_x(\omega) = \frac{2S}{(\omega_0^2 - \omega^2)^2 + \omega^2 \xi^2} \quad (1.18)$$

Note that the power spectrum of the velocity can easily be obtained using $\omega^2 S_x = S_v$.

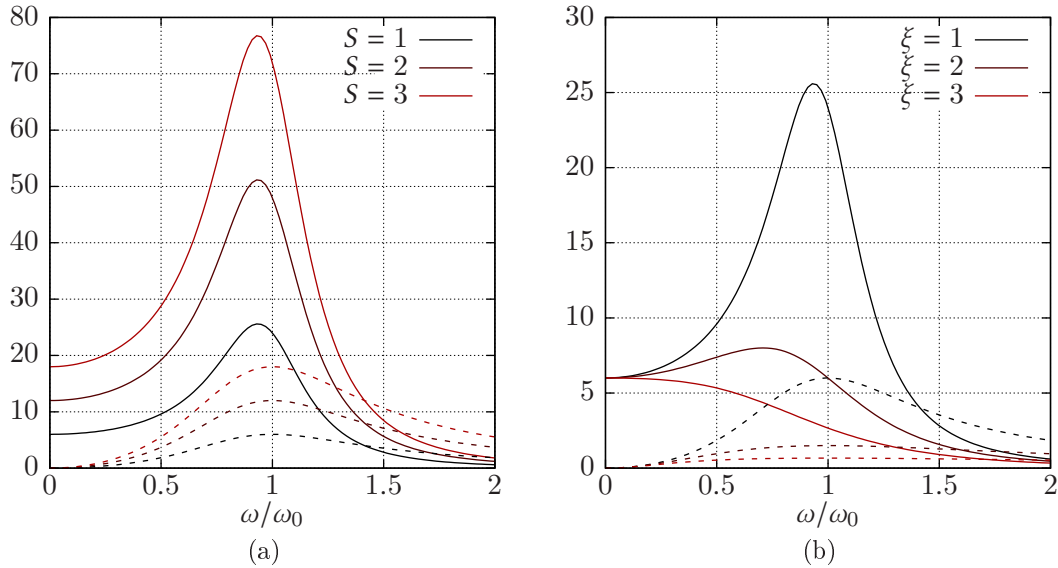


Figure 1.5.: The power spectra $S_x(\omega)$ (full) and $S_v(\omega)$ (dashed) for Brownian particles following Eq. (1.18) (a) for three different values of S with $\xi = 1$ (b) for three different values of ξ with $S = 1$

Using the Wiener-Khinchin theorem we can now obtain the autocorrelation function:

$$\langle x(t)x(t+\tau) \rangle = \frac{2S}{2\pi} \int_{-\infty}^{\infty} \frac{e^{-i\omega\tau}}{(\omega_0^2 - \omega^2)^2 + \omega^2 \xi^2} d\omega$$

1. Brownian Motion

This integral can be solved by applying the residue theorem to it. Therefore the integral should be written as contour integral in the complex plane. The residues are located at

$$\begin{aligned}\omega_0^2 - \omega^2 &= \pm i\xi\omega \\ \omega &= \pm i\frac{\xi}{2} \pm \sqrt{\omega_0^2 - \frac{\xi^2}{4}} = \pm\omega_1 \pm i\frac{\xi}{2}\end{aligned}$$

where $\omega_1^2 = \omega_0^2 - \frac{\xi^2}{4}$ denotes the natural frequency of the damped oscillator. We assume $\tau > 0$ and let $\omega = a + ib$ be a complex number, then the numerator of the fraction is $e^{y\tau - ix\tau}$ and the contour of the complex plane should be closed by a semicircle in the lower half plane. Therefore only the residues with negative complex values are needed to solve the integral $\omega = \pm\omega_1 - i\frac{\xi}{2}$. We obtain:

$$\begin{aligned}\langle x(t)x(t+\tau) \rangle &= \frac{S}{\pi} \int_{-\infty}^{\infty} \frac{e^{-i\omega\tau} d\omega}{(\omega - \omega_1 - i\xi/2)(\omega - \omega_1 + i\xi/2)(\omega + \omega_1 - i\xi/2)(\omega + \omega_1 + i\xi/2)} \\ &= -2\pi i \frac{S}{\pi} \left[\frac{e^{-i(\omega_1 - i\xi/2)\tau}}{(-i\xi)(2\omega_1 - i\xi)(2\omega_1)} + \frac{e^{-i(-\omega_1 - i\xi/2)\tau}}{(-2\omega_1 - i\xi)(-2\omega_1)(-i\xi)} \right] \\ &= \frac{2iS}{2i\omega_1\xi} e^{-\xi\tau/2} \left[\frac{(2\omega_1 + i\xi) \cdot e^{-i\omega_1\tau} + (2\omega_1 - i\xi) \cdot e^{i\omega_1\tau}}{4\omega_1^2 + \xi^2} \right]\end{aligned}$$

now taking advantage of the definition of ω_1^2 to simplify $4\omega_1^2 + \xi^2 = 4\omega_0^2$ and rearranging inside the brackets lets us use Euler's formula:

$$\begin{aligned}\langle x(t)x(t+\tau) \rangle &= \frac{S}{4\omega_0^2\omega_1\xi} e^{-\xi\tau/2} \left[2\omega_1 \cdot \underbrace{\left(e^{i\omega_1\tau} + e^{-i\omega_1\tau} \right)}_{2\cos(\omega_1\tau)} - i\xi \cdot \underbrace{\left(e^{i\omega_1\tau} - e^{-i\omega_1\tau} \right)}_{2i\sin(\omega_1\tau)} \right] = \\ &= \frac{S}{\omega_0^2\xi} e^{-\xi\tau/2} \left[\cos(\omega_1\tau) + \frac{\xi}{2\omega_1} \sin(\omega_1\tau) \right]\end{aligned}$$

We can utilise this result to calculate the missing cross-correlations and the autocorrelation of the velocity:

$$\begin{aligned}\langle x(t)v(t+\tau) \rangle &= \langle x(t) \frac{d}{d\tau} x(t) \rangle = \frac{d}{d\tau} \langle x(t)x(t+\tau) \rangle \\ &= -\frac{S}{\xi\omega_0^2} e^{-\xi\tau/2} \left[\frac{\xi^2}{4\omega_1} + \underbrace{\omega_1}_{\omega_0^2 - \xi^2/4} \right] \sin(\omega_1\tau) \\ &= -\frac{S}{\xi\omega_1} e^{-\xi\tau/2} \sin(\omega_1\tau)\end{aligned}$$

For the second cross-correlation we will use the stationarity by shifting the time axis by $-\tau$:

$$\begin{aligned}\langle v(t)x(t+\tau) \rangle &= \left\langle \frac{d}{d\tau} x(t-\tau)x(t) \right\rangle = -\frac{d}{d\tau} \langle x(t)x(t+\tau) \rangle = \\ &= \frac{S}{\xi\omega_1} e^{-\xi\tau/2} \sin(\omega_1\tau)\end{aligned}$$

The velocity auto-correlation function is therefore

$$\begin{aligned}\langle v(t)v(t+\tau) \rangle &= -\frac{d^2}{d\tau^2} \langle x(t)x(t+\tau) \rangle \\ &= \frac{S}{\xi} e^{-\xi\tau/2} \left(\cos(\omega_1\tau) - \frac{\xi}{2\omega_1} \sin(\omega_1\tau) \right)\end{aligned}$$

From this correlations one can obtain $\langle x^2 \rangle = \frac{S}{\omega_0^2 \xi} = \frac{k_B T}{m \omega_0^2}$ and the expectation value for the potential energy $\langle E_{\text{pot}} \rangle = \frac{1}{2} k_s \langle x^2 \rangle = \frac{1}{2} k_B T$, using $\omega_0^2 = \frac{k}{m}$. This result fulfills the equipartition theorem. Likewise for the kinetic energy $\langle v^2 \rangle = \frac{S}{\xi} = \frac{k_B T}{m}$, hence $\langle E_{\text{kin}} \rangle = \frac{1}{2} m \langle v^2 \rangle = \frac{1}{2} k_B T$.

1.2.1. Inactive particle in an oscillatory shear flow

Kählert and Löwen [11] studied the case of a deterministic oscillatory shearing force driving an inactive particle in a harmonic potential. They solved the case of one particle analytically and used Langevin dynamic simulations to tackle the problem of multiple particles. This case is relevant for the present work, because the active particle could be thought of as a inactive particle driven by an rotating external force. The important difference is, that the active particle's force is rotating via rotational diffusion, while the oscillatory shear force studied by Kählert and Löwen is strictly deterministic. The differences become greater when viewing multiple particles, because each active particle has it's own rotating force, while the shear force is imposed on all particles.

They first studied the problem of one particle in an oscillatory shear flow, with shear frequency Ω , imposing the force $f_{\text{shear}} = \xi \dot{s} \mathbf{y} \cos(\Omega t)$ in x -direction. Using the present work's notation, where m denotes the mass, ξ the friction and introducing the shear rate as \dot{s} , the one particle problem in a harmonic potential with trap frequency ω_0 reads

$$\dot{\chi}(t) = A(t)\chi(t) + \zeta(t)$$

where $\chi(t) = (v_x(t), v_y(t), x(t), y(t))^T$ describes the two-dimensional velocity (v_x, v_y) and position (x, y) of the particle. The vector $\zeta(t) = (f_x(t), f_y(t), 0, 0)^T/m$ describes the stochastic acceleration of the Brownian particle with

$$\langle \zeta(t) \rangle = 0, \quad \langle \zeta(t) \zeta^T(t') \rangle = D \delta(t - t')$$

where D denotes the diffusion matrix

$$D = \frac{2\xi k_B T}{m} \begin{pmatrix} 1 & 0 & 0 & 0 \\ 0 & 1 & 0 & 0 \\ 0 & 0 & 0 & 0 \\ 0 & 0 & 0 & 0 \end{pmatrix}$$

The coefficient matrix $A(t)$ is given by

$$A(t) = \begin{pmatrix} -\xi & 0 & -\omega_0^2 & \xi \dot{s} \cos(\Omega t) \\ 0 & -\xi & 0 & -\omega_0^2 \\ 1 & 0 & 0 & 0 \\ 0 & 1 & 0 & 0 \end{pmatrix}$$

1. Brownian Motion

The shear flow only affects the x -direction, therefore the equations for $v_y(t)$ and $y(t)$ are equal to the ones of an inactive particle in a harmonic trap and have been discussed in sec. 1.2.

Interestingly the solution shows for the cross moments $\langle x(t)y(t) \rangle$ and $\langle v_x(t)v_y(t) \rangle$ and the second moments $\langle x^2 \rangle$ and $\langle v_x^2 \rangle$ resonance effects for the amplitudes of these moments. The cross moments are given as

$$\begin{aligned}\langle x(t)y(t) \rangle &= \text{Wi} \left(\frac{k_B T}{m\omega_0^2} \right) A_{xy} \cos(\Omega t + \phi_{xy}) \\ \langle v_x(t)v_y(t) \rangle &= \text{Wi} \left(\frac{k_B T}{m\omega_0^2} \right) A_{v_x v_y} \cos(\Omega t + \phi_{v_x v_y})\end{aligned}$$

where $\text{Wi} = \dot{\gamma}\xi/\omega_0^2$ denotes the Weissenberg number, $\bar{\Omega} = \Omega/\omega_0$ and $\bar{\xi} = \xi/\omega_0$. The amplitudes are

$$\begin{aligned}A_{xy} &= \left[\frac{4\bar{\xi}^2 + \bar{\Omega}^2}{(\bar{\xi}^2 + \bar{\Omega}^2)[4\bar{\xi}^2\bar{\Omega}^2 + (\bar{\Omega}^2 - 4)^2]} \right]^{1/2} \\ A_{v_x v_y} &= \left[\frac{\bar{\Omega}^2}{(\bar{\xi}^2 + \bar{\Omega}^2)[4\bar{\xi}^2\bar{\Omega}^2 + (\bar{\Omega}^2 - 4)^2]} \right]^{1/2}\end{aligned}$$

and the phase angles

$$\begin{aligned}\tan \phi_{xy} &= \bar{\xi}\bar{\Omega} \left[\frac{\bar{\Omega}^2 + 4(\bar{\xi}^2 + 1)}{\bar{\Omega}^4 - 4\bar{\Omega}^2 + 4\bar{\xi}^2(\bar{\Omega}^2 - 2)} \right] \\ \tan \phi_{v_x v_y} &= \frac{\bar{\xi}}{\bar{\Omega}} \left[\frac{3\bar{\Omega}^2 - 4}{\bar{\Omega}^2 - 2\bar{\xi}^2 - 4} \right]\end{aligned}$$

And the second moments for x and v_x are given as

$$\begin{aligned}\frac{\langle x^2(t) \rangle}{k_B T/m\omega_0^2} &= 1 + \text{Wi}^2 [d_x + A_{xx} \cos(2\Omega t + \phi_{xx})] \\ \frac{\langle v_x^2(t) \rangle}{k_B T/m\omega_0^2} &= 1 + \text{Wi}^2 [d_x + A_{v_x v_y} \cos(2\Omega t + \phi_{v_x v_y})]\end{aligned}$$

The corresponding amplitudes and phase angles are quite lengthy and can be looked up in [11]. Much more enlightening are the plots of the amplitudes, phase angles and constant terms in figures 1.6 and 1.7

While the cross moments peak at $\Omega/\omega_0 = 2$ for low friction $\xi/\omega_0 \approx 10^{-2}$, the second moments show two peaks. One at $\Omega/\omega_0 = 1$ and the other at $\Omega/\omega_0 = 2$. At intermediary friction $\xi/\omega_0 \approx 10^{-1}$ the first peak becomes dominant for $\langle x^2 \rangle$.

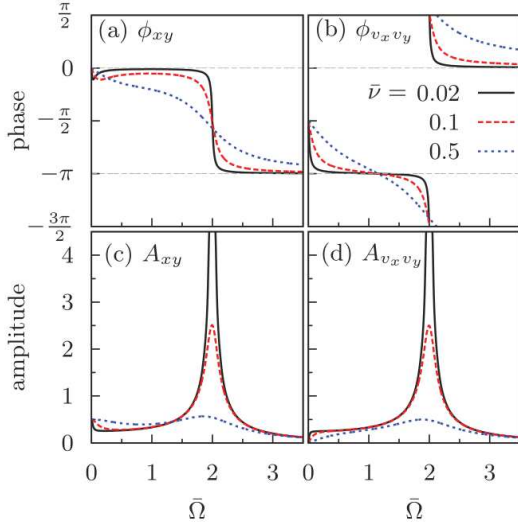


Figure 1.6.: (a) and (b) show the phase angles and (c) and (d) the Amplitudes of $\langle xy \rangle$ and $\langle v_x v_y \rangle$, Reprinted figure with permission from [11] Copyright 2018 by the American Physical Society

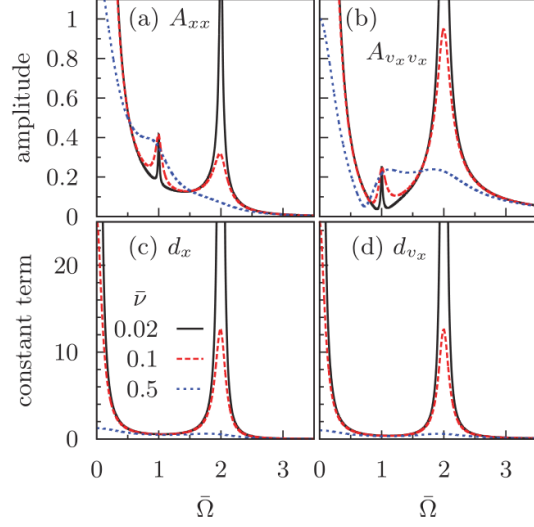


Figure 1.7.: (a) and (b) show the Amplitudes, (c) and (d) the constant terms of $\langle x^2(t) \rangle$ and $\langle v_x^2(t) \rangle$, Reprinted figure with permission from [11] Copyright 2018 by the American Physical Society

1.3. Three-dimensional case

The different components of the velocity and position in three dimensional space of the Brownian motion are independent from each other and therefore the results from above, all obtained for the one-dimensional Langevin equation, can be easily generalized to three dimensions. Because the simulations for the present thesis are done in three dimensions the important results for this case will be summarized here. The positions will be denoted as $\vec{x} = (x_1, x_2, x_3)$ and the velocities as $\vec{v} = (v_1, v_2, v_3)$.

1.3.1. Free Brownian motion

The initial position in phase space is (\vec{x}_0, \vec{v}_0) . The Langevin equation for the problem reads

$$\frac{d\vec{x}}{dt} = \vec{v} \quad \frac{d\vec{v}}{dt} = -\xi \vec{v} + \vec{A}(t)$$

with the following properties for the random acceleration $\vec{A} = (A_1, A_2, A_3)$, and $S = \xi \frac{k_B T}{m}$

$$\langle A_i(t) \rangle = 0 \quad \langle A_i(t) A_j(t') \rangle = 2S \delta_{ij} \delta(t - t')$$

Important means are $\langle \langle \cdot \rangle_{\vec{v}_0}$ denoting the mean under the assumption of $\vec{v}(0) = \vec{v}_0$:

1. Brownian Motion

$$\begin{aligned}\langle \vec{v} \rangle_{\vec{v}_0} &= \vec{v}_0 e^{-\xi t} & \langle \vec{v}^2 \rangle_{\vec{v}_0} &= \vec{v}_0^2 e^{-2\xi t} + \frac{3S}{\xi} \cdot \left(1 - e^{-2\xi t}\right) \\ \langle \vec{v}^2 \rangle &= \frac{3S}{\xi} & \langle (\vec{x} - \vec{x}_0)^2 \rangle &= \frac{6S}{\xi^3} \left(\xi t - 1 + e^{-\xi t}\right) \\ \langle E_{kin} \rangle &= \frac{3}{2} m \frac{S}{\xi} = \frac{3}{2} k_B T\end{aligned}$$

The velocity's autocorrelation reads, for $\tau \geq 0$

$$\langle \vec{v}(t) \vec{v}(t + \tau) \rangle = \frac{3S}{\xi} e^{-\xi t}$$

The Fokker-Planck equation for the probability distribution function $p(\vec{v}, t)$ reads

$$\frac{\partial p(\vec{v}, t)}{\partial t} = \xi \cdot \frac{\partial}{\partial \vec{v}} \left[\vec{v} p(\vec{v}, t) \right] + S \cdot \frac{\partial^2}{\partial \vec{v}^2} p(\vec{v}, t)$$

and the stationary solution $\partial p_0(\vec{v})/\partial t = 0$ is

$$p_0(\vec{v}) = \left(\frac{\xi}{2\pi S} \right)^{3/2} e^{-\xi \vec{v}^2 / 2S}$$

The power spectra for the position and velocity read:

$$S_{\vec{x}}(\omega) = \frac{1}{\omega^2} \cdot \frac{6S}{\xi^2 + \omega^2} \quad S_{\vec{v}}(\omega) = \frac{6S}{\xi^2 + \omega^2}$$

1.3.2. Brownian motion in a harmonic potential

The Langevin equation for the problem reads

$$\frac{d\vec{x}}{dt} = \vec{v} \quad \frac{d\vec{v}}{dt} = -\xi \vec{v} + \vec{A}(t) - \omega_0^2 \vec{x}$$

The Fokker-Planck Equation for the probability distribution $p(\vec{x}, \vec{v}, t)$ is

$$\frac{\partial p}{\partial t} + \vec{v} \frac{\partial p}{\partial \vec{x}} - \omega_0^2 \vec{x} \frac{\partial p}{\partial \vec{v}} = S \frac{\partial^2 p}{\partial \vec{x}^2} + \frac{\partial}{\partial \vec{v}} (\xi \vec{v} p)$$

The stationary solution $\partial p_0/\partial t = 0$ reads:

$$p_0(\vec{x}, \vec{v}, t) = C e^{-\xi k_s \vec{x}^2 / 2S} e^{-\xi \vec{v}^2 / 2S}$$

The auto- and cross-correlation have been obtained as - noting that ω_1 is defined via $\omega_1^2 = \omega_0^2 + \frac{\xi^2}{4}$

$$\begin{aligned}\langle \vec{x}(t) \vec{x}(t + \tau) \rangle &= \frac{3S}{\omega_0^2 \xi} e^{-\xi \tau / 2} \left[\cos(\omega_1 \tau) + \frac{\xi}{2\omega_1} \sin(\omega_1 \tau) \right] \\ \langle \vec{v}(t) \vec{x}(t + \tau) \rangle &= -\langle \vec{x}(t) \vec{v}(t + \tau) \rangle = \frac{3S}{\xi \omega_1} e^{-\xi \tau / 2} \sin(\omega_1 \tau) \\ \langle \vec{v}(t) \vec{v}(t + \tau) \rangle &= \frac{3S}{\xi} e^{-\xi \tau / 2} \left[\cos(\omega_1 \tau) - \frac{\xi}{2\omega_1} \sin(\omega_1 \tau) \right]\end{aligned}$$

1.3. Three-dimensional case

The power spectra are

$$S_{\vec{x}}(\omega) = \frac{6S}{(\omega_0^2 - \omega^2)^2 + \omega^2 \xi^2} \quad S_{\vec{v}}(\omega) = \frac{6S}{(\omega_0^2/\omega - \omega)^2 + \xi^2}$$

The means of the squares fulfill the equipartition theorem:

$$\begin{aligned} \langle \vec{x}^2 \rangle &= 3 \frac{S}{\omega_0^2 \xi} & \langle E_{pot} \rangle &= \frac{3}{2} m \frac{S}{\xi} = \frac{3}{2} k_B T \\ \langle \vec{v}^2 \rangle &= 3 \frac{S}{\xi} & \langle E_{kin} \rangle &= \frac{3}{2} m \frac{S}{\xi} = \frac{3}{2} k_B T \end{aligned}$$

2. Active Particles

2.1. Introduction

Active particles can be defined as particles undergoing Brownian motion, which can take up energy from the surrounding and convert it into a kinetic energy. This definition is broad enough to enclose motile cells, Brownian motors and artificial self-propelled particles.

There are two dominant models for active particles: the rotational diffusive and the run-and-tumble model. The present work uses only the rotational diffusive model, because it's physically closer to most artificial active particles. The run-and-tumble model is more suited for bacteria, which change their activities direction with a mean tumble rate of α . Tailleur and Cates [5] studied in which cases these two models are identical, with respect to phase separation.

2.2. Overdamped active particles

The overdamped case is insofar interesting for the present thesis, because it's the best studied case for active particles. The analytical description of the particle's motion is possible in this case, see Ref. [27], and the results of the theory will provide a first test for my simulation, as it should converge to the overdamped active particle if the friction rises. Here, I will present only the most important results for this case.

The equations of motion in the two-dimensional case read

$$\dot{x} = v_A \cos(\varphi) + \sqrt{2D_T} \zeta_x, \quad \dot{y} = v_A \sin(\varphi) + \sqrt{2D_T} \zeta_y, \quad \dot{\varphi} = \sqrt{2D_R} \zeta_\varphi$$

where v_A is the "strength" of the activity, D_T and D_R are the diffusion constants for translation and rotation, respectively, φ denotes the angle between the activity's direction and the x -axis and ζ_x , ζ_y and ζ_φ are independent white noise stochastic processes with zero mean and unit variance.

Assuming that $x(0) = x_0$, $y(0) = y_0$ and $\varphi(0) = \varphi_0$ these equations can be integrated, using $W_t^i = \int_0^t \zeta_i(t') dt'$ to denote the Wiener process, with $i = x, y, \varphi$:

$$\begin{aligned} x &= x_0 + v_A \int_0^t \cos(\varphi(t')) dt' + \sqrt{2D_T} W_t^x \\ y &= y_0 + v_A \int_0^t \sin(\varphi(t')) dt' + \sqrt{2D_T} W_t^y \\ \varphi &= \varphi_0 + \sqrt{2D_R} W_t^\varphi \end{aligned}$$

2. Active Particles

While Löwen et al. present in Ref. [27] only the equations of motion and the analytical solution to the position's average and the MSD I will use the space a master thesis grants and present the steps leading to the solution in the appendix. Taking the averages, using $\langle W_t^i \rangle = 0$ and $\langle e^{i(\varphi_0 + \sqrt{2D_R}W_t^{\varphi})} \rangle = e^{i\varphi_0} \cdot e^{-D_R t}$ (see Appendix B.1.1), one obtains, see Ref. [27],

$$\begin{aligned}\langle x - x_0 \rangle &= \frac{v_A}{D_R} \cdot \left(1 - e^{-D_R t}\right) \cdot \cos(\varphi_0) \\ \langle y - y_0 \rangle &= \frac{v_A}{D_R} \cdot \left(1 - e^{-D_R t}\right) \cdot \sin(\varphi_0) \\ \langle \varphi - \varphi_0 \rangle &= 0\end{aligned}$$

The difference to the passive particle can be seen in the expectation value for the x -component of the position. If the initial value of the activity's direction is chosen as $\varphi_0 = 0$ and therefore parallel to the positive x -axis, the particle will at first move along this direction. This movement lasts until the activity's direction is randomized enough by the rotational diffusion. Before this happens the particle moves in x -direction to a mean value of $v_A D_R^{-1}$, letting us define $\tau_R = D_R^{-1}$ as characteristic time scale for the overdamped Brownian rotational motion before rotational diffusion randomizes the direction of the activity.

The mean squared displacement can be calculated, as has been done by Löwen et al. [27], using $\langle W_t \rangle = 0$, $\langle W_t^2 \rangle = t$ and $\langle \cos(\varphi(t')) \cos(\varphi(t'')) + \sin(\varphi(t')) \sin(\varphi(t'')) \rangle = e^{-D_r(t''-t')}$ (see Appendix B.1.2):

$$\langle (x - x_0)^2 + (y - y_0)^2 \rangle = \left[4D_T + 2\frac{v_A^2}{D_R}\right] \cdot t + 2\frac{v_A^2}{D_R^2} \cdot \left(e^{-D_R t} - 1\right)$$

for long times $t \gg \tau_R$ the MSD converges to $[4D_T + 2v_A^2/D_R]t$ and is therefore steeper than the expected $4D_T t$ for an inactive particle. One could define, in an analogous way to the passive Brownian particle, an effective diffusion coefficient $D_{\text{eff}} = D_T + v_A^2/2D_R$ and for long times compare the diffusion of the active particle with the diffusion of a passive Brownian particle with a higher effective temperature

$$T_{\text{eff}} = \frac{\gamma D_{\text{eff}}}{k_B} = \frac{\gamma}{k_B} \cdot \left(D_T + v_A^2/2D_R\right)$$

This might lead to the assumption that active particles are equivalent to hotter inactive particles, but this picture only holds in simple cases, as Tailleur and Cates show in their study of active particles in external potentials [26].

Now to the velocities of the active particle. The means are

$$\langle \dot{x} \rangle = v_A e^{-D_r t} \cos(\varphi_0) \quad \langle \dot{y} \rangle = v_A e^{-D_r t} \sin(\varphi_0)$$

and the velocity's second moment $\langle \vec{v}^2 \rangle = \langle \dot{x}^2 + \dot{y}^2 \rangle$ can be calculated, using $\langle \zeta_i \rangle = 0$ and $\langle \zeta_i^2 \rangle = 1$, as

$$\begin{aligned}\langle \vec{v}^2 \rangle &= v_A^2 \langle \cos^2(\varphi(t)) \rangle + 2D_T + v_A^2 \langle \sin^2(\varphi(t)) \rangle + 2D_T \\ &= 4D_T + v_A^2\end{aligned}$$

The mean velocity reminds one of the Brownian particle's mean velocity, if they are subject to inertia. Setting $\vec{v}_0 = v_A \cdot (\cos(\varphi_0), \sin(\varphi_0))$ makes these equations identical to the ones from Ornstein and Uhlenbeck, see Eq. (1.10), where the rotational diffusion constant takes the role of the friction.

It's mathematically more complex to investigate an active particle with two rotational freedoms (φ, θ) for the direction of the particle's activity $(\sin(\theta)\cos(\varphi), \sin(\theta)\sin(\varphi), \cos(\theta))$. The MSD and the average position can be calculated using spherical harmonics like Löwen et al. did in Ref. [27]. Denoting the particles position at time t as \vec{x} and the angles defining the initial condition of the activity's direction as (φ_0, θ_0) one obtains:

$$\begin{aligned} \langle \vec{x} - \vec{x}_0 \rangle &= \frac{1}{2} \frac{v_A}{D_R} \left(1 - e^{-2D_R t} \right) \cdot \begin{pmatrix} \sin(\theta_0) \cos(\varphi_0) \\ \sin(\theta_0) \sin(\varphi_0) \\ \cos(\theta_0) \end{pmatrix} \\ \langle (\vec{x} - \vec{x}_0)^2 \rangle &= \left(6D_T + \frac{v_A^2}{D_R} \right) t + \frac{1}{2} \left(\frac{v_A}{D_R} \right)^2 \left[e^{-2D_R t} - 1 \right] \end{aligned} \quad (2.1)$$

2.3. Underdamped active particles

Underdamped active particles have been investigated, e.g. by Schweitzer et al. [21] and Schimansky-Geier et al. [17] theoretically, but these usually assumed, that the activity's direction is identical to the direction of the particle's velocity. This assumption enables one to analytically obtain the mean squared displacement, stationary velocity distribution and other statistically relevant parameters. These assumption can be extended to the model of the present paper, if the activity's rotation is slow compared to the velocity relaxation time and the activity is high compared to the particle's mean speed resulting from thermal diffusion.

2.3.1. Underdamped and freely rotating

In the present thesis the case of an underdamped active particle in three dimensions, where the activity's direction is undergoing rotational diffusion is investigated. The friction forces use Stokes' friction coefficients, for the translation $\gamma_T = 6\pi\eta R$ and for the rotation $\gamma_R = 8\pi\eta R^3$, where η is the viscosity of the medium and R the particle's radius. The activity is modeled as a force in the activity's direction \vec{a} , with $|\vec{a}| = 1$. The strength of the force is chosen in a manner that the average speed of the particle approaches a fixed value of v_A for a fixed direction, $\frac{d\vec{a}}{dt} = (0, 0, 0)$. I assume that the direction of the particle, similar to a Janus particle [4], is undergoing rotational diffusion with a diffusion coefficient $D_R = \frac{k_B T}{\gamma_R}$. The particle also experiences the translational diffusion of a passive Brownian particle with the diffusion coefficient $D_T = \frac{k_B T}{\gamma_T}$.

2. Active Particles

Accordingly, the Langevin equations read

$$\frac{d\vec{x}}{dt} = \vec{v} \quad (2.2)$$

$$m \frac{d\vec{v}}{dt} = -\gamma_T \vec{v} + \gamma_T v_A \vec{a} + \sqrt{2\gamma_T^2 D_T} \vec{\zeta}_T \quad (2.3)$$

$$\frac{d\vec{a}}{dt} = \vec{\omega} \times \vec{a} \quad (2.4)$$

$$I \frac{d\vec{\omega}}{dt} = -\gamma_R \vec{\omega} + \sqrt{2\gamma_R^2 D_R} \vec{\zeta}_R \quad (2.5)$$

where $\zeta_{R,i}$ and $\zeta_{T,i}$ are independent Gaussian processes with zero mean and unit variance and $\vec{\omega}$ denotes the angular velocity of the direction \vec{a} . The mass of the particle is m and the moment of inertia $I = \frac{2}{5}mR^2$ for a spherical particle. A similar approach has been used by Enculescu et al. [10], with the difference, that they used to model the activity with a fixed velocity, instead of a fixed acceleration. Their approach leads to an additional term of $+v_A(\vec{\omega} \times \vec{a})$ for the derivative of the translational momentum, which ensures that the particle, even if it is rotating very fast, keeps a mean speed of v_A . The equations above imply that for a fast rotating particle, the active term nearly vanishes, because the force $\gamma_T v_A \vec{a}$ changes direction faster than the velocity of the particle can, due to inertia.

The angular velocity is undergoing Brownian motion like we studied in section 1.1.2. Using these results we can write, using $\zeta_R = \frac{\gamma_R}{T}$ and $\vec{\omega}(0) = \vec{\omega}_0$:

$$\vec{\omega} = \vec{\omega}_0 e^{-\xi_R t} + e^{-\xi_R t} \int_0^t e^{\xi_R t'} \sqrt{2\xi_R^2 D_R} \vec{\zeta}_R(t') dt'$$

$$\langle \vec{\omega} \rangle = \vec{\omega}_0 e^{-\xi_R t}$$

and for the mean squared angular velocity

$$\langle \vec{\omega}^2 \rangle = \vec{\omega}_0^2 e^{-2\xi_R t} + 3\xi_R D_R \cdot \left(1 - e^{-2\xi_R t}\right)$$

The equipartition theorem for the three rotational degrees of freedom is obeyed in the long run ($t \rightarrow \infty$), if one keeps in mind that $D_R = \frac{k_B T}{I \xi_R}$ and

$$\langle E_{\text{rot}} \rangle = \frac{1}{2} I \langle \vec{\omega}^2 \rangle = \frac{3}{2} k_B T$$

The problem of describing the statistical parameters, especially the distribution and the autocorrelation function, of a unit vector's underdamped Brownian motion on a sphere has been tackled by, amongst others, Sack [19], Steele [24, 25] and Lewis et al. [12]. While Sack used the Liouville's equation and continued fractions to arrive at the complex polarization, Steele and Lewis focused on the autocorrelation function. Lewis et al. [12] derived a series to represent $\langle \vec{a}(t) \rangle$ and $\langle \vec{a}(t) \vec{a}(t+\tau) \rangle$ which is not easily extended to higher

orders. I will therefore use Steele's approximation for the autocorrelation function, which reads in the notation used in this work

$$\langle \vec{a}(t) \vec{a}(t + \tau) \rangle = \exp \left[-2 \frac{D_R}{\xi_R} \left(\xi_R \tau + e^{-\xi_R \tau} - 1 \right) \right] \quad (2.6)$$

Steele mentions that this equation is a good approximation if $\xi_R/D_R > \frac{1}{4}$, but gets worse for smaller values. In case of a small friction - $\xi_R/D_R < \frac{1}{4}$ - one can expect, the the unit vector should oscillate and this should be seen in the ACF. But Steele's approximation is positive and decreasing monotonously for all times, independent of the choice of ξ_R/D_R .

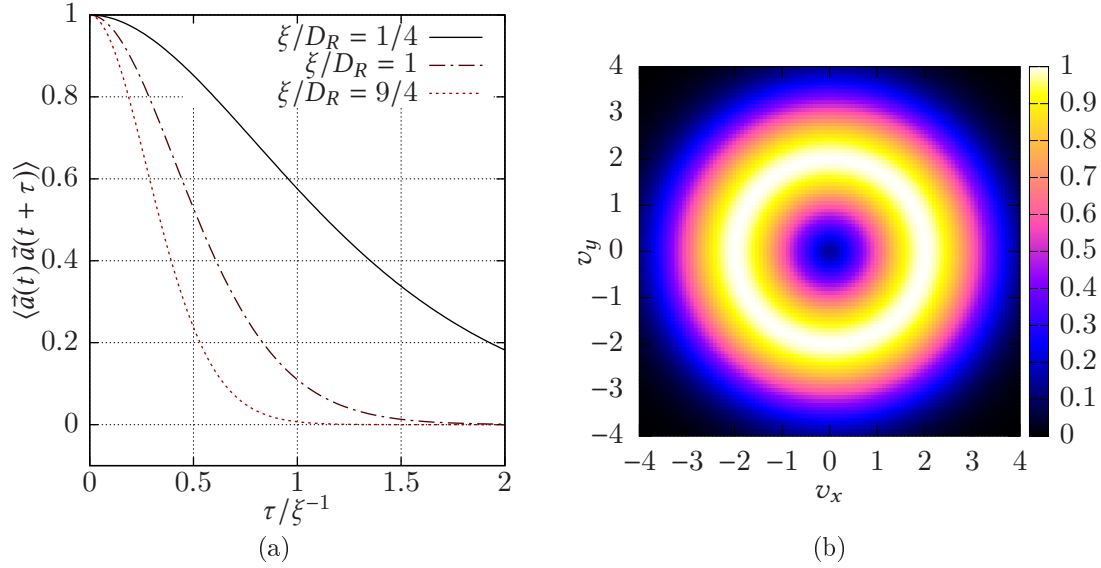


Figure 2.1.: (a) Steele's approximation for the ACF of a unit vector undergoing Brownian motion for different values of ratios of ξ_R/D_R . (b) Non-normalized velocity distribution $P_0(\vec{v})$ at $v_z = 0$, for $v_A = 2$ and $\xi_T D_T = 1$.

If the characteristic rotation time $\langle |\vec{\omega}| \rangle^{-1} = \sqrt{\pi I/8 k_B T}$ of the particle¹ is smaller than the velocity's memory ξ_T^{-1} and the activity's strength v_A is high compared to the thermal fluctuations $\sqrt{k_B T/m}$ then the velocity of the particle will be mostly parallel to the activity's direction. This is similar to the case described by Schimansky-Geier et al. [17] as "Active Brownian particles with velocity-dependent friction". The equation then reads

$$\frac{d\vec{v}}{dt} = -\xi_T \vec{v} \left(1 - \frac{v_A}{|\vec{v}|} \right) + \sqrt{2\xi_T^2 D_T} \vec{\zeta}_T \quad (2.7)$$

The first term is positive, if the particle has a speed smaller than v_A and therefore pumps energy into the system. If the speed is higher than v_A then the friction term dissipates

¹In the case of no friction, this expression is equal to the mean rotation time. For frictions bigger than zero the mean rotation time will be bigger than $\langle |\vec{\omega}| \rangle^{-1}$. Lewis et al. defined in Ref. [12] $\tau_1 = \sqrt{I/k_B T}$ as mean thermal angular period

2. Active Particles

energy. Modeling the active force in this formulation as a friction was first done by Schienbein and Gruler in 1993 [20]. The stationary velocity distribution for Eq. (2.7) reads

$$P_0(\vec{v}) = N e^{-(|\vec{v}| - v_A)^2 / (2\xi_T D_T)}$$

and can be seen in Fig. 2.1b. In three dimensions this distribution looks like a spherical shell, with the maximum at $|\vec{v}| = v_A$.

2.4. Active particles in a harmonic potential

2.4.1. Overdamped case

Overdamped active Brownian particles in a radially symmetric trapping potential have been studied analytically and via simulation by Pototsky and Stark [16]. Besides studying the case of a single particle, they applied the dynamic density functional theory (DDFT) of interacting active particles to calculate a stationary radial distribution function for multiple particles. Important for the present work is their solution for a single particle in 2D traps, because the simulation should mimic their results in the case of high friction.

They start at the overdamped equations

$$\dot{\vec{x}} = -\mu\nabla U + v_A \vec{a} + \vec{\xi}(t), \quad \dot{\vec{a}} = \vec{\eta}(t) \times \vec{a}$$

where \vec{x} is the particles position, the unit vector \vec{a} the activity's direction, $U(\vec{x})$ the trapping potential, μ the mobility, v_A the activity and $\vec{\xi}(t)$ and $\vec{\eta}(t)$ represent translational and rotational noise, respectively. These random terms fulfill $\langle \vec{\xi}(t) \vec{\xi}(t') \rangle = 2\mu k_B T \delta(t - t')$ and $\langle \vec{\eta}(t) \vec{\eta}(t') \rangle = 2D_r \delta(t - t')$.

They solve the Smoluchowski equation for this problem to calculate the probability density $\rho(\vec{x}, \vec{a}, t)$ and arrive at partial differential equations for the effective probability flux, which are not generally integrable. Only for small and large rotational diffusion coefficients D_r is the equation solvable. For convenience let's define the Peclet number $Pe = (d v_A) / (\mu k_B T)$, with d being the diameter of the particle. The Peclet number is measure for how much influence the activity of the particle has, compared to the thermal fluctuations.

In the case of small rotational diffusion the activity's direction \vec{a} is nearly constant, as far as the potential U is concerned. Therefore the activity and the trapping potential's force can be written as the force originating from an effective potential U_{eff} . This shifts the minimum of the potential from $|\vec{r}_0| = 0$ to the one obeying the condition $\frac{dU_{\text{eff}}(r)}{dr}|_{r=r_0} = Pe$. The particle will behave as an inactive Brownian particle in the effective potential. The distribution along a radius approximated to the zeroth order of D_r is obtained as

$$\rho_s^{(0)}(r) = 2\pi C e^{-U(r)} I_0(Pe r) \quad (2.8)$$

where $I_0(x)$ is the modified Bessel function of the first kind. The shape of the distribution function $\rho^{(0)}(r)$ is highly dependent on the Peclet number. For small values of Pe translational diffusion prevails and the particle stays near the origin. For large values

2.4. Active particles in a harmonic potential

the center of the effective potential shifts far enough to get a maximum of $\rho(r)$ at $r_0 > 0$. The transition is located at the critical Peclet number $Pe^{(c)} = \sqrt{2U''(0)}$. The distribution along a radius for strong trapping can be seen in Fig. 2.2 (a).

In the limit of large rotational diffusivity the distribution function along a radius changes to a bell shape with maximum at $r = 0$. They find that there is for each Peclet number a specific value of D_r to provoke the change in shape of the distribution function. If the typical rotation time $\frac{\pi^2}{D_r}$ of the particle is much smaller than the run-up time of the potential $\tau_r = \left[\frac{\partial^2 U(r)}{\partial r^2} \Big|_{r=r_0} \right]^{-1}$ then a bell-shaped distribution around $r = 0$ is to be expected.

Pototsky and Stark simulated the case of one particle in the harmonic potential and could verify their analytical results for the radial distribution function with respect to the rotational diffusion coefficient and to the strength activity. As one can see in Fig. 2.2 (b) the mean radius of the particle increases monotonically with decreasing D_r , up to a value obeying the equation $\frac{dU(r)}{dr} \Big|_{r=r_0} = Pe$.

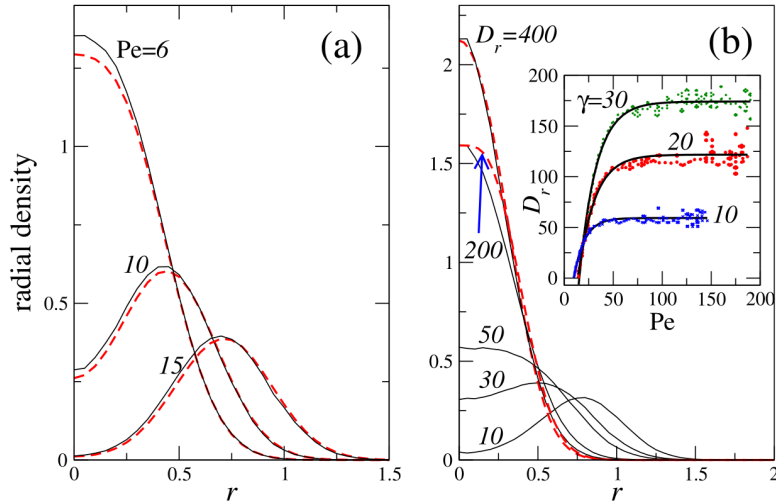


Figure 2.2.: (a) The density along a radius for slow rotational diffusivity at different Peclet numbers. The full lines represent the numerical solution of the Langevin equations, the dashed lines Eq. (2.8) (b) Transition from fast to slow rotational diffusivity at fixed Peclet number $Pe=20$. From [16]

2.4.2. Underdamped and freely rotating

The equation (2.3) is changed by adding the external force $\vec{f}_{\text{pot}} = -k_s \vec{x}$, where k_s denotes the spring constant of the potential and reads

$$m \frac{d\vec{v}}{dt} = -\gamma_T \vec{v} + \gamma_T v_A \vec{a} - k_s \vec{x} + \sqrt{2\gamma_T^2 D_T} \vec{\zeta}_T$$

2. Active Particles

The trap frequency of the potential is $\omega_0 = \sqrt{\frac{k_s}{m}}$ and we will use $\xi_T = \frac{\gamma_T}{m}$ where convenient. I will take a similar approach to Pototsky and Stark [16], discussed in a previous subsection 2.4.1, splitting the problem in the slow rotation and the fast rotation of the activity's direction.

The problem looks similar to the one studied by Kählerlert and Löwen [11], with the acceleration imposed by the activity $\xi_T v_A \vec{a}(t)$ playing the part of the shear flow $\xi_T \dot{s} y \cos(\Omega t)$. The main difference, making the analytical description far more complicated, is the stochastic direction $\vec{a}(t)$ of the acceleration. Nonetheless one can expect resonance effects, if the mean rotation frequency of the activity's direction equals the oscillation frequency ω_0 .

2.4.2.1. Slow rotation

If the characteristic time of the particle's rotation $\tau_R = \langle |\vec{\omega}| \rangle^{-1}$ is large compared to the run-up-time of the potential $\frac{2}{\omega_0}$ and the value of $\gamma_T v_A$ is small enough, then the activity's force $f_a(t) = \gamma_T v_A \vec{a}(t)$ is nearly constant for the time-scale of the oscillation $\frac{1}{\omega_0}$. Therefore the particle will be subject to an effective force $\vec{f}_{\text{eff}} = \gamma_T v_A \vec{a} - k_s \vec{x}$. This force can be rewritten as $\vec{f}_{\text{eff}} = -k_s \left(\vec{x} - \frac{\gamma_T v_A}{k_s} \vec{a} \right)$. This is the force of an harmonic potential with the minimum at $\frac{\gamma_T v_A}{k_s} \vec{a}$. As long as \vec{a} doesn't change the particle will oscillate around this new minimum, like an inactive particle, following the equation:

$$\dot{\vec{v}} = -\xi_T \vec{v} + \frac{1}{m} \vec{f}_{\text{eff}}(\vec{x}) + \sqrt{2\xi_T^2 D_T} \vec{\zeta}_T$$

We can treat this equation, like the one for the Brownian particle in sec. 1.2. To derive the potential energy, we will use the Fourier transform and the Wiener-Khinchin-theorem, assuming \vec{a} as constant. Writing $\omega_0^2 = \frac{k_s}{m}$, $r_0 = \frac{\gamma_T v_A}{k_s}$ for brevity's sake:

$$\left[(-\omega^2 + \omega_0^2)^2 + \xi_T^2 \omega^2 \right] \cdot \tilde{\vec{x}}^2 = \left(\omega_0^2 r_0 \vec{a} \delta(\omega) + \sqrt{2\xi_T^2 D_T} \cdot \tilde{\vec{\zeta}}_T \right)^2 \quad (2.9)$$

Taking the average on both sides, keeping in mind that ζ_i has zero mean, therefore $\tilde{\zeta}_i$ too, and with the above definition a power spectrum of $S_\zeta = 1$ we obtain the position's power spectrum $S_{\vec{x}}$. Using the Wiener-Khinchin-theorem leads to the auto-correlation function

$$\langle \vec{x}(t) \vec{x}(t + \tau) \rangle = r_0^2 + 3 \cdot \frac{\xi_T D_T}{\omega_0^2} \cdot e^{-\xi_T \tau / 2} \cdot \left[\cos(\omega_1 \tau) + \frac{\xi_T}{2\omega_1} \sin(\omega_1 \tau) \right] \quad (2.10)$$

where $\omega_1^2 = \omega_0^2 - \frac{\xi_T^2}{4}$. For $\tau = 0$ we obtain

$$\langle \vec{x}^2(t) \rangle = r_0^2 + 3 \cdot \frac{\xi_T D_T}{\omega_0^2} \quad (2.11)$$

and for the potential energy

$$\langle E_{\text{pot}} \rangle = \frac{m\omega_0^2}{2} \langle \vec{x}^2(t) \rangle = \frac{m\omega_0^2}{2} r_0^2 + \frac{3}{2} \gamma_T D_T$$

using $D_T = \frac{k_B T}{\gamma_T}$ and r_0 from above:

$$\langle E_{\text{pot}} \rangle = \frac{\gamma_T^2 v_A^2}{2k_s} + \frac{3}{2} k_B T \quad (2.12)$$

The kinetic energy would be, for quasi-static \vec{a} , only as big as the stochastic term allows: $\langle E_{\text{kin}} \rangle = \frac{3}{2} k_B T$. We obtain the autocorrelation function of the velocity by taking the second negative derivative of the position's autocorrelation function:

$$\langle \vec{v}(t) \vec{v}(t + \tau) \rangle = 3\xi_T D_T e^{-\xi_T \tau / 2} \left[\cos(\omega_1 \tau) - \frac{\xi_T}{2\omega_1} \sin(\omega_1 \tau) \right] \quad (2.13)$$

this is exactly the autocorrelation for the inactive particle, as expected.

The energies stop following the equipartition theorem for slow rotation and active particles. For quasi-static \vec{a} the kinetic energy will be equal to the inactive particle $\frac{3}{2} k_B T$. It's easy to see in Eq. (2.12) that the potential energy is the sum of an inactive part and an active part.

In the long run the activity's direction \vec{a} should be equi-distributed over the unit sphere. Slow changes, as assumed above with $\tau_R \gg \frac{2}{\omega_0}$ and $v_0 \omega_0 \gg \gamma_T v_A$, will result in slow changes of the minimum and the particle has time to follow accordingly. In the equilibrium state ($t \rightarrow \infty$) the probability distribution is radial symmetric. The maxima of the distribution should be found at the circle with radius $r_0 = \frac{\gamma_T v_A}{k_s}$, for $r_0 \gg l_0$.

The distribution of the position $\rho(\vec{x})$ should be proportional to $e^{-\beta U_{\text{eff}}(\vec{x})}$ and therefore

$$\rho(\vec{x}) = C \cdot e^{-U_{\text{eff}}(\vec{x})}$$

The effective potential reads $U_{\text{eff}} = \frac{k_s}{2} (\vec{x} - r_0 \vec{a})^2$. Simplifying and using $\vec{x}^2 = r^2$ and denoting the angle between \vec{a} and \vec{x} as ψ : $U_{\text{eff}} = \frac{k_s}{2} r^2 - k_s r_0 r \cos(\psi) + \frac{k_s}{2} r_0^2$. The distribution then reads

$$\tilde{\rho}(r, \psi) = C_1 \cdot e^{-k_s r^2 / 2 + k_s r_0 r \cos(\psi)}$$

absorbing the constant term of the potential into the constant C_1 . To obtain the distribution along a radius, we will need to integrate over ψ . This approach is very similar to the one Pototsky and Stark [16] used, and yields

$$\rho(r) = 2\pi C e^{-k_s r^2 / 2} I_0(\gamma_T v_A r)$$

where C can be calculated using the normalization $\int_0^\infty \rho(r) dr = 1$, and $I_0(x)$ denotes the modified Bessel function of the first kind.

The velocities for a slow rotating particle should stay Gaussian distributed. The exact treatment of the distribution's second moment follows in the next subsection.

2. Active Particles

2.4.2.2. Rotation period near oscillation period

Pototsky and Stark [16] found in their study of the overdamped active particle in a harmonic potential only a transition from the state of the fast rotation to the slow rotation. In contrast to this paper I expect to find resonant behaviour of the particle for the underdamped case, like Kählert et al. [11] did for a deterministic force.

This expectation can be justified as follows: The activity is pumping additional energy into the system, which is dissipated through (translational) friction. The amount of energy per unit time that can be absorbed by the system is highly dependent on the frequency of the activity. While Kählert et al. used an external force with a single frequency, the frequency spectrum of the stochastic activity is continuous. It can be analyzed by examining the power spectrum of the activity's direction.

The total absorbed energy per unit time P_{abs} is then, see e.g. Chandler's "Introduction to modern statistical mechanics" [6] chapter 8, proportional to

$$P_{\text{abs}} \propto \int \omega^2 S_x^i(\omega) S_f(\omega) d\omega \quad (2.14)$$

where S_x^i denotes the power spectrum of the position of the unperturbed, inactive particle, S_f the power spectrum of the force disturbing the system, consisting of the random thermal fluctuations and the activity, and ω the frequency.

The power spectrum of the inactive particle has been calculated in sec. 1.3.2 as

$$S_x^i = \frac{6 \xi_T^2 D_T}{(\omega_0^2 - \omega^2)^2 + \omega^2 \xi_T^2}$$

The perturbation's power spectrum is defined as

$$S_f(\omega) = \left\langle \left| \int e^{i\omega t} [v_A \xi_T \vec{a}(t) + \sqrt{2\xi_T^2 D_T} \vec{\zeta}_T(t)] dt \right|^2 \right\rangle$$

Because the activity and the random thermal fluctuations are independent, the power spectrum of the total force is essentially the sum of the power spectrum of the thermal fluctuation, which is known from subsec. 1.1.4, and the power spectrum of the activity's force:

$$S_{\text{active}}(\omega) = \left\langle \left| \int e^{i\omega t} v_A \xi_T \vec{a}(t) dt \right|^2 \right\rangle = v_A^2 \xi_T^2 \cdot \left\langle \left| \int e^{i\omega t} \vec{a}(t) dt \right|^2 \right\rangle$$

The last expression is simply the power spectrum of the activity's direction $S_{\vec{a}}$ and can be calculated via the Wiener-Khinchin theorem if the autocorrelation function $\langle \vec{a}(t) \vec{a}(t + \tau) \rangle$ is known. Using the autocorrelation function, see Eq. 2.6:

$$S_{\vec{a}}(\omega) = \int e^{-i\omega\tau} \langle \vec{a}(t) \vec{a}(t + \tau) \rangle d\tau \quad (2.15)$$

$$= \int \exp \left\{ -2 \frac{D_R}{\xi_R} \left[\left(1 + i \frac{\omega}{2D_R}\right) \xi_R \tau + e^{-\xi_R \tau} - 1 \right] \right\} d\tau \quad (2.16)$$

2.4. Active particles in a harmonic potential

Now we can rewrite Eq. (2.14) as

$$P_{\text{abs}} = C \cdot \int_{-\infty}^{\infty} \omega^2 S_{\vec{x}}^i(\omega) \cdot (6\xi_T^2 D_T + v_A^2 \xi_T^2 S_{\vec{a}}(\omega)) d\omega \quad (2.17)$$

To calculate C , let's compare the integral above with the power that should be dissipated by the friction term of the Langevin equation in the case of an inactive particle. The work the friction force $-\gamma \vec{v}$ performs is simply $-\gamma \vec{v} \cdot d\vec{x}$. The corresponding power, being work per unit time, is therefore $-\gamma \vec{v} \cdot \frac{d\vec{x}}{dt}$. This means that the mean dissipated power for an inactive particle is:

$$P_{\text{dis}} = -\gamma \langle \vec{v}^2 \rangle = -3\gamma m k_B T$$

Then C can be calculated requiring stationarity $P_{\text{dis}} + P_{\text{abs}} = 0$ with $v_A = 0$, as

$$C = \frac{m^2}{k_B T} \cdot \frac{1}{12\pi}$$

For an active particle we can write

$$P_{\text{dis}} = -\gamma \frac{2}{m} \langle E_{\text{kin}} \rangle$$

$$P_{\text{abs}} + P_{\text{dis}} = 0$$

$$C v_A^2 \xi_T^2 \int \omega^2 S_{\vec{x}}^i(\omega) S_{\vec{a}}(\omega) d\omega + C 6 \xi_T^2 D_T \int \omega^2 S_{\vec{x}}^i(\omega) d\omega - 2\xi_T \langle E_{\text{kin}} \rangle = 0$$

The second term should evaluate to the case of the inactive particle with $2\xi_T \langle E_{\text{kin,passive}} \rangle = 3\xi_T k_B T$

$$\langle E_{\text{kin}} \rangle = \frac{m^2}{k_B T} \frac{\xi_T v_A^2}{24\pi} \int_{-\infty}^{\infty} \omega^2 S_{\vec{x}}^i(\omega) S_{\vec{a}}(\omega) d\omega + \frac{3}{2} k_B T$$

Because the integral in the last equation is independent from the activity v_A , the kinetic energy and the second moment of the velocity distribution are always going to rise quadratically with respect to v_A . It's not so simple for the friction ξ_T , because $S_{\vec{x}}$ and $S_{\vec{a}}$ both change with respect to ξ and the integral is not analytically solvable.

The integrals (2.17) and (2.16) can be solved numerically, to discuss the expected absorbed power, see Fig. 2.3.

Now to the potential energy and the second moment of the position $\langle \vec{x}^2 \rangle$. In the subsec. 2.4.2.1 concerning the slow rotating particle, we calculated $\langle \vec{x}^2 \rangle$ via Fourier transformation of the Langevin equation. Furthermore we assumed that the activity's direction \vec{a} is constant and therefore $\vec{a} = \vec{a} \delta(\omega)$. Let's now drop the last assumption and rewrite Eq. (2.9):

$$\left[(-\omega^2 + \omega_0^2)^2 + \xi_T^2 \omega^2 \right] \cdot \vec{x}^2 = \left(\xi_T v_A \vec{a} + \sqrt{2\xi_T^2 D_T} \vec{\zeta} \right)^2 \quad (2.18)$$

One can now write for the power spectrum of the position, using that $\langle \vec{\zeta} \rangle = 0$, $\langle |\vec{\zeta}_T|^2 \rangle = 3$ and that $\vec{\zeta}_T$ and \vec{a} are mutually independent:

$$S_{\vec{x}}(\omega) = \frac{\xi_T^2 v_A^2 S_{\vec{a}}(\omega)}{(-\omega^2 + \omega_0^2)^2 + \xi_T^2 \omega^2} + \frac{6\xi_T^2 D_T}{(-\omega^2 + \omega_0^2)^2 + \xi_T^2 \omega^2}$$

2. Active Particles

The second term is equal to the position's power spectrum of an inactive particle, splitting the total power spectrum into an active and an inactive part. The ACF of the position then reads, using the Wiener-Khinchin theorem

$$\begin{aligned}\langle \vec{x}(t) \vec{x}(t + \tau) \rangle &= \frac{1}{2\pi} \int_{-\infty}^{\infty} S_{\vec{x}}(\omega) e^{i\omega\tau} d\omega \\ \langle \vec{x}(t) \vec{x}(t + \tau) \rangle &= \frac{1}{2\pi} \int_{-\infty}^{\infty} \frac{\xi_T^2 v_A^2 S_{\vec{a}}(\omega) e^{i\omega\tau}}{(-\omega^2 + \omega_0^2)^2 + \xi_T^2 \omega^2} d\omega + \langle \vec{x}(t) \vec{x}(t + \tau) \rangle_{\text{inactive}}\end{aligned}$$

This can be further simplified by using the power spectrum of the inactive particle $S_{\vec{x}}^i$

$$\langle \vec{x}(t) \vec{x}(t + \tau) \rangle = \frac{\gamma_T v_A^2}{12\pi k_B T} \int_{-\infty}^{\infty} S_{\vec{x}}^i(\omega) S_{\vec{a}}(\omega) e^{i\omega\tau} d\omega + \langle \vec{x}(t) \vec{x}(t + \tau) \rangle_{\text{inactive}}$$

To obtain the potential energy, we are only interested in $\langle \vec{x}^2 \rangle$, setting $\tau = 0$ and using $\langle \vec{x}^2 \rangle_{\text{inactive}} = 3 \frac{k_B T}{\omega_0^2 m}$:

$$\langle \vec{x}^2 \rangle = \frac{\gamma_T v_A^2}{12\pi k_B T} \int_{-\infty}^{\infty} S_{\vec{x}}^i(\omega) S_{\vec{a}}(\omega) d\omega + 3 \frac{k_B T}{\omega_0^2 m}$$

The potential energy reads

$$\langle E_{\text{pot}} \rangle = \frac{k_s \gamma_T v_A^2}{24\pi k_B T} \int_{-\infty}^{\infty} S_{\vec{x}}^i(\omega) S_{\vec{a}}(\omega) d\omega + \frac{3}{2} k_B T \quad (2.19)$$

This calculation can also be done for the velocity. The power spectrum of the velocity is easily obtained by $S_{\vec{v}} = \omega^2 S_{\vec{x}}$. Following the train of thought from above, one arrives at

$$\langle \vec{v}^2 \rangle = \frac{\gamma_T v_A^2}{12\pi k_B T} \int_{-\infty}^{\infty} \omega^2 S_{\vec{x}}^i(\omega) S_{\vec{a}}(\omega) d\omega + 3 \frac{k_B T}{m}$$

and for the kinetic energy

$$\langle E_{\text{kin}} \rangle = \frac{m \gamma_T v_A^2}{24\pi k_B T} \int_{-\infty}^{\infty} \omega^2 S_{\vec{x}}^i(\omega) S_{\vec{a}}(\omega) d\omega + \frac{3}{2} k_B T \quad (2.20)$$

which is exactly the same result - notice, that $m \xi_T = \gamma_T$ - as obtained above using the absorbed power of the harmonic oscillator. Note that these derivations are independent of the way $\vec{a}(t)$ is obtained.

The kinetic and potential energy have been determined by numerically calculating the integrals in eqs. (2.19) and (2.20) and plotted in Fig. 2.3. The potential energy transitions for high friction from the slow rotating case of (see Eq. (2.12) above) to the fast rotating case. If the friction decreases, the potential energy can show a peak at intermediate rotation frequencies.

The kinetic energy will always have a peak with respect to the rotational frequency, and the value of the frequency is depending on ξ_T . One can see, that the lower the viscosity

2.4. Active particles in a harmonic potential

the nearer is the peak of the kinetic energy to $\langle |\vec{\omega}| \rangle / \omega_0 = 1$. If the mean rotation time of the particle is near to the frequency of the harmonic trap the absorbed power should be at a maximum and therefore the kinetic energy too. The exact value of $\langle |\vec{\omega}| \rangle$ for the maximum is not easy to find via the numerical solution, because the slope is quite flat over a wide range of values. For $\xi_T / \omega_0 = 0.5$ it seems that the maximum is indeed at a $\langle |\vec{\omega}| \rangle$ higher than the natural oscillation frequency, see Fig. 2.3b, and at $\xi_T / \omega_0 = 0.25$ the maximum is definitely nearer to $\langle |\vec{\omega}| \rangle = \omega_0$. Because the absolute value of the active force depends on the activity's strength v_A and the friction ξ_T the maximum value of the absorbed power decreases with decreasing friction. If one would keep the active force constant over different values of ξ_T by defining $v_A = \frac{1}{\xi_T}$ the maximum value of the absorbed power would rise with decreasing friction ξ_T . One can also see that for fast rotations the equipartition theorem seems to be obeyed again.

2.4.2.3. Fast rotation

If the rotation is fast with respect to the oscillation period, then the active force will appear as random, equi-distributed force to the potential. The force exerted by the activity will sum up to zero, over one period of oscillation and therefore the behaviour of the particle shouldn't differ from a passive particle. There will be occurrences, when the preferred direction will change slower, then the particle will get a boost in that direction. This should be equivalent to a stochastic force, like we introduced for the Brownian motion. Added to the Brownian Motion the particle already performs, it should look like a Brownian motion in a heat bath with a higher temperature. Therefore the positions and velocities should stay Gaussian distributed, but with $\langle \vec{x}^2 \rangle$ and $\langle \vec{v}^2 \rangle$ rising with respect to the activity v_A .

For the frequencies where $S_x^i \gg 0$ one can assume that the power spectrum of the activity's direction is nearly constant $S_{\vec{a}}(\omega) = S_{\vec{a}}(0)$, see Fig. 2.4.

Using the derivation from before, we can state that

$$\langle E_{\text{kin}} \rangle = \frac{m^2}{k_B T} \frac{\xi_T v_A^2}{24\pi} S_{\vec{a}}(0) \int_{-\infty}^{\infty} \omega^2 S_x^i(\omega) d\omega + \frac{3}{2} k_B T$$

integration yields

$$\begin{aligned} \langle E_{\text{kin}} \rangle &= \frac{m^2}{k_B T} \frac{\xi_T v_A^2}{24\pi} S_{\vec{a}}(0) 3\pi \frac{k_B T}{m} + \frac{3}{2} k_B T \\ &= \frac{\gamma_T v_A^2}{8} S_{\vec{a}}(0) + \frac{3}{2} k_B T \end{aligned}$$

2. Active Particles

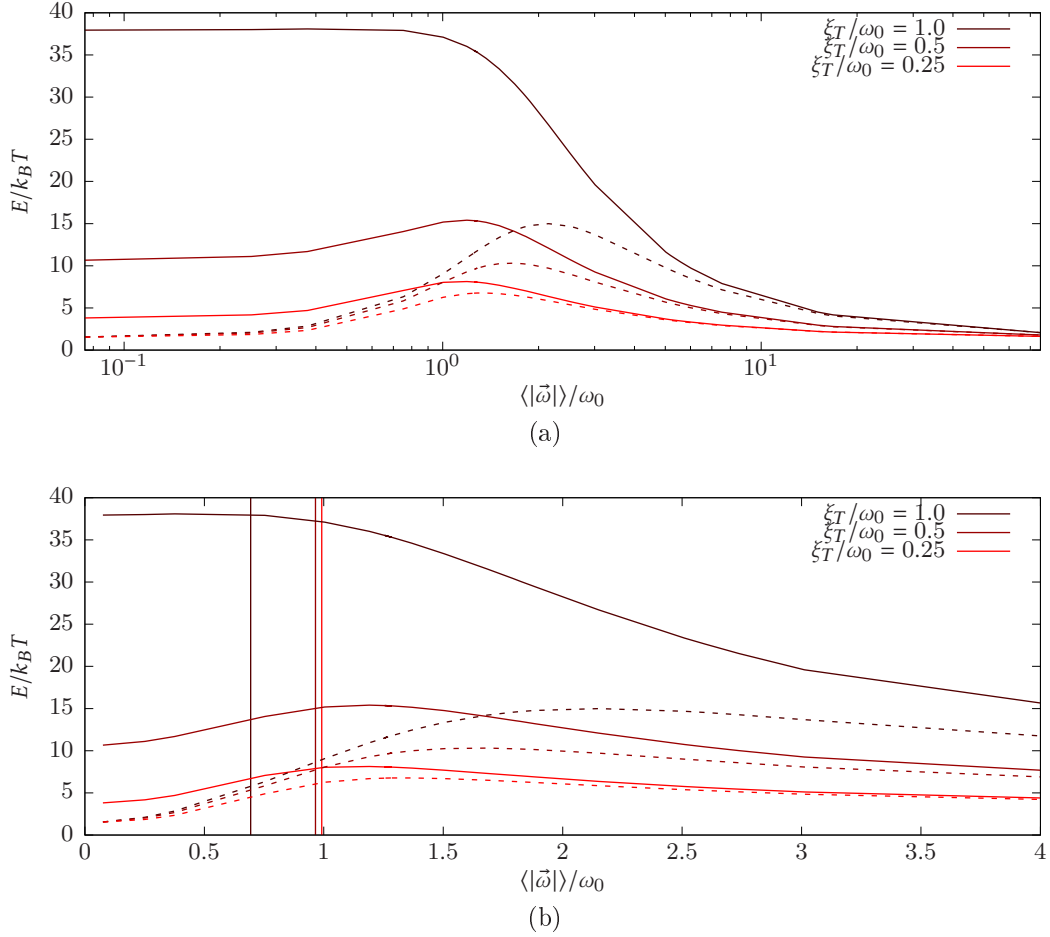


Figure 2.3.: Numerical solutions of the integral in Eq. (2.20) for the potential energy (full) and Eq. (2.19) for the kinetic energy (dashed) for different values of the translational friction ξ_T/ω_0 with respect to the rotational diffusion $\langle|\vec{\omega}|\rangle/\omega_0$. The natural oscillation frequency $\omega_1 = \sqrt{\omega_0^2 - \xi^2/4}$ is highlighted as a vertical line in the bottom graph, for each of the solutions. The activity's strength was fixed at $v_A/\sqrt{k_B T/m} = 8$

2.4. Active particles in a harmonic potential

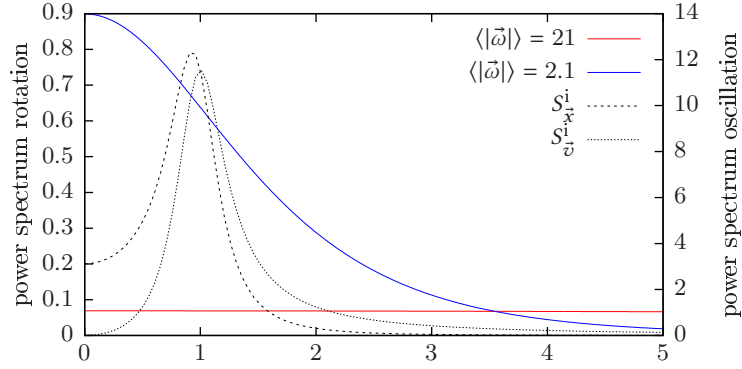


Figure 2.4.: The power spectra for the inactive particle in a harmonic potential $S_{\vec{x}}^i$ and $S_{\vec{v}}^i$ and the power spectra obtained by integrating Steele's approximation for two different mean rotational frequencies $\langle |\vec{\omega}| \rangle$ with $\xi_T = 0.5$, $\omega_0 = 1$, $m = 1$. One can clearly see that the power spectrum for the fast rotating particle ($\langle |\vec{\omega}| \rangle = 21$) is nearly constant where $S_{\vec{x}}^i \gg 0$.

And the potential energy can be written as

$$\begin{aligned}
 \langle E_{\text{pot}} \rangle &= \frac{k_s \gamma_T v_A^2}{24\pi k_B T} S_{\vec{a}}(0) \int_{-\infty}^{\infty} S_{\vec{x}}^i(\omega) d\omega + \frac{3}{2} k_B T \\
 &= \frac{k_s \gamma_T v_A^2}{24\pi k_B T} S_{\vec{a}}(0) \cdot 3 \frac{k_B T}{m\omega_0^2} + \frac{3}{2} k_B T \\
 &= \frac{\gamma_T v_A^2}{8} S_{\vec{a}}(0) + \frac{3}{2} k_B T
 \end{aligned}$$

which is identical to the kinetic energy, as proposed.

For the effective temperature one obtains:

$$T_{\text{eff}} = T + \frac{\gamma_T v_A^2}{12 k_B} S_{\vec{a}}(0)$$

3. Simulations

In this chapter I will present the algorithms used for the Langevin dynamics simulations. While the translational motion uses the unmodified OVRVO algorithm by Sivak, Chodera and Crooks [23], the algorithm had to be modified for the rotational motion.

The rotational motion has been studied via simulation using two different dynamics. The first dynamic views the source of the activity as moving on the surface of the particle, using the tangential velocity \vec{w} and the position of the source \vec{a} - I shall call it moving source (MS)-dynamics, while the sphere's coordinate system doesn't rotate. For small rotational friction this leads to movement of the source on great circles on the sphere. The second algorithm for rotational motion uses the angular velocity $\vec{\omega}$ and the activity's direction \vec{a} , as we discussed in the previous chapter, this dynamics will be called rotating sphere (RS)-dynamics, while the source stays fixed in the sphere's coordinate system.

Subsequently the results of the simulations will be compared with the theoretical work from the previous chapter.

3.1. The algorithms

3.1.1. Moving source-dynamics

For the translation and the rotation of the particle I used the OVRVO algorithm by Sivak, Chodera and Crooks [23]. The dynamics of the rotating unit vector are obtained imagining the source of the activity is moving on the surface of the sphere, therefore the algorithm had to be adjusted for the constraint of the rotation, namely the activity's direction \vec{a} should stay a unit vector and the tangential velocity \vec{w} should stay perpendicular to the direction, i. e. $\vec{a} \cdot \vec{w} = 0$. The continuous equations read, using the tangential velocity instead of the angular velocity:

$$\frac{d\vec{a}}{dt} = \vec{w} \quad (3.1)$$

$$I \frac{d\vec{w}}{dt} = -\gamma_R \vec{w} + \sqrt{2\gamma_R^2 D_R} \vec{\zeta}_R \quad (3.2)$$

where $\gamma_R = 8\pi\eta R^3$ is the Stokes' friction coefficient, with η the viscosity and R the particles radius. I is the sphere's momentum of inertia and $D_R = \frac{k_B T}{\gamma_R}$ is the rotational diffusion coefficient. The moments of the random process $\vec{\zeta}_R$ are defined as $\langle \zeta_{R,i} \rangle = 0$ and $\langle \zeta_{R,i}(t) \zeta_{R,j}(t') \rangle = \delta_{ij} \delta(t - t')$ for $i, j = 1, 2, 3$, δ_{ij} being the Kronecker-delta and $\delta(t - t')$ the delta distribution. Defining $\xi_R := \frac{\gamma_R}{I}$, the second equation can be written as:

$$\frac{d\vec{w}}{dt} = -\xi_R \vec{w} + \sqrt{2\xi_R^2 D_R} \vec{\zeta}_R$$

3. Simulations

To take one time step from n to $n + 1$ of the size Δt the algorithm of Sivak and Chodera for the set of equations (3.1) and (3.2) reads:

$$\begin{aligned}\vec{w}\left(n + \frac{1}{2}\right) &= \sqrt{c} \vec{w}(n) + \sqrt{(1-c)\xi_R D_R} \vec{\zeta}\left(n + \frac{1}{2}\right) \\ \vec{a}\left(n + 1\right) &= \vec{a}(n) + b \cdot \Delta t \cdot \vec{w}\left(n + \frac{1}{2}\right) \\ \vec{w}\left(n + 1\right) &= \sqrt{c} \vec{w}\left(n + \frac{1}{2}\right) + \sqrt{(1-c)\xi_R D_R} \vec{\zeta}(n)\end{aligned}$$

where $c = \exp(-\xi_R \Delta t)$ and ζ_i are independent normally distributed random variables with a mean of zero and a variance of one and $b = \sqrt{\frac{2}{\xi_R \Delta t} \tanh\left(\frac{\xi_R \Delta t}{2}\right)}$. These equations do not ensure, that \vec{a} stays on the unit sphere $|\vec{a}| = 1$ and that the tangential velocity is perpendicular to \vec{a} .

One has therefore to introduce a constraint $\Theta(\vec{a}_n)$, where $\vec{a}_n = \vec{a}(n)$. Because the constraint should keep the position \vec{a}_n on a sphere of radius R it reads $\Theta(\vec{a}_n) = \vec{a}_n^2 - R^2$ and therefore $\vec{\nabla}\Theta(\vec{a}_n) = 2\vec{a}_n$. The equations have to be rewritten to:

$$\begin{aligned}\vec{w}_{n+\frac{1}{2}} &= -\sqrt{c} \vec{w}_n + \sqrt{(1-c)\xi_R D_R} \vec{\zeta}_{n+\frac{1}{2}} - \lambda_1 \vec{\nabla}\Theta(\vec{x}_n) \\ \vec{a}_{n+1} &= \vec{a}_n + b \Delta t \cdot \vec{w}_{n+\frac{1}{2}} \\ \vec{w}_{n+1} &= -\sqrt{c} \vec{w}_{n+\frac{1}{2}} + \sqrt{(1-c)\xi_R D_R} \cdot \vec{\zeta} - \lambda_2 \vec{\nabla}\Theta(\vec{x}_{n+1})\end{aligned}$$

The Langragian multipliers λ_1 and λ_2 have to be chosen in a way that $\Theta(\vec{a}_{n+1}) = 0$ and $\vec{w}_{n+1} \cdot \vec{\nabla}\Theta(\vec{a}_{n+1}) = 0 \iff \vec{w}_{n+1} \cdot \vec{a}_{n+1} = 0$.

$$\begin{aligned}\vec{a}_{n+1} &= \vec{a}_n + b \Delta t \left(-\sqrt{c} \vec{w}_n + \sqrt{(1-c)\xi_R D_R} \vec{\zeta}_{n+\frac{1}{2}} - \lambda_1 2\vec{a}_n \right) \\ \vec{a}_{n+1} &= -2b \Delta t \lambda_1 \vec{a}_n + \underbrace{\vec{a}_n + b \Delta t \left(-\sqrt{c} \vec{w}_n + \sqrt{(1-c)\xi_R D_R} \vec{\zeta}_{n+\frac{1}{2}} \right)}_{=: \vec{C}_n}\end{aligned}\tag{3.3}$$

Now let's make sure that the vector stays on the sphere $\Theta(\vec{a}_{n+1}) = 0$:

$$\begin{aligned}\vec{a}_{n+1}^2 - R^2 &= 0 \\ (-2b \Delta t \lambda_1 \vec{a}_n + \vec{C}_n)^2 - R^2 &= 0 \\ \vec{C}_n^2 - 4b \Delta t \lambda_1 \vec{C}_n \vec{a}_n + 4b^2 \Delta t^2 \lambda_1^2 \vec{a}_n^2 - R^2 &= 0 \\ (4b^2 \Delta t^2 \vec{a}_n^2) \lambda_1^2 - (4b \Delta t \vec{C}_n \vec{a}_n) \lambda_1 + \vec{C}_n^2 - R^2 &= 0\end{aligned}$$

using $\Theta(\vec{a}_n) = 0$, therefore $\vec{a}_n^2 = R^2$:

$$4b^2 \Delta t^2 R^2 \lambda_1^2 - 4b \Delta t \vec{C}_n \vec{a}_n \lambda_1 + \vec{C}_n^2 - R^2 = 0$$

solving the quadratic equation yields

$$\lambda_1^\pm = \frac{4b \Delta t \vec{C}_n \vec{a}_n \pm \sqrt{(4b \Delta t \vec{C}_n \vec{a}_n)^2 - 4(4b^2 \Delta t^2 R^2 (\vec{C}_n^2 - R^2))}}{8b^2 \Delta t^2 R^2}$$

$$\lambda_1^\pm = \frac{\vec{C}_n \vec{a}_n \pm \sqrt{(\vec{C}_n \vec{a}_n)^2 - R^2 (\vec{C}_n^2 - R^2)}}{2b \Delta t R^2}$$

Only one of the two solutions can be the Langrangian multiplier that is needed. For small time steps the value of \vec{a}_{n+1} should be approximately \vec{a}_n . Using this criteria lets one choose the right solution for λ_1 .

For small Δt the vector \vec{C}_n is approximately \vec{a}_n . For the positive sign, using $\vec{a}_n^2 = R^2$:

$$\lambda_1^+ \approx \frac{R^2 + \sqrt{R^4 - R^2(R^2 - R^2)}}{2b \Delta t R^2} = \frac{2R^2}{2b \Delta t R^2} = \frac{1}{b \cdot \Delta t}$$

putting this in (3.3) yields

$$\vec{a}_{n+1} \approx \vec{a}_n - 2b \Delta t \frac{1}{b \Delta t} \vec{a}_n = -\vec{a}_n$$

The positive sign puts one on the other side of the sphere.

And looking at the negative sign, using $\vec{a}_n^2 = R^2$:

$$\lambda_1^- \approx \frac{R^2 - \sqrt{R^4 - R^2(R^2 - R^2)}}{2b \Delta t R^2} = 0$$

$$\vec{a}_{n+1} \approx \vec{a}_n - 0 = \vec{a}_n$$

keeps \vec{a}_n nearly constant for very small Δt . The first Langrangian multiplier therefore reads:

$$\lambda_1 = \frac{\vec{C}_n \vec{a}_n - \sqrt{(\vec{C}_n \vec{a}_n)^2 - R^2 (\vec{C}_n^2 - R^2)}}{2b \Delta t R^2}$$

Let's look at λ_2 . This parameter should make sure, that the velocity stays perpendicular to the sphere. And therefore

$$\vec{w}_{n+1} \vec{\nabla} \Theta(\vec{a}_{n+1}) = 0$$

$$\vec{w}_{n+1} 2\vec{a}_{n+1} = 0$$

$$\vec{w}_{n+1} \vec{a}_{n+1} = 0$$

$$\left[-\sqrt{c} \vec{w}_{n+\frac{1}{2}} + \sqrt{(1-c)\xi_R D_R} \vec{\zeta}_{n+1} - \lambda_2 \vec{\nabla} \Theta(\vec{a}_{n+1}) \right] \vec{a}_{n+1} = 0$$

yielding

$$\lambda_2 = \frac{\left(\sqrt{c} \vec{v}_{n+\frac{1}{2}} - \sqrt{(1-c)\xi_R D_R} \vec{\zeta}_{n+1} \right) \vec{a}_{n+1}}{2 \vec{a}_{n+1}^2}$$

3. Simulations

and using $\vec{a}_{n+1}^2 = R^2$

$$\lambda_2 = \frac{\left(\sqrt{c} \vec{w}_{n+\frac{1}{2}} - \sqrt{(1-c)\xi_R D_R} \vec{\zeta}_{n+1} \right) \vec{a}_{n+1}}{2 R^2}$$

as long as $R > 0$ this fraction exists.

The algorithm reads:

1. Draw three random numbers $\vec{\zeta}_{n+\frac{1}{2}} = (\zeta_{n+\frac{1}{2},1}, \zeta_{n+\frac{1}{2},2}, \zeta_{n+\frac{1}{2},3})$ from a Gaussian distribution with $\langle \zeta_{n+\frac{1}{2},i} \rangle = 0$ and $\langle \zeta_{n+\frac{1}{2},i}^2 \rangle = 1$ for $i = 1, 2, 3$.
2. Compute $\vec{C}_n = \vec{a}_n + b \Delta t \left(-\sqrt{c} \vec{w}_n + \sqrt{(1-c)\xi_R D_R} \vec{\zeta}_{n+\frac{1}{2}} \right)$
3. Determine the Langrange multiplier λ_1

$$\lambda_1 = \frac{\vec{C}_n \vec{a}_n - \sqrt{(\vec{C}_n \vec{a}_n)^2 - R^2(\vec{C}_n^2 - R^2)}}{2b \Delta t R^2}$$

4. Calculate the intermediate velocity

$$\vec{w}_{n+\frac{1}{2}} = -\sqrt{c} \vec{w}_n + \sqrt{(1-c)\xi_R D_R} \vec{\zeta}_{n+\frac{1}{2}} - \lambda_1 \vec{\nabla} \Theta(\vec{a}_n)$$

5. Get the new positions

$$\vec{a}_{n+1} = \vec{a}_n + b \Delta t \vec{w}_{n+\frac{1}{2}}$$

6. Draw three new random numbers $\vec{\zeta}_n$ following the instructions in 1.
7. Determine the Langrange multiplier λ_2

$$\lambda_2 = \frac{\left(\sqrt{c} \vec{w}_{n+\frac{1}{2}} - \sqrt{(1-c)\xi_R D_R} \vec{\zeta}_{n+1} \right) \vec{a}_{n+1}}{2 \vec{a}_{n+1}^2}$$

8. Get the new velocity

$$\vec{w}_{n+1} = -\sqrt{c} \vec{w}_{n+\frac{1}{2}} + \sqrt{(1-c)\xi_R D_R} \vec{\zeta}_{n+1} - \lambda_2 \vec{\nabla} \Theta(\vec{a}_{n+1})$$

3.1.2. Rotating sphere-dynamics

The rotating sphere-dynamics uses a rotating sphere, with the unit vector fixed in the sphere's coordinate system. Using the Eq. 2.4 and 2.5 and defining $\xi_R := \frac{YR}{I}$ leads to the following set of equations:

$$\begin{aligned}\frac{d\vec{a}}{dt} &= \vec{\omega} \\ \vec{\omega} &= \vec{\omega} \times \vec{a} \\ \frac{d\vec{\omega}}{dt} &= -\xi_R \vec{\omega} + \sqrt{2\xi_R^2 D_R} \vec{\zeta}_R\end{aligned}$$

To take one time step from n to $n+1$ of the size Δt the OVRVO algorithm reads

$$\begin{aligned}\vec{\omega}\left(n + \frac{1}{2}\right) &= \sqrt{c} \vec{\omega}(n) + \sqrt{(1-c)\xi_R D_R} \vec{\zeta}\left(n + \frac{1}{2}\right) \\ \vec{a}(n+1) &= \vec{a}(n) + b \cdot \Delta t \cdot \left[\vec{\omega}\left(n + \frac{1}{2}\right) \times \vec{a}(n) \right] \\ \vec{\omega}(n+1) &= \sqrt{c} \vec{\omega}\left(n + \frac{1}{2}\right) + \sqrt{(1-c)\xi_R D_R} \vec{\zeta}(n)\end{aligned}$$

where $c = \exp(-\xi_R \Delta t)$ and ζ_i are independent normally distributed random variables with a mean of zero and a variance of one and $b = \sqrt{\frac{2}{\xi_R \Delta t} \tanh\left(\frac{\xi_R \Delta t}{2}\right)}$. This algorithm doesn't ensure that \vec{a} stays on the unit sphere, because we are not taking infinite small steps which are perpendicular to \vec{a} .

For each step we take, we want the direction \vec{a} to move a length of $b \cdot \Delta t \cdot \left| \vec{\omega}\left(n + \frac{1}{2}\right) \times \vec{a}(n) \right|$ on the unit sphere's surface. This length is equal to the angle the direction should change, because the sphere has a radius of one. To change the direction accordingly, we simply add an vector of length $\tan\left(b \cdot \Delta t \cdot \left| \vec{\omega}\left(n + \frac{1}{2}\right) \times \vec{a}(n) \right|\right)$ and direction $\vec{\omega}\left(n + \frac{1}{2}\right) \times \vec{a}(n)$ to $\vec{a}(n)$ and normalize the result, see Fig. 3.1.

The algorithm then reads:

$$\begin{aligned}(1) \quad \vec{\omega}\left(n + \frac{1}{2}\right) &= \sqrt{c} \vec{\omega}(n) + \sqrt{(1-c)\xi_R D_R} \vec{\zeta}\left(n + \frac{1}{2}\right) \\ (2) \quad \vec{w}\left(n + \frac{1}{2}\right) &= \tan\left(b \cdot \Delta t \cdot \left| \vec{\omega}\left(n + \frac{1}{2}\right) \times \vec{a}(n) \right|\right) \frac{\vec{\omega}\left(n + \frac{1}{2}\right) \times \vec{a}(n)}{\left| \vec{\omega}\left(n + \frac{1}{2}\right) \times \vec{a}(n) \right|} \\ (3) \quad \vec{a}(n+1) &= \frac{\vec{a}(n) + \vec{w}\left(n + \frac{1}{2}\right)}{\left| \vec{a}(n) + \vec{w}\left(n + \frac{1}{2}\right) \right|} \\ (4) \quad \vec{\omega}(n+1) &= \sqrt{c} \vec{\omega}\left(n + \frac{1}{2}\right) + \sqrt{(1-c)\xi_R D_R} \vec{\zeta}(n)\end{aligned}$$

3. Simulations

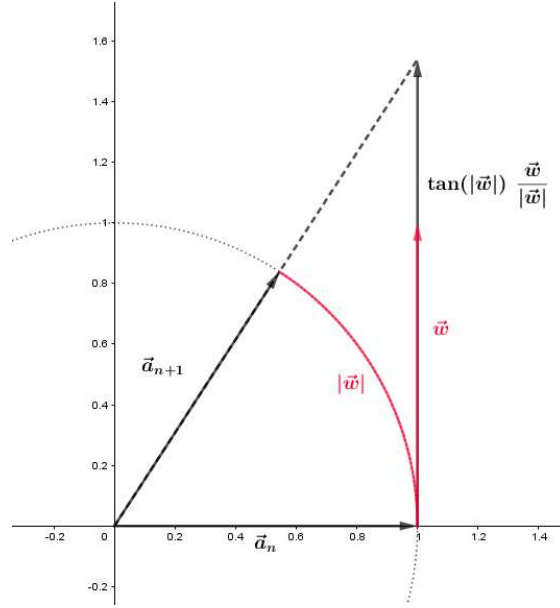


Figure 3.1.: Sketch of the changes made to the algorithm, where $\vec{w} = b \cdot \Delta t \cdot \left[\vec{\omega} \left(n + \frac{1}{2} \right) \times \vec{a}(n) \right]$, $\vec{a}_n = \vec{a}(n)$ and $\vec{a}_{n+1} = \vec{a}(n+1)$.

3.1.3. Translational motion

Like in the last section the algorithm by Sivak, Chodera and Crooks [23] will be used to simulate the free translational motion, governed by the Langevin equation

$$\begin{aligned} \frac{d\vec{x}}{dt} &= \vec{v} \\ \frac{d\vec{v}}{dt} &= -\xi_T \vec{v} + \xi_T v_A \cdot \vec{a} + \sqrt{2\xi_T^2 D_T} \cdot \vec{\zeta}_T \end{aligned}$$

where $\xi_T = \frac{\gamma_T}{m}$ and $\xi_T v_A \vec{a}$ will be treated as an external force. For the particle in the harmonic potential $U = \frac{k_s}{2} \vec{x}^2$ an additional external force will be added $\vec{f}_{\text{pot}} = -k_s \vec{x}$,

where k_s denotes the spring constant. The algorithm then reads

$$\begin{aligned}
 (1) \quad \vec{v}\left(n + \frac{1}{4}\right) &= \sqrt{c} \vec{v}(n) + \sqrt{(1-c)\xi_T D_T} \zeta\left(n + \frac{1}{2}\right) \\
 (2) \quad \vec{v}\left(n + \frac{1}{2}\right) &= v\left(n + \frac{1}{2}\right) + \frac{b\Delta t}{2} \frac{\vec{f}(n)}{m} \\
 (3) \quad \vec{x}(n+1) &= \vec{x}(n) + b\Delta t v\left(n + \frac{1}{2}\right) \\
 (4) \quad \vec{v}\left(n + \frac{3}{4}\right) &= \vec{v}\left(n + \frac{1}{2}\right) + \frac{b\Delta t}{2} \frac{\vec{f}(n+1)}{m} \\
 (5) \quad \vec{v}(n+1) &= \sqrt{c} \vec{v}\left(n + \frac{3}{4}\right) + \sqrt{(1-c)\xi_T D_R} \vec{\zeta}(n+1)
 \end{aligned}$$

where $c = \exp(-\xi_T \Delta t)$, $\vec{f}(n)$ denotes force acting on the particle at timestep n and the components of $\vec{\zeta}(n)$ and $\vec{\zeta}(n + \frac{1}{2})$ are independent, normally distributed random variables with zero mean and a variance of one. The time-step rescaling is done by multiplication with $b = \sqrt{\frac{2}{\xi_T \Delta t} \tanh\left(\frac{\xi_R \Delta t}{2}\right)}$.

Because the activity is treated as an external force, the rotational step from $\vec{a}(n)$ to $\vec{a}(n+1)$ has to take place between steps (3) and (4) of the translational algorithm.

3.2. Underdamped active particles

The units used for this section are $E_0 = k_B T_0 = 1$, the particle's radius l_0 as unit length, the particle's mass m_0 as unit mass, $v_0 = \sqrt{E_0/m_0}$ and $t_0 = l_0/v_0$.

As discussed in subsec. 2.4.2.2 the power spectrum of the rotation will be analyzed and compared with Steele's approximation Eq. (2.6). As can be seen in Fig. 3.2 the approximation holds for $\langle |\vec{\omega}| \rangle \approx \omega_0$ and smaller $\langle |\vec{\omega}| \rangle$ for both rotational dynamics, but deviates for higher rotation frequencies. Unsurprisingly Steele's approximation holds far longer for the RS-dynamics. The approximations also deviates if the friction gets lower. The ACF of the MS-dynamics arrives at negative values for fast rotations and low friction, implying that the activity's direction moves in average at least a fourth of the great circle, before rotational diffusion randomizes the direction. In contrast the ACF of the RS-dynamics arrives near zero and rises again for fast rotation and low friction, because the activity's direction only moves on great circles if it's perpendicular to the angular velocity. The activity's direction is therefore more likely to arrive at values near the starting value, than at angles bigger than $\pi/4$.

Because the interesting part of our analysis lies in this range of the rotational frequency, I still expect the resonance phenomenon, despite the deviations from Steele's approximation.

For the overdamped active particle the mean squared displacement could be solved analytically, see Eq. (2.1). For small frictions $\xi_T, \xi_R \ll 1$ the rotational diffusion constant

3. Simulations

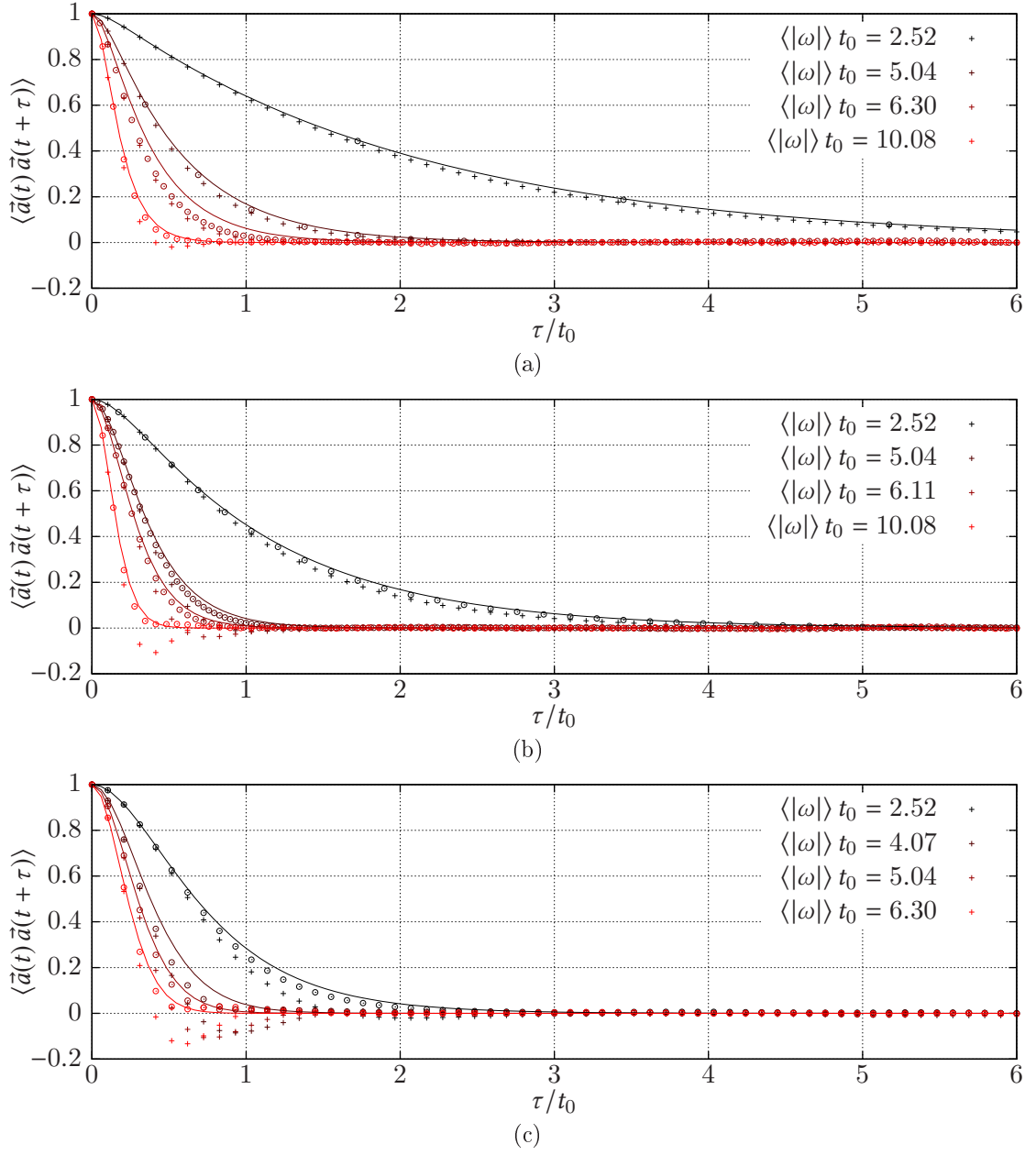


Figure 3.2.: Autocorrelation functions for the activity's direction $\vec{a}(t)$ (crosses for the MS-dynamics, circles for the RS-dynamics) and Steele's approximation (line) Eq. (2.6) for decreasing friction from (a) $\xi_T t_0 = 4.5$, (b) $\xi_T t_0 = 1.5$ to (c) $\xi_T t_0 = 0.75$

3.2. Underdamped active particles

increases and the formula reads in the limit $D_R \gg v_A^2$

$$\langle (\vec{x} - \vec{x}_0)^2 \rangle = 6D_T t$$

In Fig. 3.3 one can see that the overdamped formula arrives at a linear function for small frictions. The simulation shows for such small frictions, that - like for an inactive particle - the particle's MSD looks ballistic for small times.

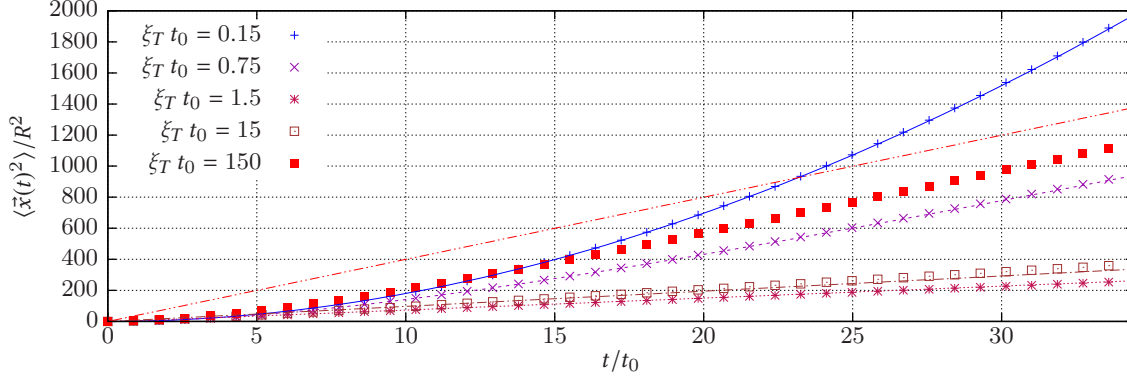


Figure 3.3.: The mean squared displacement as function of time for various frictions ξ_T (rotational: $\xi_R = \frac{10}{3}\xi_T$). Simulated values are represented as dots, the lines represent MSD for the overdamped limit, see Eq. (2.1).

Let's take a look at the velocity distribution function. In Fig. 3.4 one can see, that the distributions are crater-like, if the activity is high enough. In 3D the distribution then looks like a spherical shell, with the maximum of the distribution at $\sqrt{v_x^2 + v_y^2 + v_z^2} \leq v_A$. The higher the particle's mean rotation time is with respect to ξ_T^{-1} , i.e. if $D_R \ll \xi_T$, the nearer the mean speed of the particle will get to v_A . In Fig. 3.4 one can see, that the maximum of the distribution is considerably smaller than v_A with $\xi_T/D_R = 3$.

3. Simulations

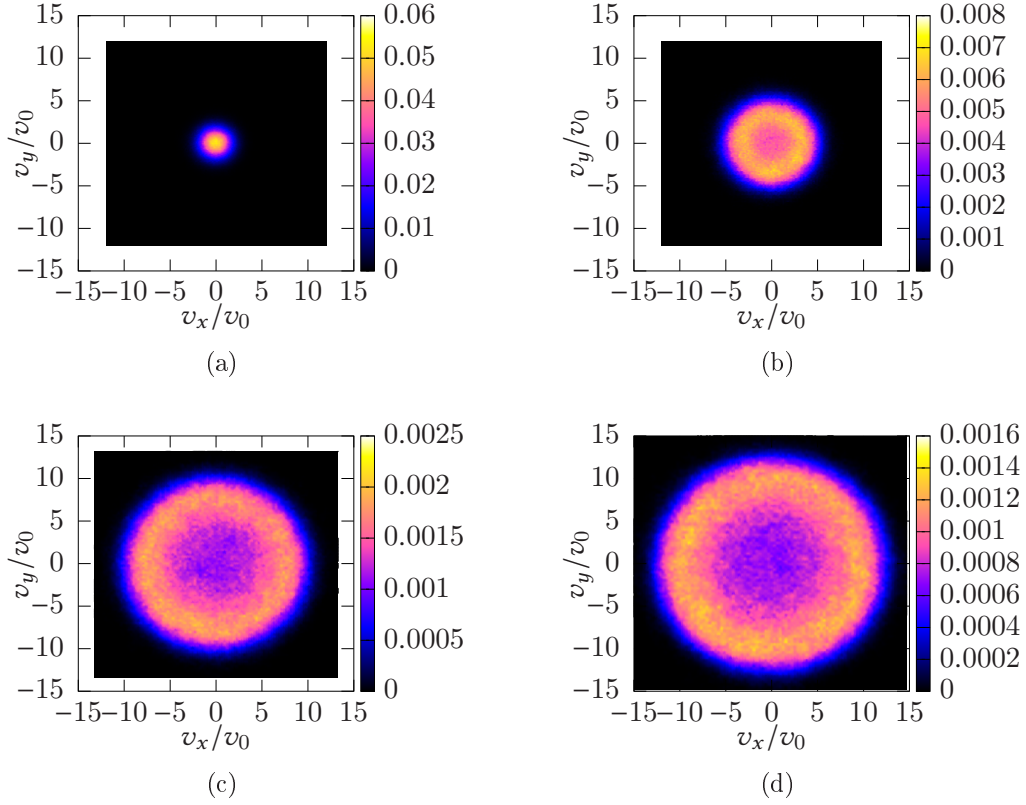


Figure 3.4.: The (v_x, v_y) - distribution for different activity strengths (a) $v_A/v_0 = 1.36$ (b) $v_A/v_0 = 5.45$ (c) $v_A/v_0 = 10.9$ (d) $v_A/v_0 = 13.6$ at $\xi_T t_0 = 1.5$ and $\langle |\vec{\omega}| \rangle_{t_0} = 2.2$. The distribution is not as sharp as the one in 2.1b, because it is the marginal distribution and not the cut at $v_z = 0$.

3.3. Underdamped active particles in a harmonic potential

3.3.1. Units and particle properties

For convenience the results will be presented with respect to reduced units. The energy unit E_0 is defined via the unit temperature T_0 as $E_0 = k_B T_0$. The frequency unit corresponds to the trap frequency $\omega_0 = 1$. The mass unit is equal to the particle's mass $m_0 = 1$. All other units needed for the present thesis can be derived from this three, e. g. the unit length is $l_0 = \sqrt{E_0/m_0\omega_0^2}$ and the unit velocity is $v_0 = l_0\omega_0$. Then the diffusion constants are $D_T/\omega_0 = \frac{1}{\xi_T/\omega_0}$ and $D_R/\omega_0 = \frac{2\omega_0 l_0^2}{5R^2 \xi_R}$.

3.3.2. Slow rotation

To study the case of a slow rotation compared to the oscillation period a ratio of about $\langle |\vec{\omega}| \rangle / \omega_0 \approx 1/12$ was chosen. For slow rotation both rotational dynamics provide the same results. In subsection 2.4.2.1 was proposed that in the case of a nearly constant activity direction the particle would be subject to an effective potential with a minimum at

$$r_0 = \frac{\gamma_T v_A}{k_s}$$

If the direction changes slowly enough the potential's minimum will change too, but the radius of the location will be constant and the particle has enough time to accommodate to this new minimum. The radial distribution for different activities v_A of the particle is shown in Fig. 3.5b. The distribution along a radius changes from the inactive particle for small v_A to a distribution centered around a distinct radius r_0 . The radius' mean value for $r_0 \gg l_0$ is expected to be:

$$\langle r \rangle = \frac{\xi_T}{\omega_0^2} v_A \quad (3.4)$$

For small activities $r_0 \ll l_0$ the expectation value will be equal to that of an inactive particle. The simulation is in good agreement with this assumption as can be seen in Fig. 3.6a. The description using an effective potential is sufficient for the case of a slow rotating particle and describes the radial distribution. A two-dimensional histogram of the position's first and second component can be seen in Fig. 3.10. While at low activity strengths the distribution is Gaussian distributed, one can see that for higher activity the distribution will transform into a ring-like distribution.

Furthermore I gave an analytical solution for the potential energy. While the kinetic and the rotational energy stay nearly constant, as we would expect for inactive particles at $\frac{3}{2}E_0$, the potential energy rises quadratically with respect to the activity. This is confirmed by the simulation, as can be seen in Fig. 3.7a. Furthermore it rises quadratically with the friction constant, see Fig. 3.7b. One can see that for high values of $\xi_T v_A$ the kinetic energy starts to deviate from the constant value, because the changes of $\xi_T v_A \vec{a}(t)$ start to be bigger than our assumption allows for.

3. Simulations

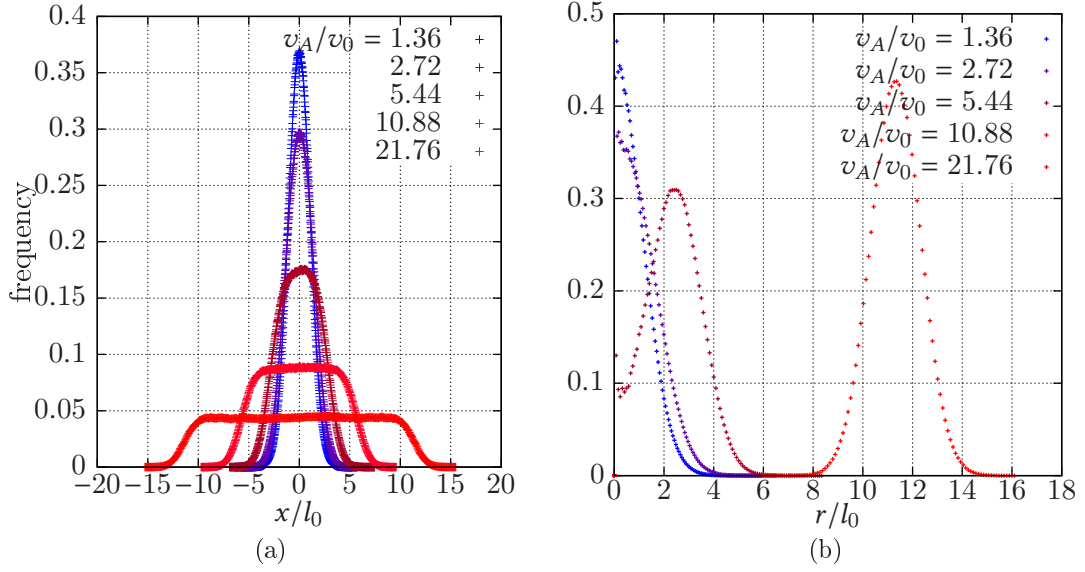


Figure 3.5.: (a) distribution of the position's x -coordinate with respect to different activities v_A ; (b) distribution along a radius with respect to different activities v_A (both done at $\xi_T/\omega_0 = 0.52$)

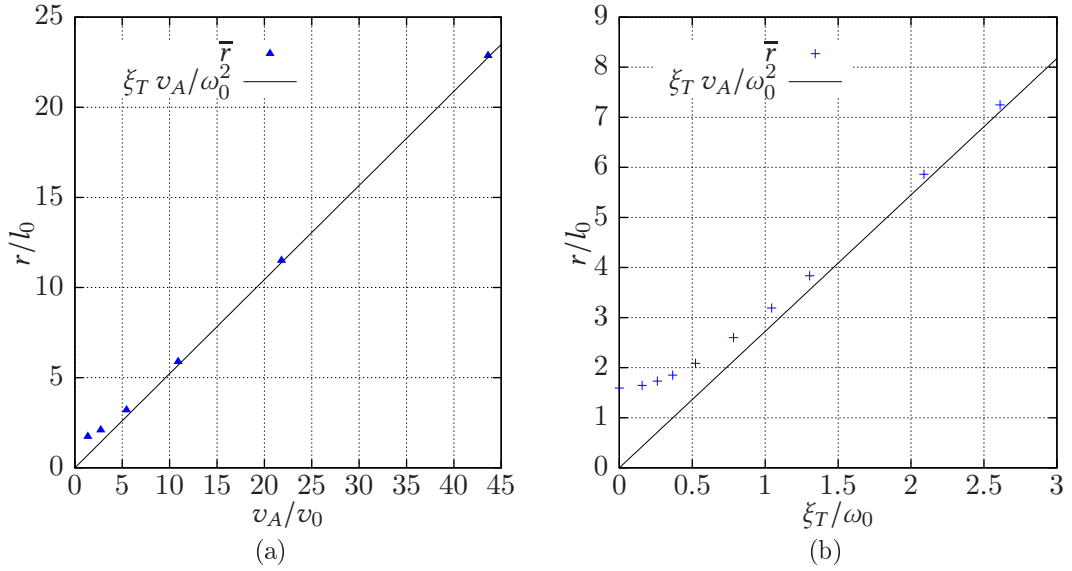


Figure 3.6.: the simulated means of the position's radius and Eq. (3.4) (a) at $\xi_T/\omega_0 = 0.5$ (b) at $v_A/v_0 = 2.7$

3.3. Underdamped active particles in a harmonic potential

The simulation is furthermore in good accordance with the assumption that the velocity distribution doesn't deviate from an inactive particle, if the rotation is slow enough. This can be seen in Fig. 3.8 for a range of activity strengths. The velocity's autocorrelation function, as shown in Fig. 3.9b, does confirm that the velocity doesn't deviate from the one of an inactive particle.

The ACF for the position has also been calculated in subsec. 2.4.2.1 and the simulation's results confirm this derivation, see Fig. 3.9a. The deviation from the theory occur when the changes of $v_A \xi_T \vec{a}$ get too big. The bigger the product $v_A \xi_T$ the bigger the impact of even slow changes of $\vec{a}(t)$, and therefore the assumption is only valid if $v_A \xi_T \frac{d\vec{a}}{dt}$ is small enough.

3. Simulations

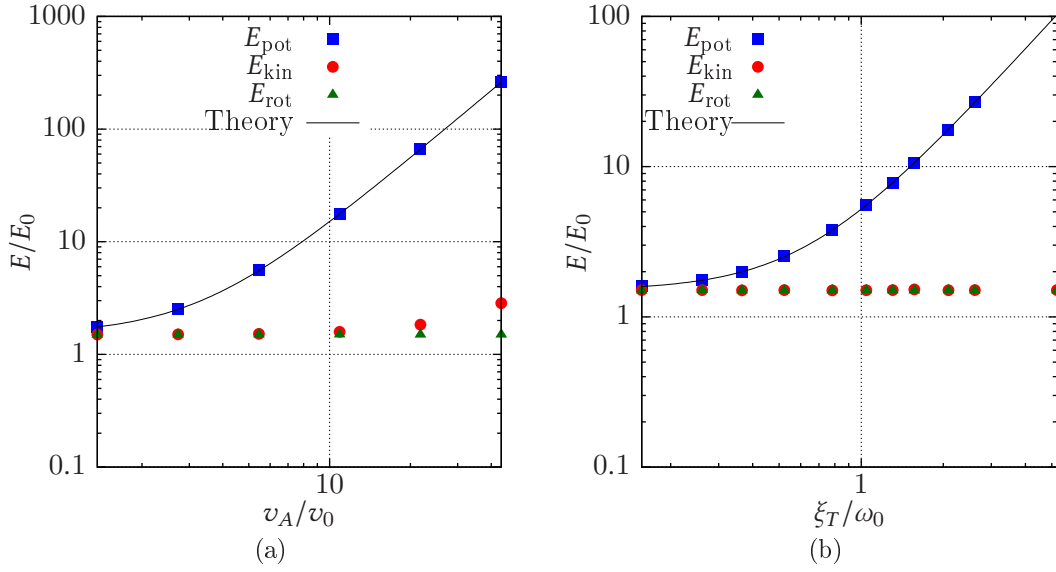


Figure 3.7.: Mean kinetic, potential and rotational energies at (a) $\xi_T/\omega_0 = 0.52$ with respect to different activities (b) $v_A/v_0 = 2.73$ with respect to different frictions ξ_T - 'Theory' denotes Eq. (2.12)

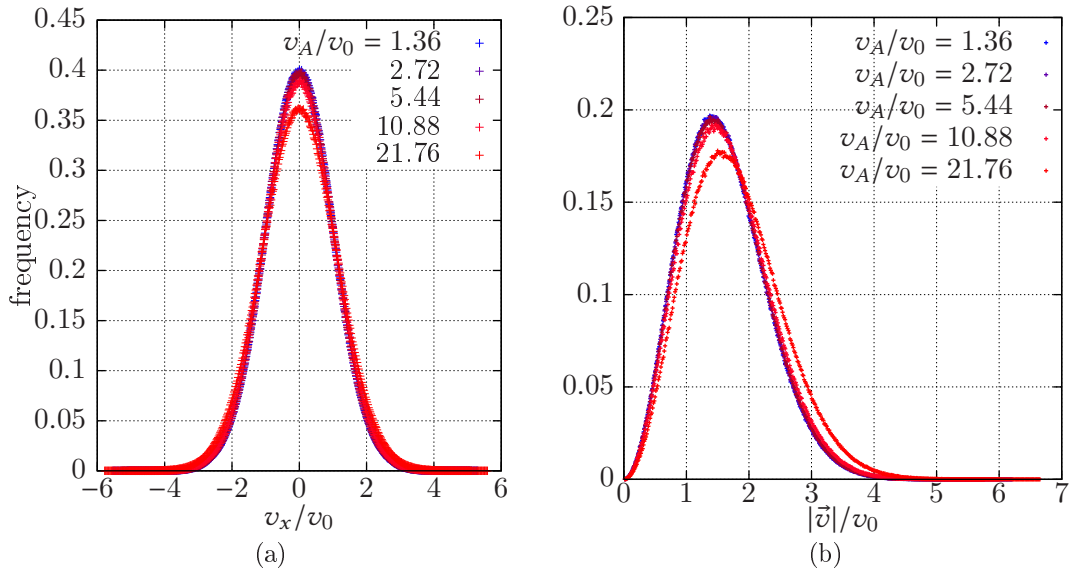


Figure 3.8.: The distributions of (a) the velocity's first component v_x , (b) the speed $|\vec{v}|$ of the particle at $\xi_T/\omega_0 = 0.5$ for different activity strengths v_A .

3.3. Underdamped active particles in a harmonic potential

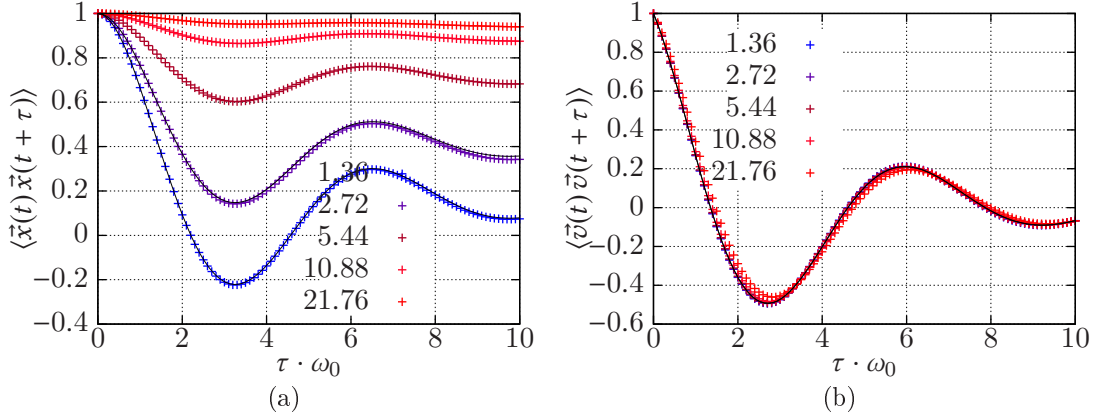


Figure 3.9.: Normalized ACFs for the (a) position (b) velocity for different activity strengths v_A/v_0 at $\xi_T/\omega_0 = 0.5$. Dots are obtained from the simulation the lines represent Eq. (2.10) and (2.13) respectively

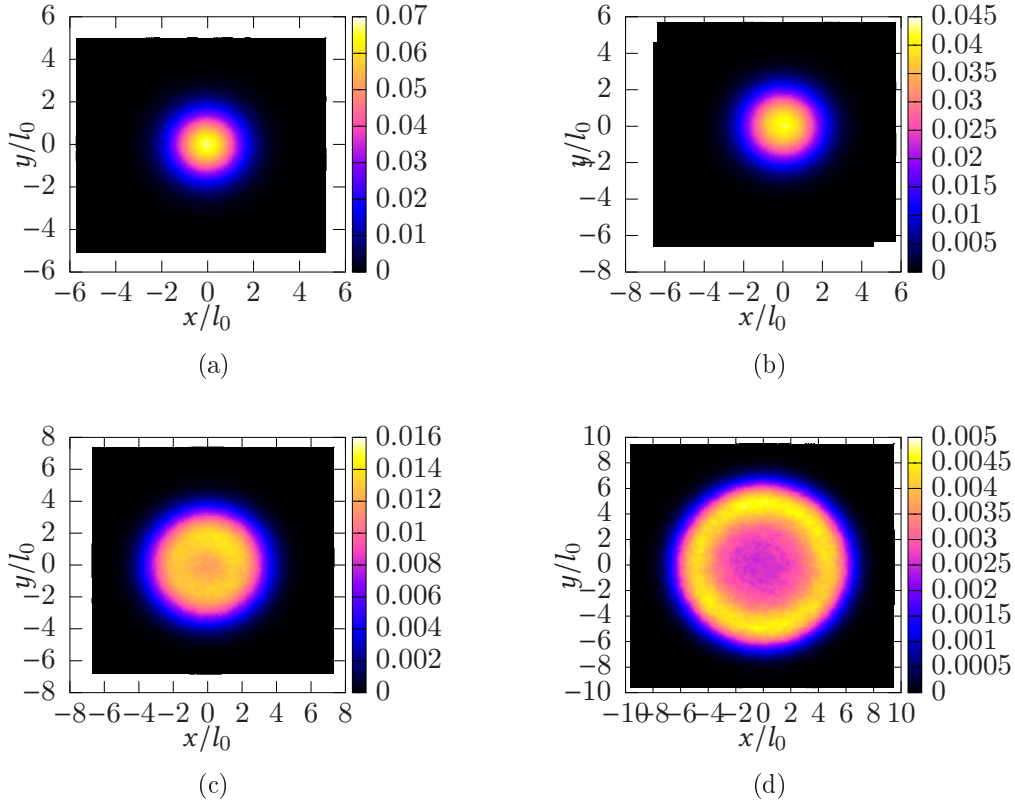


Figure 3.10.: The (x, y) - distribution for different activity strengths (a) $v_A/v_0 = 1.36$ (b) $v_A/v_0 = 2.72$ (c) $v_A/v_0 = 5.45$ (d) $v_A/v_0 = 10.9$ at $\xi_T/\omega_0 = 0.5$.

3. Simulations

3.3.3. Rotation period near oscillation period

Let's look at the total absorbed power

$$P_{\text{abs}} \propto \xi_T^2 v_A^2 \int \omega^2 S_{\vec{a}}(\omega) S_{\vec{x}}^i(\omega) d\omega \quad (3.5)$$

Comparing it to the kinetic energy yields:

$$\langle E_{\text{kin}} \rangle / E_0 = \frac{P_{\text{abs}}}{2\xi_T} + \frac{3}{2} = \frac{\xi_T v_A^2}{24\pi\omega_0 v_0^2} \int_{-\infty}^{\infty} \omega^2 S_{\vec{x}}^i(\omega) S_{\vec{a}}(\omega) d\omega + \frac{3}{2}$$

For the power spectrum of the activity's direction $S_{\vec{a}}$ the autocorrelation function was calculated based on the time series obtained from the simulation. For the position's power spectrum $S_{\vec{x}}^i$ the analytic solution is known from Eq. (1.18) and was used for the numerical integration of the integral in (3.5). Comparing the power spectra resulting from the two different rotational dynamics shows, that they differ mostly for small friction and higher values of the mean angular velocity $\langle |\vec{\omega}| \rangle$. As can be seen in Fig. 3.11 the MS-dynamics shows in the power spectrum a distinct peak for lower frictions, because the activity's direction tends to rotate on great circles. The RS-dynamics first shows a knee in the power spectrum, very near to $\omega = \langle |\vec{\omega}| \rangle$, and at low frictions a small peak, but the global maximum of the power spectrum tends to stay at $\omega = 0$.

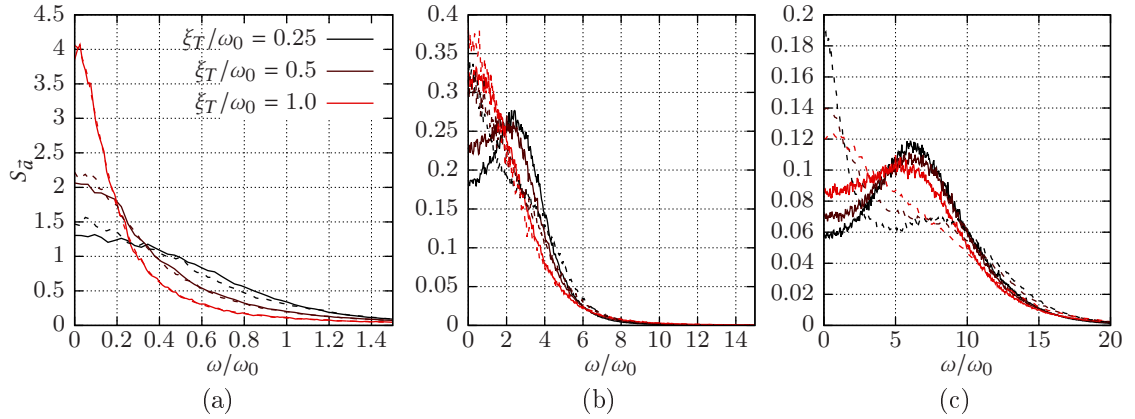


Figure 3.11.: Power spectra of the activity's direction $S_{\vec{a}}(\omega)$ for different values of the average absolute value of the angular velocity $\langle |\vec{\omega}| \rangle / \omega_0$ (a) 0.87 (b) 3.5 (c) 8.7. Both dynamics are plotted, the MS-dynamics with full lines, the RS-dynamics with dashed lines.

Using the power spectra of the two algorithms to calculate the absorbed energy using the integral from Eq. (3.5) yields Fig. 3.12. The absorbed energy is for slow and fast rotation nearly zero, but for intermediate average angular velocities they show a peak. The higher the friction the higher is the value of the average angular velocity, where the peak is located. As we have discussed in the power spectrum and ACF of the activity's direction the differences between the two different rotational dynamics is mostly at low friction and higher average angular velocities. But while the power spectra are qualitatively

3.3. Underdamped active particles in a harmonic potential

different the absorbed power derived from these show the same characteristics and differ only quantitatively.

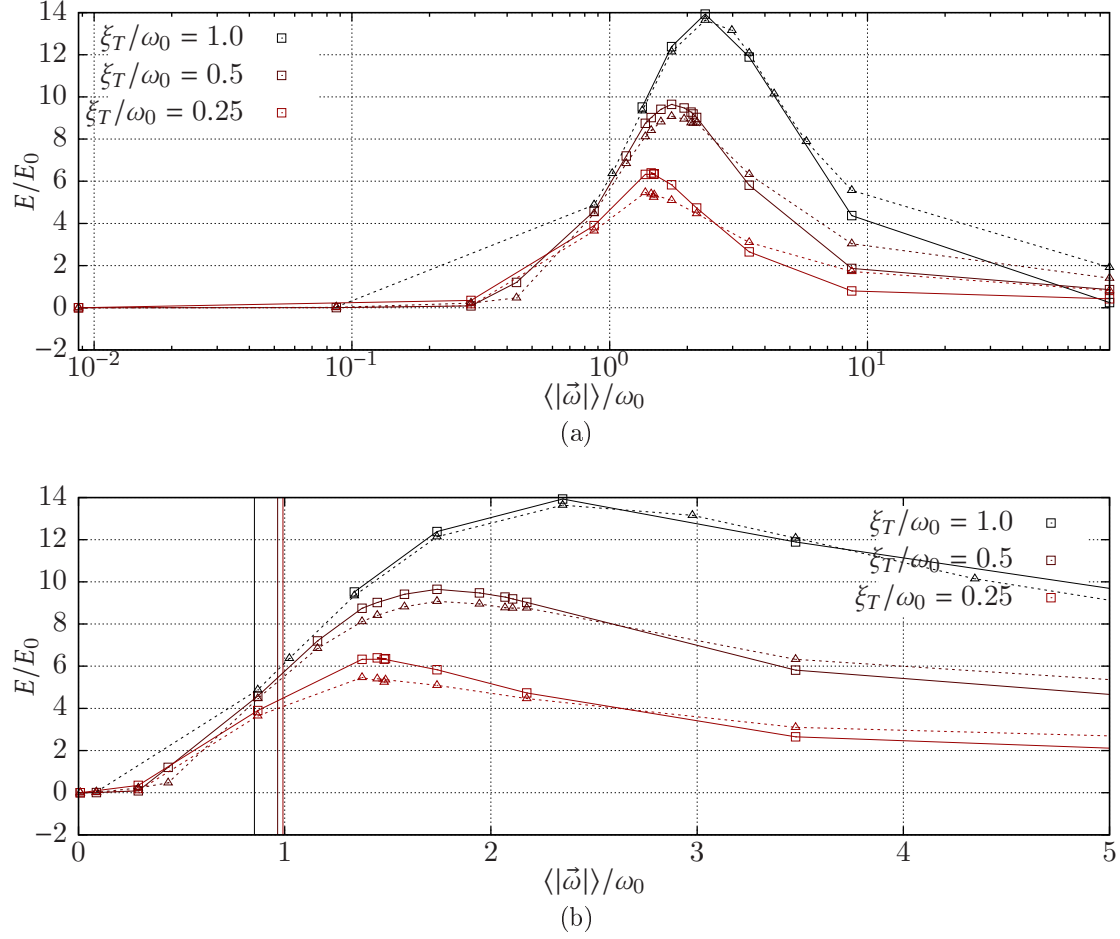


Figure 3.12.: Numerical integration of (3.5) using the simulated ACF for the activity's direction, for different values of the translational friction ξ_T with respect to the mean angular velocity $\langle |\vec{\omega}| \rangle$. Both rotational dynamics are shown, the MS-dynamics (full) and the RS-dynamics (dashed). For the underdamped case is natural oscillation frequency $\omega_1 = \sqrt{\omega_0^2 - \xi^2/4}$ highlighted as a vertical line in (b).

The calculated absorbed energy does indeed have an impact on the system. In Figs. 3.13 and 3.14 the potential and kinetic energies obtained from the simulation are plotted with respect to the mean angular velocity. The kinetic energy equals the one calculated via the absorbed power. As shortly discussed in sec. 2.4.2.2 the absorbed energy can only be dissipated via translational friction and this friction only rises with the particle's speed.

In the case of a damped, but not overdamped, system at $\xi_T / \omega_0 = 1.0$ the potential energy dominates. Steele's approximation and both algorithms are in good agreement in

3. Simulations

this case. As can be seen the potential energy only transitions from the state of the slow rotating particle with $\langle E_{\text{pot}} \rangle / E_0 = \left(\frac{v_A}{v_0} \cdot \frac{\xi_T}{\omega_0} \right)^2 + \frac{3}{2}$ to the one of the fast rotating particle with $E_{\text{pot}} / E_0 \approx 1.5$. The kinetic energy has a peak at about $\langle |\vec{\omega}| \rangle / \omega_0 = 2$ with a value of approximately $3E_0$. The figures for the kinetic and potential energy are similar to those obtained via numerical integration, using Steele's approximation. The important features are the same: the peak in the potential energy at lower friction, the peak in the kinetic energy and the limits for high and low rotation frequencies. This confirms the derivations done in subsec. 2.4.2.2.

While the mean kinetic and potential energies both rise with the square of the activity v_A the description with respect to the translational friction ξ_T is more complicated, as can be seen in Fig. 3.15. The kinetic energy rises with the friction until a threshold value, which depends on the rotation frequency.

The histograms for the potential and kinetic energies in Fig. 3.16 illustrate the behaviour of the second moments of the position and velocity. The shape of the histograms is identical for both rotation algorithms. While to position's second moment transitions from the "hotter" inactive state at fast rotations via a very broad distribution - which only occurs at small friction values - to the distinct peak, where the particle oscillates in the effective potential. The distribution of the kinetic energy is for fast and slow rotation very similar and is at it's broadest at about $\langle |\vec{\omega}| \rangle / \omega_0 = 1.6$.

3.3. Underdamped active particles in a harmonic potential

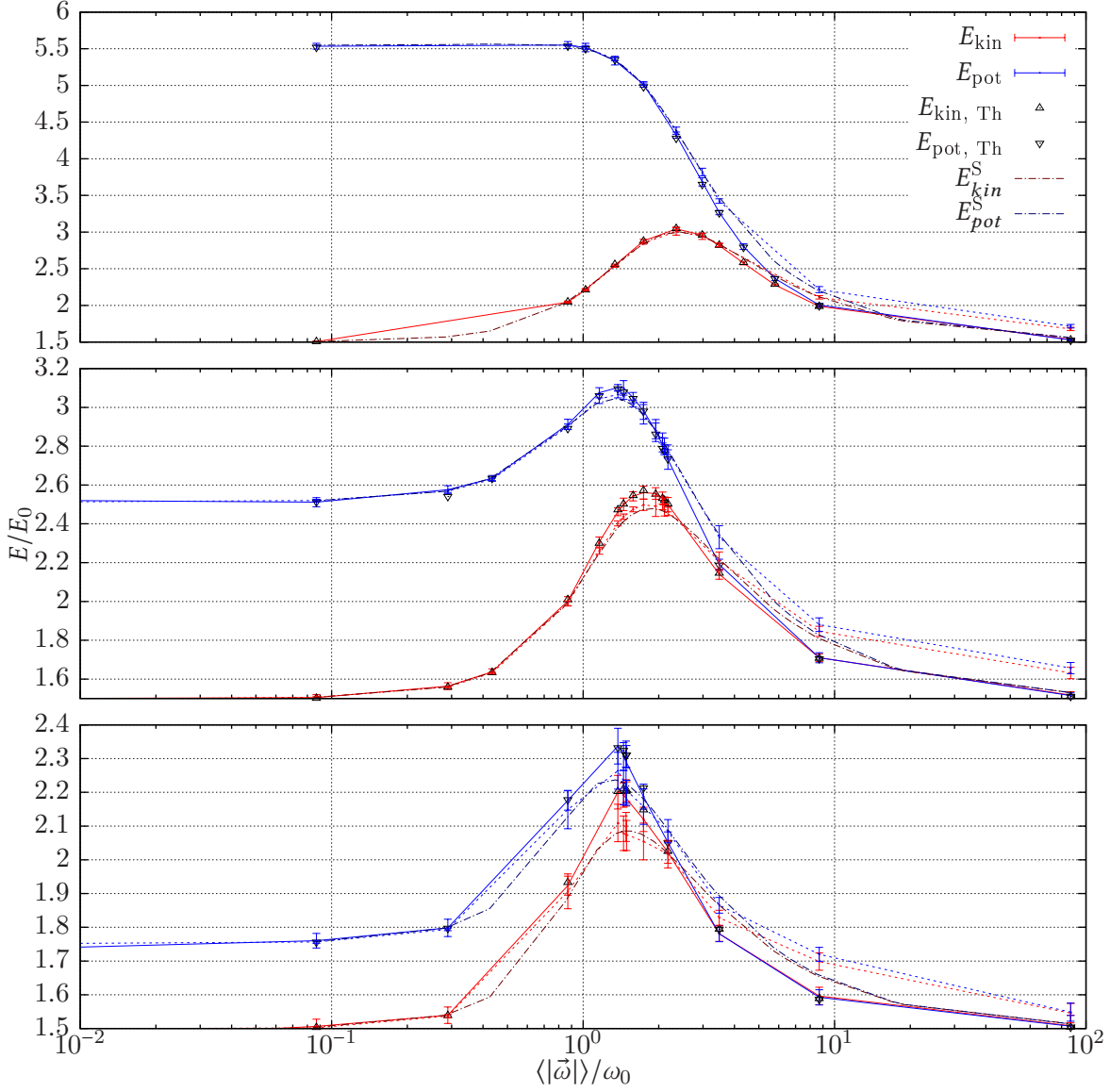


Figure 3.13.: The average kinetic and potential energy at $v_A/v_0 = 2.7$ and $\xi_T/\omega_0 = 1, 0.5$ and 0.25 (from top to bottom) with respect to the rotation frequency D_R/ω_0 . The numerically solved Eq. (2.19) and (2.20) have been plotted as $E_{\text{pot, Th}}$ and $E_{\text{kin, Th}}$, respectively, using the simulated AFC, while E_{pot}^S and E_{kin}^S have been obtained using Steele's approximation. Both rotational algorithms are shown, the one using the tangential velocity (full lines) and the one using the angular velocity (dashed lines).

3. Simulations

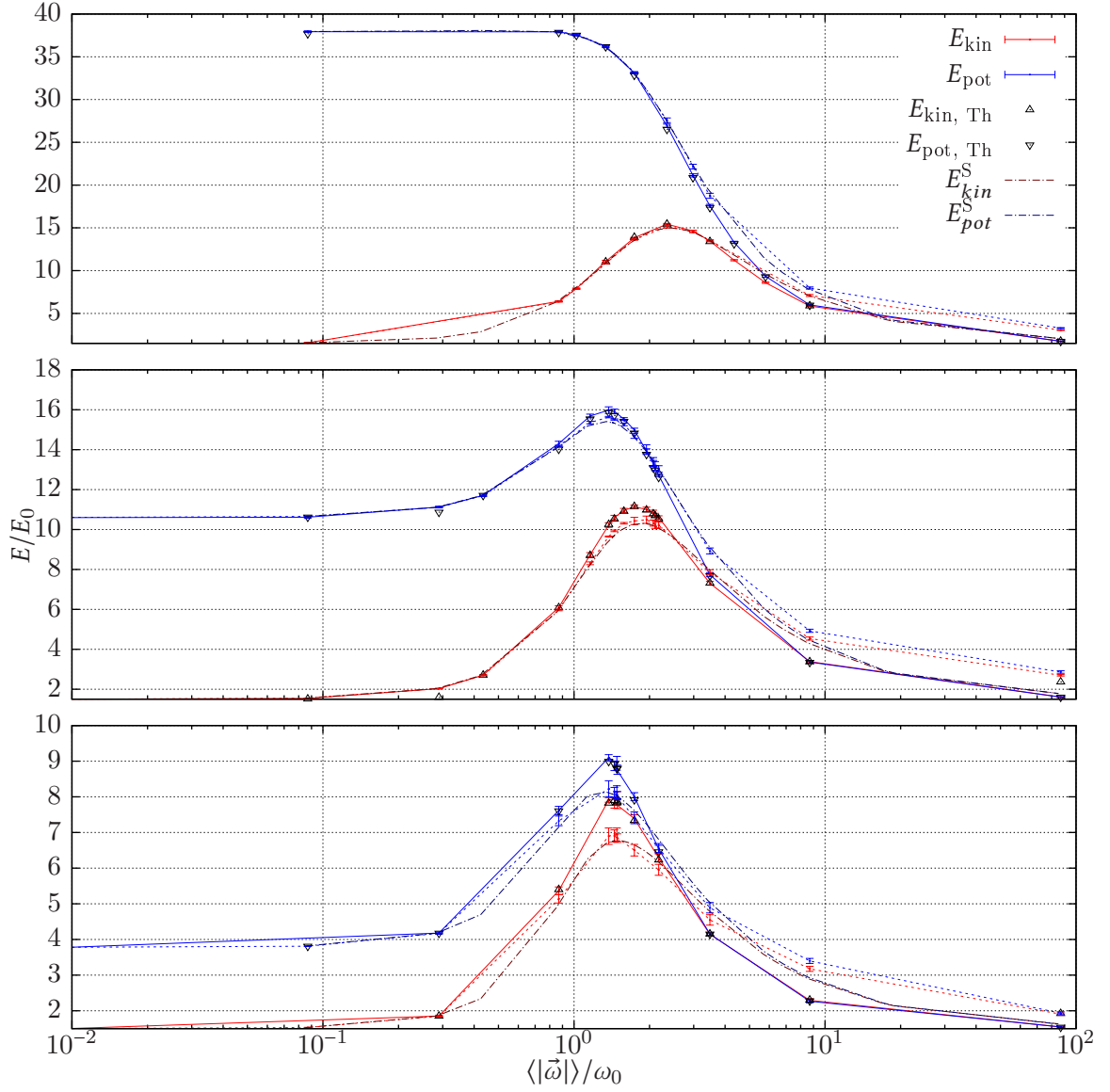


Figure 3.14.: The average kinetic and potential energy at $v_A/v_0 = 8.2$ and $\xi_T/\omega_0 = 1, 0.5$ and 0.25 (from top to bottom) with respect to the rotation frequency $\langle|\vec{\omega}|\rangle/\omega_0$. The numerically solved Eq. (2.19) and (2.20) have been plotted as $E_{\text{pot, Th}}$ and $E_{\text{kin, Th}}$, respectively, using the simulated AFC, while E_{pot}^S and E_{kin}^S have been obtained using Steele's approximation. Both rotational dynamics are shown, the MS-dynamics (full lines) and RS-dynamics (dashed lines).

3.3. Underdamped active particles in a harmonic potential

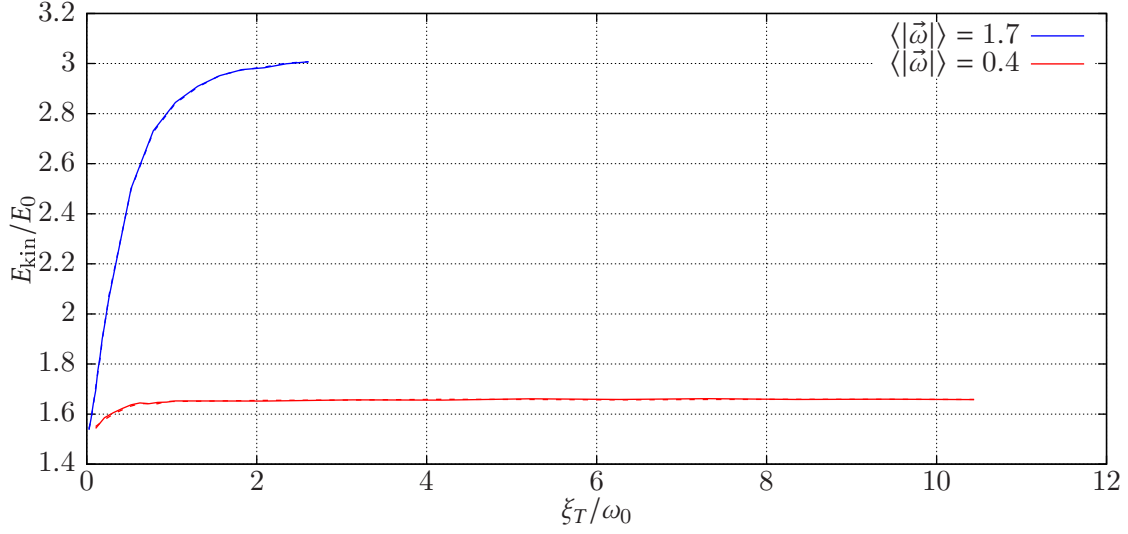


Figure 3.15.: The average kinetic energy (points) with respect to the translational friction ξ_T for different rotation frequencies $\langle |\vec{\omega}| \rangle$ at an activity of $v_A/v_0 = 2.7$. Both rotational dynamics return identical results for this range of rotation frequencies and frictions.

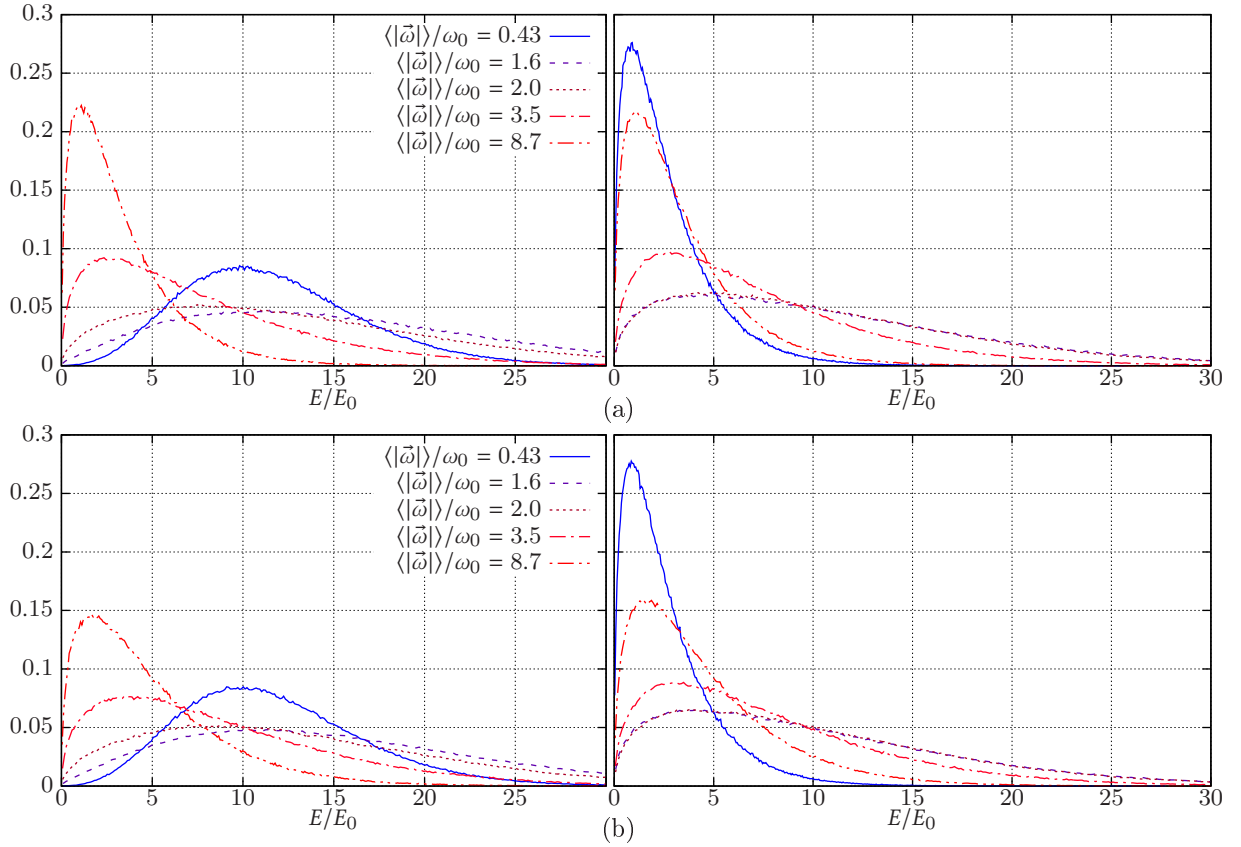


Figure 3.16.: Distributions of the potential and kinetic energy, respectively. Values obtained at $\xi_T/\omega_0 = 0.5$ and $v_A/v_0 = 8$

3. Simulations

3.3.4. Fast rotation

A rotational diffusion constant of $\langle|\vec{\omega}|\rangle/\omega_0 = 21$ has been used to arrive at the fast rotation limit.

In sec. 2.4.2.3 the foundation of the theory for fast rotating particle, was the assumption that the force due to the activity acts like a random white noise for the harmonic potential. To justify this assumption the power spectrum of the activity's direction $S_{\vec{a}}$ should be nearly constant over the frequencies which are important to the potential, i.e. where $S_{\vec{x}}^i(\omega)\omega^2 \gg 0$. Looking at Fig. (3.17) the simulation confirms this assumption. While $S_{\vec{a}}$ changes drastically over the important frequencies at $\langle|\vec{\omega}|\rangle/\omega_0 = 1.7$, the power spectrum stays nearly constant for $\langle|\vec{\omega}|\rangle/\omega_0 = 87$, but the values differ between the two different rotational dynamics.

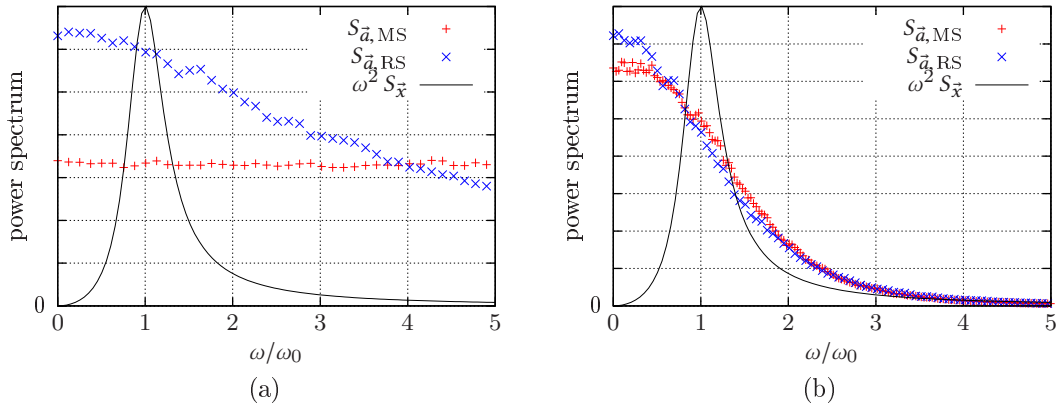


Figure 3.17.: The power spectrum of the activity's direction $S_{\vec{a},MS}$, obtained by the MS-dynamics, and $S_{\vec{a},RS}$, obtained by the RS-dynamics, for (a) $\langle|\vec{\omega}|\rangle/\omega_0 = 87$ fast rotation, (b) $\langle|\vec{\omega}|\rangle/\omega_0 = 1.7$ near resonance and $\omega^2 S_{\vec{x}}^i$ for $\xi_R/\omega_0 = 0.52$. For the relevant frequencies, where $S_{\vec{x}}^i\omega^2 \gg 0$, the activity's power spectrum is nearly constant for a fast rotating particle.

It has been shown in subsec. 2.4.2.3 that the equipartition theorem holds in the limit of the fast rotation

$$\langle E_{\text{kin}} \rangle / E_0 = \langle E_{\text{pot}} \rangle / E_0 = \frac{\gamma_T v_A^2}{8v_0^2 \omega_0} S_{\vec{a}}(0) + \frac{3}{2}$$

If the friction is fixed, the kinetic and potential energy will just depend on square of the activity's strength v_A . In the case of $\xi_T/\omega_0 = 0.52$ and $\langle|\vec{\omega}|\rangle/\omega_0 = 21$ and using the algorithm for the tangential velocity the function after evaluating the power spectrum reads

$$\langle E_{\text{kin}} \rangle / E_0 = \langle E_{\text{pot}} \rangle / E_0 = 0.0093 v_A^2 + \frac{3}{2} \quad (3.6)$$

In Fig. (3.18) one can see, that indeed the theoretical work is in good agreement with the simulation. Using Steele's approximation for $S_{\vec{a}}(\omega)$ the deviation for fast rotating particles is quite high, it would give us a function of $\langle E_{\text{kin}} \rangle / E_0 = 0.02 v_A^2 + 1.5$. As

3.3. Underdamped active particles in a harmonic potential

discussed before Steele's approximation is not in agreement with the simulation of the fast rotating particle.

The result for the effective temperature doesn't converge to the overdamped limit presented in sec. 2.2, because our model treats the activity as a force with a fixed absolute value, independent of the rotation period. The overdamped model always assumes a speed of v_A , regardless of the rotation period. As can be seen in the speed distributions, see Fig. 3.19, the fast rotation hinders the particle from arriving at a mean speed of v_A .

If the mean rotation time is small with respect to the oscillation time of the particle, then we expect Gaussian distributions for the components of velocity and position. Only the variance of the distribution should be subject to change, if the activity v_A rises. This can be quantified using the energies, described by Eq. (3.6), above:

$$\langle \vec{x}^2 \rangle = \frac{2}{\omega_0^2 m} \langle E_{\text{pot}} \rangle \quad \langle \vec{v}^2 \rangle = \frac{2}{m} \langle E_{\text{kin}} \rangle$$

The simulation agrees with this assumption and the distributions can be seen in Fig. 3.20. Accordingly the shape of the speed and radial distribution should not change, these can be seen in Fig. 3.19.

The ACFs of the position and the velocity, see Fig. 3.21, only solidify the equality between the inactive particle in a harmonic potential and the fast rotating, active particle.

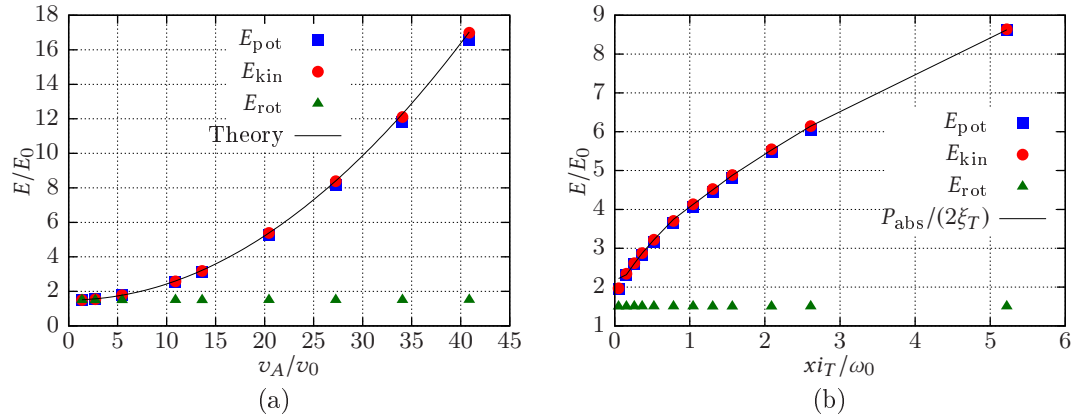


Figure 3.18.: Energies with respect to (a) activity v_A , at $\xi_T/\omega_0 = 0.5$ (b) translational friction ξ_T at $v_A/v_0 = 13.5$. For the fit see Eq. (3.6).

3. Simulations

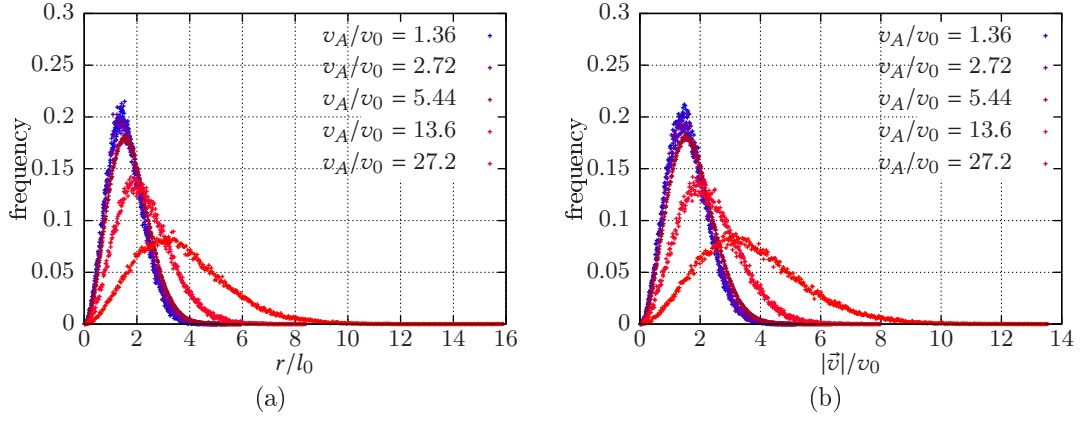


Figure 3.19.: Distributions of (a) the position's radius r (b) the speed $|\vec{v}|$ of the particle with different activities v_A at $\xi_T/\omega_0 = 0.52$

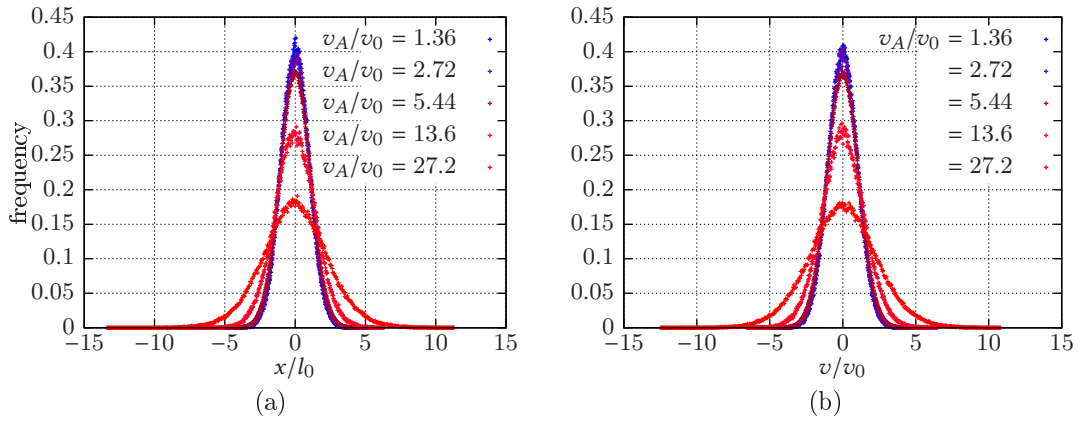


Figure 3.20.: Distributions of a (a) position component (b) velocity component with different activities v_A at $\xi_T/\omega_0 = 0.5$

3.3. Underdamped active particles in a harmonic potential

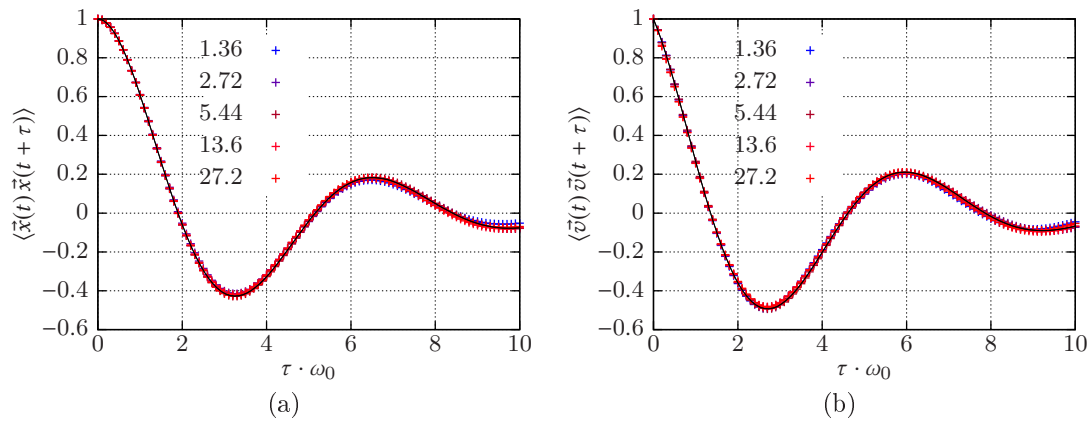


Figure 3.21.: Normalized ACFs for the (a) position (b) velocity for different activity strengths v_A/v_0 at $\xi_T/\omega_0 = 0.5$. Dots are obtained from the simulation the lines represents the analytical solutions for the inactive particle

4. Conclusion

In the present thesis the case of an underdamped active particle in a harmonic potential has been investigated.

The harmonically trapped particle was at first studied theoretically, where the partition in slow, fast and medium rotation with respect to the oscillation period simplified the problem.

In the simplest case, the slow rotation, the power spectrum and the ACF of the position and velocity could be obtained analytically by means of an effective harmonic potential. Therefore the potential and kinetic energy and the shape of the position and velocity distribution functions could be predicted. The simulation for the slow rotation at $\langle |\vec{\omega}| \rangle / \omega_0 \approx 1/12$ was in good agreement with the theoretical work. These results are independent of the details of how the activity's direction moves. In this case both rotational dynamics used in this thesis have been in full agreement.

To address the challenge of a mean rotation time near the oscillation period the sum of the active force and the thermal fluctuations was treated as a perturbation of the harmonic oscillator. Studying the power absorbed by the particle lead to an - at least numerically - simple expression for the particle's kinetic energy. An equivalent expression has been obtained by calculating the power spectrum and Fourier transforming it at $\tau = 0$, to obtain the second moments of the position and velocity distribution. Therefore the kinetic and the potential energy could be described using the power spectrum of the activity's direction. This expression predicts a peak in the kinetic energy if the particle rotates approximately as fast as it oscillates for all friction values. The potential energy showed a peak at about $\langle |\vec{\omega}| \rangle / \omega_0 = 1$ only for low friction. For high friction values and slow particle rotation Steele's approximation yields results which are in good agreement with the simulation using both different rotational dynamics. For low friction values and faster particle rotation the RS-dynamics produced results which were in better agreement with Steele's approximation than the MS-dynamics. Despite the qualitative differences in the power spectra of the activity's direction obtained by the two rotational dynamics, the results for the second moments of the position and velocity only differed slightly.

For predictions in an experimental framework one could either try to measure the direction's autocorrelation function or obtain the autocorrelation function via simulating a rotating unit vector. Two different rotational dynamics and the corresponding algorithms for this problem has been presented in section 3.1.

For the fast rotating particle the expression for the kinetic and potential energy from the medium rotation time can be reused. These expressions could be further simplified by assuming that the power spectrum is nearly constant in the relevant interval around ω_0 . Furthermore it has been shown that the equi-partition would hold again and therefore that the particle would just behave like an hotter inactive particle. The corresponding

4. Conclusion

temperature can be derived from the kinetic energy. For the simulation of the fast rotating a particle a rotational diffusion coefficient of $\langle |\vec{\omega}| \rangle / \omega_0 = 21$ has been chosen and the results are in good agreement with the theory.

The study of the activity's direction's autocorrelation function revealed, that there is still theoretical work to be done. While Steele's approximation is sufficient for the overdamped case, the case of an underdamped rotating unit vector is still hard to tackle analytically in a way that is numerically easy to use.

Pototsky and Stark [16] studied not only the single particle case, but also multiple interacting particles. One could study underdamped, interacting active particles in a harmonic trap and compare the results to the overdamped results from Pototsky and Stark [16].

A. Testing the Simulation

A.1. Brownian particle

A.1.1. Free particle

The parameters defining the motion of the Brownian particle are the friction ξ , the mass m and the temperature T :

$$\frac{d\vec{x}}{dt} = \vec{v} \quad \frac{d\vec{v}}{dt} = -\xi \vec{v} + \vec{A}(t)$$

with the following properties for the random acceleration $\vec{A} = (A_1, A_2, A_3)$, and $S = \xi \frac{k_B T}{m}$

$$\langle A_i(t) \rangle = 0 \quad \langle A_i(t) A_j(t') \rangle = 2S \delta_{ij} \delta(t - t')$$

Then, see sec. 1.3,

$$\langle (\vec{x} - \vec{x}_0)^2 \rangle = \frac{6S}{\xi^3} \left(\xi t - 1 + e^{-\xi t} \right) \quad (\text{A.1})$$

$$\langle \vec{v}(t) \vec{v}(t + \tau) \rangle = \frac{3S}{\xi} e^{-\xi t} \quad (\text{A.2})$$

$$p_0(v_x) = \left(\frac{1}{2\pi S} \right)^{3/2} e^{-\xi v_x^2 / 2S} \quad (\text{A.3})$$

Setting $m = 1$, $k_B T = 1/300$ and varying ξ shows good agreement between simulation and theory, see Fig. A.1.

A.1.2. In harmonic potential

An additional parameter is added in terms of the potential's frequency ω_0 . The equations read:

$$\frac{d\vec{x}}{dt} = \vec{v} \quad \frac{d\vec{v}}{dt} = -\xi \vec{v} + \vec{A}(t) + \omega_0^2 \vec{x}$$

A.2. Overdamped active particle

The MSD for the active particle has been obtained by Löwen et al. [27] as:

$$\langle (\vec{x} - \vec{x}_0)^2 \rangle = \left(6D_T + \frac{v_A^2}{D_R} \right) t + \frac{1}{2} \left(\frac{v_A}{D_R} \right)^2 \left[e^{-2D_R t} - 1 \right] \quad (\text{A.4})$$

Now testing this for different values of v_A at $\xi_T = 100$, with $R = 1$, $k_B T = 1$ and $m = 1$ shows good agreement between simulation and theory, Fig. A.3.

A. Testing the Simulation

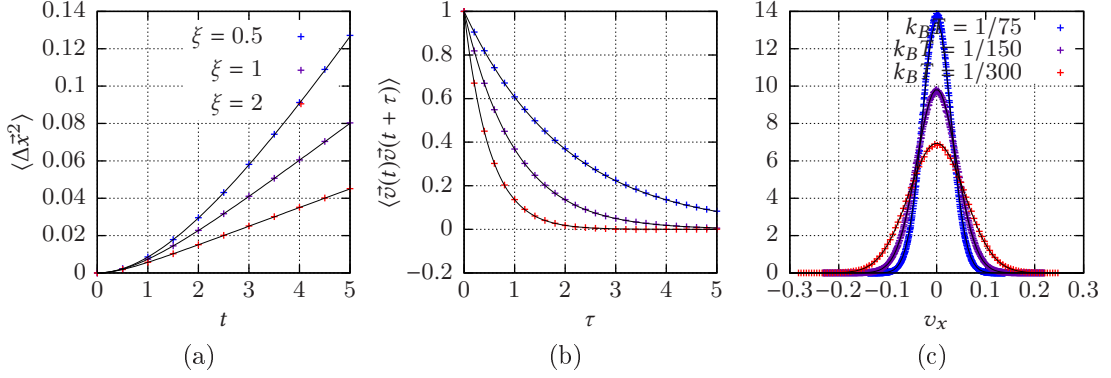


Figure A.1.: (a) The MSD and (b) the ACF of the velocity for three different values of ξ ; (c) the distribution of v_x for different values of $k_B T$ at $\xi = 0.5$. The simulation is plotted as dots, Eq. (A.1), (A.2), (A.3) respectively as black line.

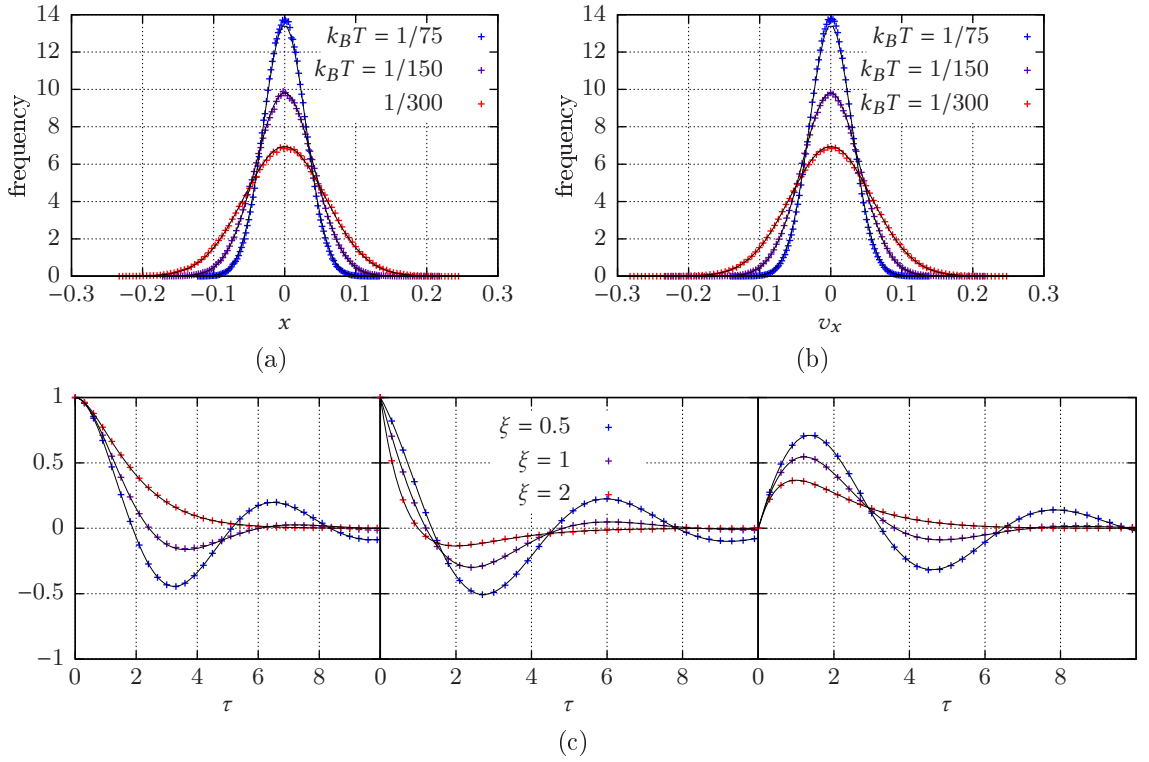


Figure A.2.: (a) and (b) show the distribution of x and v_x for different values of T respectively. The ACF $\langle \vec{x}(t) \vec{x}(t+\tau) \rangle$, $\langle \vec{v}(t) \vec{v}(t+\tau) \rangle$ and the cross-correlation function $\langle \vec{x}(t) \vec{v}(t+\tau) \rangle$ for different values of ξ are plotted in (c).

A.2. Overdamped active particle

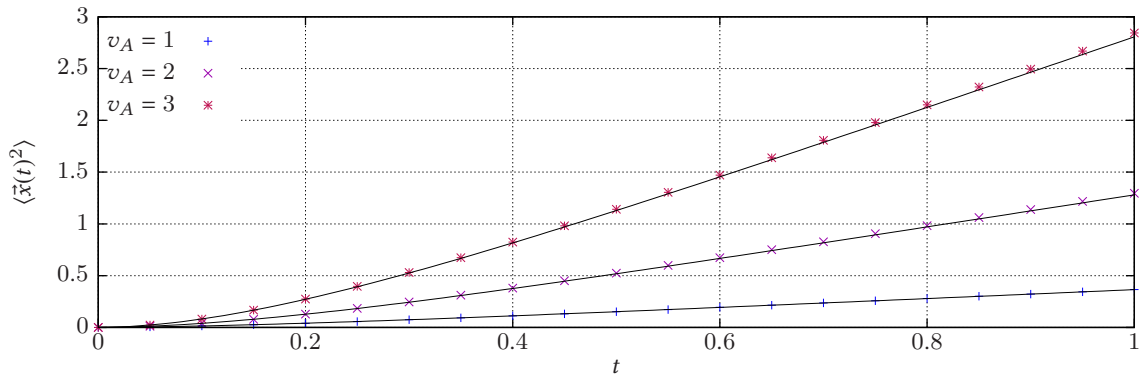


Figure A.3: MSD for the overdamped ($\xi_T = 100$) active particle for different activity strengths v_A . Simulation is plotted as dots, Eq. (A.4) as line.

B. Supplementary Calculations

B.1. Overdamped active particles

B.1.1. Position's expectation value

The equations to average are $x = x_0 + v_A \cdot \int_0^t \cos(\varphi(t')) dt' + \sqrt{2D_T} W_t^x$ and $y = y_0 + v_A \cdot \int_0^t \sin(\varphi(t')) dt' + \sqrt{2D_T} W_t^y$, with $\varphi(t) = \varphi_0 + \sqrt{2D_R} W_t^\varphi$. The Wiener process W_t^i is $\mathcal{N}(0, t)$ -distributed, therefore $\langle W_t^i \rangle = 0$ ($i = x, y, \varphi$). Hence

$$\begin{aligned}\langle x - x_0 \rangle &= v_A \int_0^t \langle \cos(\sqrt{2D_R} W_{t'}^\varphi) \rangle dt' \\ \langle y - y_0 \rangle &= v_A \int_0^t \langle \sin(\sqrt{2D_R} W_{t'}^\varphi) \rangle dt'\end{aligned}$$

Let's take a closer look at $\langle \cos(a \cdot W_t) \rangle$ using the Euler formula:

$$\langle \cos(\varphi_0 + a \cdot W_t) \rangle = \langle \Re \left\{ e^{i(\varphi_0 + a W_t)} \right\} \rangle = \Re \left\{ e^{i\varphi_0} \langle e^{ia W_t} \rangle \right\}$$

To calculate the expectation value, we will use that W_t is $\mathcal{N}(0, t)$ -distributed and get:

$$\begin{aligned}\langle e^{ia W_t} \rangle &= \frac{1}{\sqrt{2\pi t}} \int_{-\infty}^{\infty} e^{iax} \cdot e^{-x^2/2t} dx \\ &= \frac{1}{\sqrt{2\pi t}} \int_{-\infty}^{\infty} e^{-(x^2/2t - ia x)} dx\end{aligned}$$

by completing the square and substituting $y = x/\sqrt{2t} - ia/\sqrt{2}$:

$$\begin{aligned}\langle e^{ia W_t} \rangle &= \frac{1}{\sqrt{2\pi t}} \int_{-\infty}^{\infty} e^{-(x/\sqrt{2t} - ia/\sqrt{2})^2 - a^2/2} dx \\ &= \frac{1}{\sqrt{2\pi t}} e^{-a^2/2} \cdot \int_{-\infty}^{\infty} e^{-y^2} \sqrt{2t} dy \\ &= \frac{1}{\sqrt{\pi}} e^{-a^2/2} \cdot \sqrt{\pi} \\ &= e^{-a^2/2}\end{aligned}$$

Using the above result, we obtain

$$\langle \cos(\varphi_0 + \sqrt{2D_R} W_{t'}^\varphi) \rangle = \cos(\varphi_0) \cdot e^{-D_R t'}$$

B. Supplementary Calculations

and subsequently:

$$\begin{aligned}\langle x - x_0 \rangle &= v_A \cdot \cos(\varphi_0) \cdot \int e^{-D_R t'} dt' \\ &= \frac{v_A}{D_R} \cdot \left(1 - e^{-D_R t}\right) \cdot \cos(\varphi_0)\end{aligned}$$

For the average of the y -position $\langle y \rangle$, we use that $\langle \sin(a \cdot W_t) \rangle = \Im \left\{ e^{i\varphi_0} \langle e^{iaW_t} \rangle \right\} = \sin(\varphi_0) \cdot e^{-D_R t}$, to obtain

$$\langle y - y_0 \rangle = \frac{v_A}{D_R} \cdot \left(1 - e^{-D_R t}\right) \cdot \sin(\varphi_0)$$

B.1.2. Mean squared displacement

For the mean squared displacement $\langle (\vec{r} - \vec{r}_0)^2 \rangle = \langle (x - x_0)^2 + (y - y_0)^2 \rangle$ we will at first look at $(x - x_0)^2$ and $(y - y_0)^2$ separately:

$$\langle (x - x_0)^2 \rangle = v_A^2 \cdot \left(\int_0^t \cos(\varphi(t')) dt' \right)^2 + 2v_A \cdot \int_0^t \cos(\varphi(t')) dt' \cdot \sqrt{2D_T} W_t^x + 2D_T (W_t^x)^2$$

averaging the above expression, using the properties for a Wiener process W_t : $\langle W_t \rangle = 0$ and $\langle W_t^2 \rangle = t$, and writing the squared integral as two integrals:

$$\langle (x - x_0)^2 \rangle = v_A^2 \int_0^t \int_0^t \langle \cos(\varphi(t')) \cos(\varphi(t'')) \rangle dt'' dt' + 2D_T t \quad (\text{B.1})$$

The interesting part is the two-dimensional integral, it's argument is the autocorrelation function of the angle's cosine. Using $\varphi(t) = \varphi_0 + \sqrt{2D_R} \cdot W_t^\varphi =: \varphi_t$ we will take a closer look

$$\begin{aligned}& \int_0^t \int_0^t \langle \cos(\varphi_{t'}) \cos(\varphi_{t''}) \rangle dt'' dt' = \\ &= \int_0^t \int_{t'}^t \langle \cos(\varphi_{t'}) \cos(\varphi_{t''}) \rangle dt'' dt' + \int_0^t \int_{t''}^{t'} \langle \cos(\varphi_{t'}) \cos(\varphi_{t''}) \rangle dt' dt''\end{aligned}$$

The two integrals in the last line are identical, because the argument of the mean commutes, and using the property of the Wiener process, that $W_{t''} = W_{t'} + W_{t''-t'} - W_{t'} = W_{t'} + W_{t''-t'}$ and $\varphi_{t''-t'} := \varphi_{t''} - \varphi_{t'} = \sqrt{2D_R} \int_{t'}^{t''} \xi_\varphi(s) ds$ we obtain

$$2 \int_0^t \int_{t'}^t \langle \cos(\varphi_{t'}) \cos(\varphi_{t'} + \varphi_{t''-t'}) \rangle dt'' dt'$$

now using $\cos(a + b) = \cos(a)\cos(b) - \sin(a)\sin(b)$

$$2 \int_0^t \int_{t'}^t \langle \cos^2(\varphi_{t'}) \cos(\varphi_{t''-t'}) \rangle - \langle \cos(\varphi_{t'}) \sin(\varphi_{t'} + \varphi_{t''-t'}) \rangle dt'' dt'$$

B.1. Overdamped active particles

because $W_{t'}$ describes the Wiener process up to t' and $W_{t''-t'}$ the process from t' to t'' these are independent from each other, and therefore the angles $\varphi_{t'}$ and $\varphi_{t''-t'}$ are independent and we can write:

$$2 \int_0^t \int_{t'}^t \langle \cos^2(\varphi_{t'}) \rangle \langle \cos(\varphi_{t''-t'}) \rangle - \langle \cos(\varphi_{t'}) \sin(\varphi_{t'}) \rangle \langle \sin(\varphi_{t''-t'}) \rangle dt'' dt'$$

After rewriting the two-dimensional integral we will put it back in Eq. (B.1)

$$\langle x^2 \rangle = 2v_A^2 \int_0^t \int_{t'}^t \langle \cos^2(\varphi_{t'}) \rangle \langle \cos(\varphi_{t''-t'}) \rangle - \langle \cos(\varphi_{t'}) \sin(\varphi_{t'}) \rangle \langle \sin(\varphi_{t''-t'}) \rangle dt'' dt' + 2D_T t$$

In an analogous manner, using $\sin(a+b) = \sin(a)\cos(b) + \cos(a)\sin(b)$ one can obtain

$$\langle y^2 \rangle = 2v_A^2 \int_0^t \int_{t'}^t \langle \sin^2(\varphi_{t'}) \rangle \langle \cos(\varphi_{t''-t'}) \rangle + \langle \cos(\varphi_{t'}) \sin(\varphi_{t'}) \rangle \langle \sin(\varphi_{t''-t'}) \rangle dt'' dt' + 2D_T t$$

We can now calculate the MSD

$$\langle x^2 + y^2 \rangle = 2v_A^2 \int_0^t \int_{t'}^t \langle \cos^2(\varphi_{t'}) + \sin^2(\varphi_{t'}) \rangle \langle \cos(\varphi_{t''-t'}) \rangle dt'' dt' + 4D_T t$$

and using the result from the previous section B.1.1 $\langle \cos(\varphi_{t''-t'}) \rangle = e^{-D_R(t''-t')}$

$$\begin{aligned} \langle x^2 + y^2 \rangle &= 2v_A^2 \int_0^t \int_{t'}^t e^{-D_R(t''-t')} dt'' dt' + 4D_T t \\ &= 2v_A^2 \int_0^t \frac{1}{D_R} \left(1 - e^{-D_R(t-t')} \right) dt' + 4D_T t \\ &= 2v_A^2 \left[\frac{1}{D_R} \cdot t - \frac{1}{D_R^2} \left(1 - e^{-D_R t} \right) \right] + 4D_T t \\ &= \left[4D_T + \frac{2v_A^2}{D_R} \right] \cdot t + \frac{2v_A^2}{D_R^2} \cdot \left(e^{-D_R t} - 1 \right) \end{aligned}$$

Bibliography

- [1] Jörg Bartnick, Andreas Kaiser, Hartmut Löwen, and Alexei V Ivlev. Emerging activity in bilayered dispersions with wake-mediated interactions. *The Journal of Chemical Physics*, 144(22):224901, 2016.
- [2] Clemens Bechinger, Roberto Di Leonardo, Hartmut Löwen, Charles Reichhardt, Giorgio Volpe, and Giovanni Volpe. Active particles in complex and crowded environments. *Reviews of Modern Physics*, 88(4):045006, 2016.
- [3] Howard C Berg. *E. coli in Motion*. Springer Science & Business Media, 2008.
- [4] Ivo Buttinoni, Giovanni Volpe, Felix Kümmel, Giorgio Volpe, and Clemens Bechinger. Active brownian motion tunable by light. *Journal of Physics: Condensed Matter*, 24(28):284129, 2012.
- [5] Michael E Cates and Julien Tailleur. When are active brownian particles and run-and-tumble particles equivalent? consequences for motility-induced phase separation. *EPL (Europhysics Letters)*, 101(2):20010, 2013.
- [6] David Chandler. *Introduction to modern statistical mechanics*. Oxford University Press, 1987.
- [7] William T Coffey and Yuri P Kalmykov. *The Langevin equation: with applications to stochastic problems in physics, chemistry and electrical engineering*. World Scientific, 2004.
- [8] Geertruida L de Haas-Lorentz. *Die Brownsche Bewegung und einige verwandte Erscheinungen*. Springer-Verlag, 2013.
- [9] Albert Einstein. On the motion of small particles suspended in liquids at rest required by the molecular-kinetic theory of heat. *Annalen der Physik*, 17:549–560, 1905.
- [10] Mihaela Enculescu and Holger Stark. Active colloidal suspensions exhibit polar order under gravity. *Physical Review Letters*, 107(5):058301, 2011.
- [11] Hanno Kählert and Hartmut Löwen. Resonant behavior of trapped brownian particles in an oscillatory shear flow. *Physical Review E*, 86(4):041119, 2012.
- [12] John T Lewis, James McConnell, and Brendan KP Scaife. Relaxation effects in rotational brownian motion. In *Proceedings of the Royal Irish Academy. Section A: Mathematical and Physical Sciences*, pages 43–69. JSTOR, 1976.

Bibliography

- [13] David Lindley. *Boltzmann's Atom: The Great Debate that Launched a Revolution in Physics*. Free Press, 2001.
- [14] Andrei Manoliu and Charles Kittel. Correlation in the langevin theory of brownian motion. *American Journal of Physics*, 47(8):678–680, 1979.
- [15] Leonard S Ornstein. On the brownian motion. In *Proc. Amst*, volume 21, pages 96–108, 1919.
- [16] Andriy Pototsky and Holger Stark. Active brownian particles in two-dimensional traps. *EPL (Europhysics Letters)*, 98(5):50004, 2012.
- [17] Pawel Romanczuk, Markus Bär, Werner Ebeling, Benjamin Lindner, and Lutz Schimansky-Geier. Active brownian particles. *The European Physical Journal Special Topics*, 202(1):1–162, 2012.
- [18] Gerd Röpke. *Statistische Mechanik für das Nichtgleichgewicht*. Deutscher Verlag der Wissenschaften, 1987.
- [19] Robert A Sack. Relaxation processes and inertial effects ii: Free rotation in space. *Proceedings of the Physical Society. Section B*, 70(4):414, 1957.
- [20] Manfred Schienbein and Hans Gruler. Langevin equation, fokker-planck equation and cell migration. *Bulletin of Mathematical Biology*, 55(3):585–608, 1993.
- [21] Frank Schweitzer. *Brownian agents and active particles: collective dynamics in the natural and social sciences*. Springer Science & Business Media, 2007.
- [22] Padma K Shukla and Abdullah A Mamun. *Introduction to dusty plasma physics*. CRC Press, 2015.
- [23] David A Sivak, John D Chodera, and Gavin E Crooks. Time step rescaling recovers continuous-time dynamical properties for discrete-time langevin integration of nonequilibrium systems. *The Journal of Physical Chemistry B*, 118(24):6466–6474, 2014.
- [24] William A Steele. Molecular reorientation in liquids. i. distribution functions and friction constants. *The Journal of Chemical Physics*, 38(10):2404–2410, 1963.
- [25] William A Steele. Molecular reorientation in liquids. ii. angular autocorrelation functions. *The Journal of Chemical Physics*, 38(10):2411–2418, 1963.
- [26] Julien Tailleur and Michael E Cates. Sedimentation, trapping, and rectification of dilute bacteria. *EPL (Europhysics Letters)*, 86(6):60002, 2009.
- [27] Borge ten Hagen, Sven van Teeffelen, and Hartmut Löwen. Brownian motion of a self-propelled particle. *Journal of Physics: Condensed Matter*, 23(19):194119, 2011.